



Corso di dottorato di ricerca in:

“Scienze Biomediche e Biotecnologiche”

in convenzione con Centro di Riferimento Oncologico di Aviano, IRCCS

Ciclo 36°

Titolo della tesi

“Epithelioid hemangioma and hemangioendothelioma:
at the root of tumor spreading”

Dottoranda

Ilaria De Benedictis

Supervisore

Dott.ssa Roberta Maestro

Anno 2024

INDEX

ABSTRACT	1
INTRODUCTION	3
1. Mesenchymal tumors: classification and genetics.....	4
2. Vascular tumors	4
2.1. Epithelioid hemangioma	6
2.1.1. Molecular genetics of EH	7
2.2. Epithelioid hemangioendothelioma	9
2.2.1. Molecular genetics of EHE	11
3. Angiogenesis.....	12
3.1. Angiogenic pathway alterations in vascular tumors	14
4. Passive and active mechanisms of tumor spreading	16
AIMS.....	18
RESULTS	20
5. Clinical data of EH of bone patients.....	21
6. Fusion transcriptome profiling of multiple EHs	22
7. Fusion transcriptome profiling of multiple EHEs.....	29
8. Whole transcriptome profiling of EHE vs. EH.....	31
DISCUSSION.....	38
CONCLUSIONS AND FUTURE PERSPECTIVES	43
MATERIALS AND METHODS	45
9. Tumor samples analyzed	46
10. RNA and DNA extraction.....	46
11. Targeted RNA-sequencing and fusion calling	46
12. Retro-transcription (RT)-PCR and Sanger sequencing	46
13. Whole transcriptome RNA-sequencing and data processing.....	47
14. Functional data annotation	49
REFERENCES	51
ACKNOWLEDGEMENTS	64

ABSTRACT

Epithelioid hemangioendothelioma (EHE) and epithelioid hemangioma (EH), are ultra-rare vascular tumors characterized by recurrent chromosomal rearrangements. WWTR1::CAMTA1 fusions typify ~90% of EHEs, while less than 10% carry the YAP1::TFE3 gene fusion. Instead, fusions involving FOS or FOSB are detected in ~70% of EH. EHE is classified as a malignant tumor, while EH is a controversial entity. In fact, the WHO classification of Soft Tissue and Bone tumors classifies it differently depending on the site of origin: EH is considered a benign tumor if arisen in soft tissues whilst is classified as an intermediate grade tumor if developed in bones due to the common infiltrative growth pattern.

Both EHE and EH show high propensity to multifocal presentation. Approximately 60% of EHE and up to 25% of EH develop synchronous or metachronous lesions in different bones or organs. Given its malignant nature, multifocal EHE lesions are by default considered metastases. Conversely, whether multifocal EH are independent lesions or rather represent metastatic spreading of the primary neoplasm is debated. Understanding if multicentric tumors are clonally related clearly impacts on the prognosis and patients' management. To shed light on this issue, and in particular to elucidate the clinical and pathological characteristics of EH, we combined a clinical study with a thorough molecular characterization of EH multiplicity and used the fusion breakpoint as a clonality marker. In parallel, malignant EHE were analyzed as a reference.

The clinical characterization of 42 EH of bone patients demonstrated that their prognosis, irrespective of whether they developed synchronous or metachronous lesions and irrespective of the type of treatment, was excellent. Thus, EH is clearly a clinically benign tumor.

Molecular analyses showed that in both EH and EHE, multiple lesions arisen in the same patients shared an identical breakpoint, indicating a common clonal origin. This result demonstrates that, irrespective of benign looking histological appearance and irrespective to the excellent prognosis, from a biological standpoint EH feature an intrinsic propensity to metastatic spreading, similar to an overt malignant tumor such as EHE. This paradox may be explained by phenomena of passive spreading, whereby EH, being vascular lesions, shed tumor cells into the circulation which colonize distal sites while maintaining their intrinsic benign biological nature.

Furthermore, EHE and EH comparison through differential gene expression analysis allowed us to pinpoint some pathways potentially implicated in the aggressive clinical behavior of EHE.

INTRODUCTION

1. Mesenchymal tumors: classification and genetics

Mesenchymal tumors are a heterogeneous group of neoplasms of mesenchymal nature that include benign and malignant entities (sarcomas). The classification of these tumors is based on morphological characteristics, lineage and site of origin. The World Health Organization (WHO) divides mesenchymal tumors in two main categories: Soft Tissue and Bone tumors. Soft tissue tumors arise in fat, muscle, blood vessel and nerve tissue, while bone tumors typically interest cartilage and bone and comprise not only bone-derived neoplasms, but also tumors of different origin but with bone localization ¹. Genetically, they are divided into: complex karyotype tumors, with no recurrent genetic alterations; simple karyotype tumors, which are characterized by specific genetic alterations such as chromosomal translocations, amplifications or oncogenic mutations ².

About 1/3 of mesenchymal tumors carry histotype-specific fusion transcripts, which are helpful in the diagnosis, prognosis and management of patients ³. Chromosomal rearrangements giving origin to reciprocal or non-reciprocal translocations can result in the production of highly specific fusion genes ⁴. Not only translocations, but also inversions, deletions and insertions are responsible for the generation of gene fusions⁵. Since in certain mesenchymal tumors gene fusions represent the predominant aberration and these tumors have a low tumor mutational burden, the fusion product is considered the driver oncogenic event that hallmarks the lesion ⁶⁻⁹. Thus, fusion products are considered diagnostic tools and the fusion breakpoint may be employed as a clonality marker ¹⁰⁻¹².

2. Vascular tumors

Vascular tumors belong to the class of mesenchymal tumors and represent a rare and heterogeneous group arising in the blood vessels of different anatomic sites. Several tumors belong to this group, ranging from benign entities such as hemangiomas to highly aggressive tumors like angiosarcomas¹. Diagnosis is based on morphology, histologic features (e.g. abnormal vascular growth) and expression of typical endothelial markers such as CD31, CD34 and ERG ^{1,13}. However, in the case of vascular tumors with epithelioid morphology, diagnosis may be challenging¹⁴. In fact, mesenchymal tumors with epithelioid morphology, which include epithelioid hemangioma (EH), pseudomyogenic hemangioendothelioma (PHE), epithelioid hemangioendothelioma (EHE) and epithelioid angiosarcoma ¹, show histological and immunological characteristics that overlap with other pathological entities

such as metastatic carcinomas or epithelioid sarcomas^{14,15}, a fact that may be source of erroneous diagnoses and inapt treatments¹⁶.

Luckily, the progressive identification of histotype-specific genetic alterations such as recurrent chromosomal aberration giving raise to fusion genes (**Table 1**) has offered the opportunity to solve these diagnostic dilemmas. Indeed, epithelioid vascular tumors represent a paradigmatic example on how the inclusion of molecular analyses have dramatically reduced diagnostic errors^{14,17}. Importantly, EH and EHE were originally considered the same tumor entity¹⁸, because of highly similar histologic appearance (well-defined cell borders, abundant densely eosinophilic cytoplasm, cytologic atypia)¹⁹. Subsequently, the two tumors were recognized as distinct entities^{16,20–22}, and the difference is further supported by the identification of different chromosomal rearrangements^{12,23–26}.

Table 1. Recurrent fusion genes identified in vascular tumors.

Vascular tumor	Gene fusion	Fusion reported	Studies in which was reported
EH	FOS rearrangement	FOS::VIM (a.k.a FOS::chr10)	24,26,27
		FOS::LMNA	27
		FOS::lincRNA	24
		FOS::MBNL1	24
	FOSB rearrangement	ZFP36::FOSB	26,28,29
		WWTR1::FOSB	26,28,30
		SETD1B::FOSB	31
		ACTB::FOSB	32
FOXO1 rearrangement	GATA6::FOXO1	33	
PHE	FOSB rearrangement	SERPINE1::FOSB	34,35
		ACTB::FOSB	32,36
		CLTC::FOSB	37
		WWTR1::FOSB	38,39
EHE	WWTR1 rearrangement	WWTR1::CAMTA1	12,23,40–47
		WWTR1::MAML2 WWTR1::ACTL6A	48
	YAP1 rearrangement	YAP1::TFE3	25,43,44,47,49–53
Angiosarcoma	CIC rearrangement	CIC::LEUTX, Unknown partner	54
	Other rearrangements	NUP160::SLC43A3	55

Epithelioid vascular tumors include tumors of different grades and clinical behavior, from benign to very aggressive forms. In this context, the classification of EH is quite

controversial. EH is classified as a benign tumor if arisen in soft tissues but it is considered an intermediate-locally aggressive tumor if developed in bones ¹. Indeed, bone EH may be characterized by a locally destructive growth pattern, sometimes associated with lymph node involvement. Moreover, these tumors may show multifocal presentation ^{1,56,57}. These facts are in apparent contradiction with the benign looking histologic appearance and would suggest an aggressive clinical behavior. Indeed, whether these EH multiple lesions from the same patient are distinct entities or they are rather clonally related is still debated ^{19,56}. Shedding light on this issue is of paramount importance not only for understanding the biology of the disease but also for adequate patients' management.

EH and EHE will be discussed in detail further on, since they are the focus of this thesis.

2.1. Epithelioid hemangioma

Epithelioid hemangioma (EH) is an ultra-rare vascular tumor. EH is composed of endothelial cells that exhibit an epithelioid morphology ¹.

EH occurs in soft tissue, bone but also in other sites. Macroscopically, the tumor has a nodular appearance. Loose connective tissue composes the stroma of the tumor and is often enriched with inflammatory cells such as eosinophils ^{19,22,58}. When developed in bone, EH appears as a lytic mass that can extend into the soft tissues and erode the cortex ⁵⁷.

The main histologic categories of EH are classic or atypical/cellular ²⁹. Classic EH (**Figure 1**) shows thin well-developed blood vessels lined by large epithelioid endothelial cells that may occasionally project into the lumina. Only a few mitosis and small foci of necrosis can be observed. The atypical/cellular variant of EH (**Figure 2**) shows a more solid growth, increased cellularity, nuclear pleomorphism and necrosis.

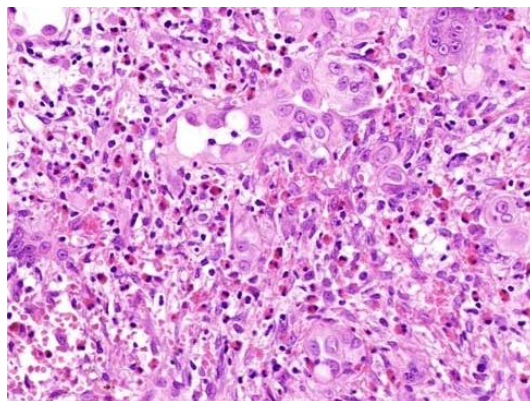


Figure 1. Histology of a classic variant of EH. From Righi et al.²⁹.

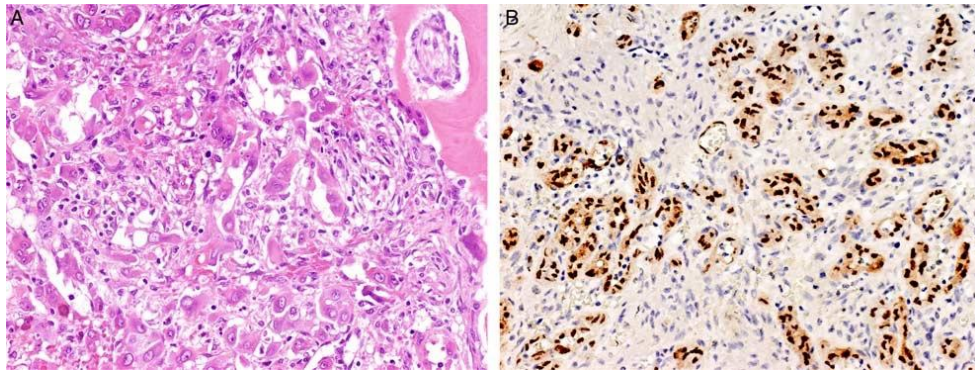


Figure 2. (A) Histology of an atypical/cellular variant of EH evidences an increased nuclear atypia compared to the classic variant. (B) Some cases show a strong and diffuse nuclear expression of FOSB antibody. From Righi et al. ²⁹.

The tumor cells are positive for the endothelial markers CD31, CD34, FLI1, ERG, and the factor VIII-related antigen. Positivity for keratin and EMA have also been observed ^{20,58}. EH is hallmarked by gene rearrangements involving either FOS or FOSB and resulting in increased protein expression ^{24,26,28,29}. EH enters in differential diagnosis with angiosarcoma and EHE ^{19,59}. However, morphologically angiosarcoma differs from EH for the lack of lobular architecture, presence of nuclear atypia and higher mitotic index; EHE do not have the well-developed vasculature that typify EH ¹. From a genetic standpoint, the detection of the pathognomonic fusions that characterize EH and EHE plays an important role in differential diagnosis.

Approximately 25% of EH present as multifocal lesions, phenomenon particularly common for EH developing in bone ^{19,22,58,60} where tumor foci may involve the same bone, contiguous bones but also non-contiguous, distal bones ^{22,61,62}. Invasion of adjacent soft tissues may also be observed. Treatment includes *en bloc* resection, curettage and radiotherapy ²².

2.1.1. Molecular genetics of EH

Pathognomonic genetic rearrangements of EH involve the genes FOS (~70% of cases) or, less commonly, FOSB (**Figure 3**). FOS gene fusions seem more common in EH of bone than in EH at other anatomical sites ^{26,27}. FOS fusions are truncating fusions. In fact, the intra or interchromosome rearrangement involving FOS results in the generation of a premature stop codon downstream the exon 4. This results in the removal of the C-terminal regulatory domain of the protein, leading to FOS increased stability and hyperactivation ^{24,63}.

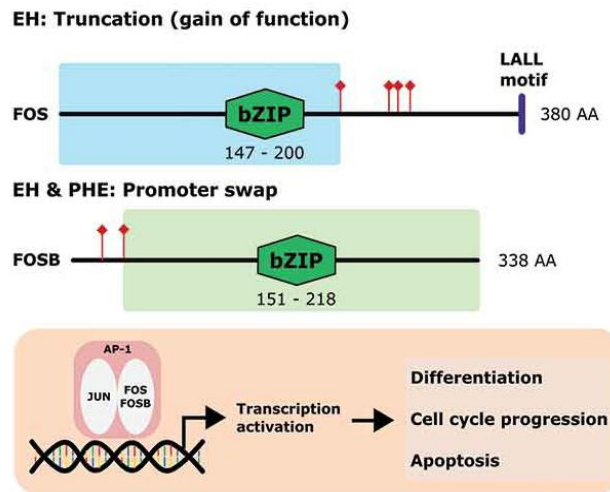


Figure 3. Graphical representation of EH fusions, adapted from Ong et al. ¹⁷. FOS and FOSB fusions lead to constitutive activation of the AP-1 transcription factor and transcription of its downstream genes, leading to increased proliferation and survival.

Specifically, the truncated FOS allele resulting from FOS fusions retains the basic leucine zipper (bZIP) domain, responsible for initiating transcriptional activity, but loses the LALL motifs that physiologically are responsible for the turnover of FOS. Functional studies revealed that truncated FOS is resistant to ubiquitin-mediated degradation and is therefore more stable and promotes endothelial sprouting and abnormal vessel formation in HUVEC cell lines ⁶³.

Being truncating events, there is no preferential gene partner for FOS fusions and that these fusions often involve intergenic, non-coding region of the genome ^{24,63}.

FOS fusion events reported in the literature include: intergenic regions as in the case of FOS::VIM ^{24,26,27}; long non-coding RNAs such as lincRNA (RP11-326N17.1) ²⁴ or intronic regions of protein coding genes as in MBNL1 ²⁴ and LMNA ²⁷.

Different from FOS, the fusions involving FOSB generate chimeric proteins. FOSB usually fuses downstream with the Zinc Finger Protein 36 (ZFP36) ^{26,28,29} or WW Domain Containing Transcription Regulator 1 (WWTR1) ^{28,30} leading to ZFP36::FOSB or WWTR1::FOSB fusions. The promoter swap event in FOSB rearranged EHs leads to overexpression of FOSB. Consequently, FOSB-regulated pathways are overactivated and promote vascular tumorigenesis, as demonstrated in *in vitro* studies in HUVEC cells ⁶⁴.

FOS and FOSB belong to the FOS family of transcription factors, which also includes FOSL1, FOSL2 and ΔFOSB. Under physiological conditions, wild-type FOS and FOSB heterodimerize with JUN to form the transcription factor Activator Protein (AP)-1, which is responsible for the induction of cell growth, differentiation, and apoptosis. Their activity is

normally turned off by the cellular proteasome machinery ⁶⁵. However, cancer cells evolved different mechanisms to prolong or increase the activity of these proteins to constitutively activate the transcription of genes involved in cancer initiation and progression. A role for AP-1 proteins has been described in several cancer types ⁶⁶. In particular, FOS ⁶⁷ has been found to be overexpressed in osteosarcoma, endometrial cancer, ovarian cancer, melanoma and lung cancer, while the role of FOSB has been well characterized in breast cancer, where its expression is associated with a well-differentiated phenotype and is downregulated in poorly differentiated tumors ⁶⁶.

In bone tumors, FOS plays a key role in oncogenic transformation: it is a marker for osteoid/osteomas and osteblastomas ⁶⁸. Similar to EHEs, osteblastomas are characterized by FOS truncating rearrangements ⁶⁹, while osteosarcomas and chondrosarcomas require the expression of this protein for tumor formation ⁷⁰. FOSB oncogenic role has been explored in detail in another vascular tumor, the PHE, which shares FOSB fusions with EHE ^{64,71,72}.

2.2. Epithelioid hemangioendothelioma

Epithelioid hemangioendothelioma (EHE) is an ultra-rare vascular tumor, with an incidence of 0.038/100000/year ⁷³. The tumor is constituted by epithelioid endothelial cells and is commonly localized in soft tissue, bone, but also lung, liver and skin ^{1,74,75}.

Macroscopically, EHE of soft tissues appears as a solid mass surrounded by the vessel wall in soft tissues, whereas EHE of bone is usually a lytic lesion that may erode the cortex ⁵⁸. EHE can extend to the surrounding tissues such as skeletal muscle or fat ^{16,74}.

There are two EHE histological variants. The classic and most common variant (about 90% of the cases) consists of epithelioid and spindle-shaped cells in a myxohyaline stroma, with copious eosinophilic cytoplasm and is genetically characterized by the expression in most cases of the WWTR1::CAMTA1 gene fusion ^{40,41}. The other, less common variant, is defined YAP1::TFE3 EHE variant due to the expression of the YAP1::TFE3 gene fusion (**Figure 4**). YAP1::TFE3 rearranged tumors tend to growth as solid sheets of well-formed vessels and their cells show abundant cytoplasm with moderate nuclear atypia. The myxohyaline stroma is usually absent ²⁵.

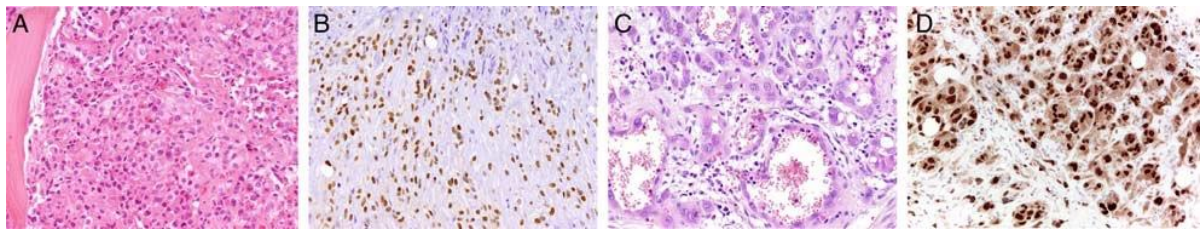


Figure 4. (A) EHE CAMTA1 positive. Tumor cells with glassy eosinophilic cytoplasm and sharply defined cell borders, and round to ovoid bland, vesicular nucleus with small, centrally located nucleoli. (B) they show a strong nuclear expression of CAMTA1. (C) TFE3 positive EHEs exhibit variable vasoformative features, ranging from the presence of prominent and readily discernible open lumina to focal and more subtle findings. (D) They show a strong nuclear expression of TFE3. From Righi et al. ²⁹.

EHE tumor cells express endothelial markers such as CD31, CD34, ERG, FLI1, factor VIII-related antigen and podoplanin (D2-40), PROX1, markers of lymphatic differentiation. Positivity for keratin and EMA may also be present ^{16,74,76,77}. SMA is expressed in the 50% of cases ⁷⁸. The immunohistochemical positivity for CAMTA1 or TFE3 fusion products may help in the identification of fusion-driven tumors, although sensitivity and specificity of the immunohistochemical approach are not optimal ^{43,79}.

EHE can be confused with metastatic carcinomas, because of positivity for keratins, with epithelioid angiosarcomas and with EH. However, the detection of the pathognomonic fusion is discriminant in these cases ^{45,80}.

The prognosis of EHE is influenced by tumor location and genetics. EHE of skin have an excellent prognosis; EHE of soft tissues tend to be relatively indolent although in about 20% of the cases the tumor metastasizes; EHE of bones tend to have a poorer prognosis and the development of multifocal, metastatic lesions is quite common. These lesions may involve the same bone or non-contiguous separate bones ⁷⁴. Moreover, TFE3 rearranged tumors tend to be more aggressive than WWTR1::CAMTA1 tumors ²⁵.

Treatment usually consists in wide resection, and, in the case of metastatic lesions, systemic therapy including antiangiogenics ^{73,81}. Additional treatments include MEK inhibitors ⁸², mTOR inhibitors ⁸³, the microtubule inhibitor Eribulin ⁸⁴, or TEAD inhibitors (NCT05228015). The mortality rate for these tumors is about 20%. Multifocal EHEs are associated with a bad prognosis. Clinically, EHE of bone can be indolent for several years and then suddenly become aggressive. Currently, there are no biomarkers that can be associated with the clinical course of the disease ⁸⁵.

The monoclonality of multifocal, metastatic EHE lesions was demonstrated by using the gene fusion breakpoint as a clonality marker ^{12,29}.

2.2.1. Molecular genetics of EHE

WWTR1::CAMTA1 fusion typify the 90% of EHE, while <10% of tumors harbor YAP1::TFE3 fusion. Both are responsible for the deregulation of the Hippo pathway.

The mechanism by which these fusions drive tumorigenesis and tumor progression is highly similar (**Figure 5**).

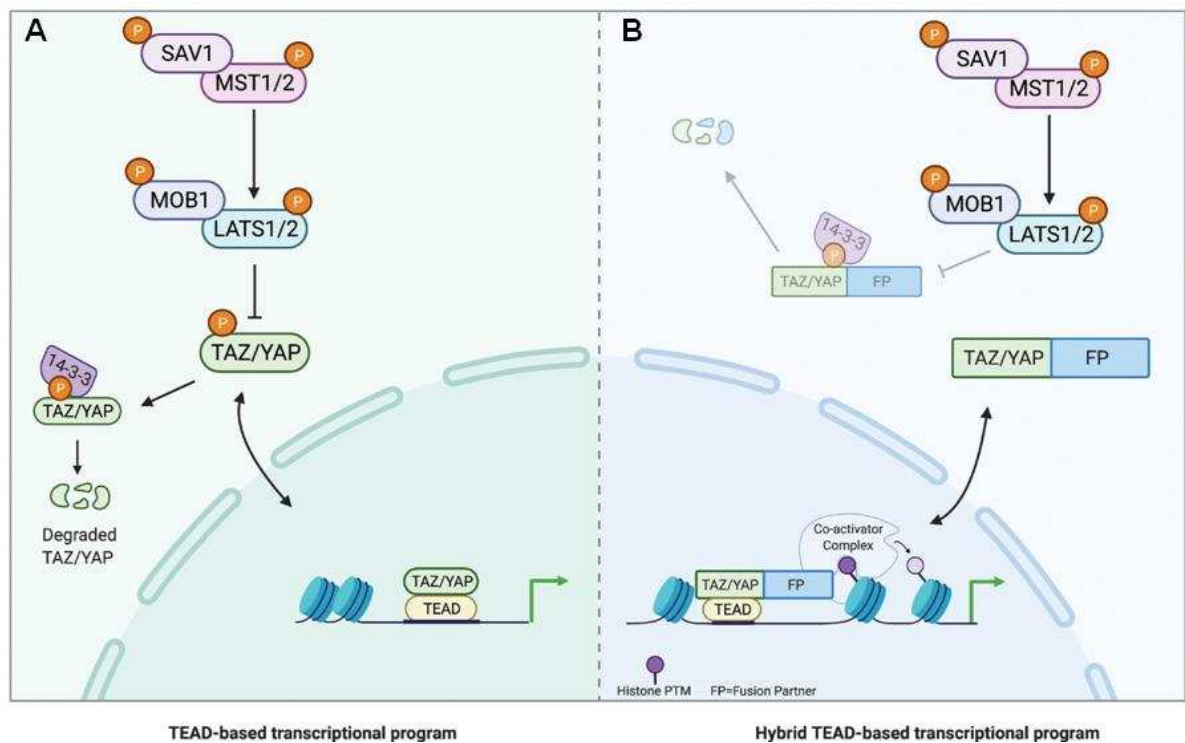


Figure 5. Adapted from Garcia et al. ⁸⁶ (A) Hippo pathway activation results in a series of phosphorylation events involving the serine/threonine kinases the mammalian sterile 20-like 1/2 (MST1/2) and large tumor suppressor kinase 1/2 (LATS 1/2), that in turn phosphorylate and activate TAZ and YAP. In physiological conditions, TAZ/YAP shuttle from the nucleus into the cytosol under external stimuli. Binding of TAZ/YAP to 14-3-3 proteins and their ubiquitin-mediated degradation and inactivation of the pathway. (B) TAZ/YAP fusion proteins escape from Hippo pathway regulation and degradation, allowing them to accumulate in the nucleus. In addition to interacting with the TEAD family of transcription factors, fusion partners can recruit chromatin/transcriptional co-activator complexes, to drive an altered TEAD-based transcriptional program that is responsible of tumorigenesis.

The WWTR1::CAMTA1 fusion joins the first exons of WWTR1 (a.k.a. TAZ) with CAMTA1, a transcriptional activator usually expressed in the nervous system ^{87,88}. The YAP1::TFE3 fusion retains the N-terminal domain of YAP and links it with the C-terminus of TFE3. The N-terminal domain of TAZ (WWTR1) and YAP contains a DNA binding domain and the TEAD binding site, which is responsible for the interaction with other transcription factors. The C-terminal fusion partners provide a nuclear localization sequence that is essential for aberrant transcription of the chimeric factor ^{49,89-91}. WWTR1::CAMTA1 is insensitive to the inhibitory Hippo signals and constitutively activates the TAZ (WWTR1)

transcriptome⁹⁰. The YAP/TAZ pathway is involved in cancer development and metastatic spreading^{89,92}. YAP/TAZ have been reported to be upregulated in prostate cancer, cervical cancer, melanoma and ovarian cancer, among others. Mutations or gene fusions involving YAP/TAZ and conferring constitutive activation and nuclear localization have been reported in sarcomas and brain tumors^{93,94}.

Besides the pathognomonic fusions, few studies have addressed the additional genetic events involved in EHE pathogenesis. The most common secondary genetic alteration associated with the EHE is the loss of CDKN2A⁹⁵ that functionally contributes to EHE tumor progression *in vivo*⁹⁶ and promotes genomic instability and senescence⁹⁷. Other common variants include CDKN2B, RB1, ATRX, APC and FANCA, which are involved in cell cycle regulation, growth signaling and DNA damage response⁹⁵. NOTCH3 missense mutations⁹⁸ and MSH2 mutations⁹⁹ have also been reported.

3. Angiogenesis

Angiogenesis is a key process that consists in new blood vessels formation starting from a pre-existing vascular network. In physiologic conditions, it is a finely regulated and coordinated process, in which endothelial cells (ECs) differentiation, proliferation and migration are under the control of several pro-angiogenic and anti-angiogenic factors¹⁰⁰. There are different models of neo vessel formation¹⁰¹. In the conventional model of angiogenesis¹⁰², the sprouting angiogenesis, a hypoxic environment is required to drive vascular endothelial growth factor A (VEGF-A) secretion (**Figure 6**).

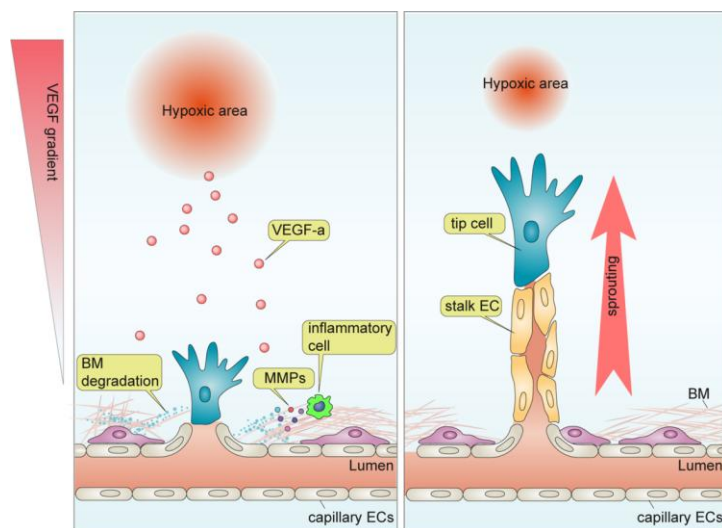


Figure 6. Conventional angiogenesis model. From Lee et al.¹⁰⁰.

This molecule acts on the capillary bed cells that start migrating towards a VEGF-A gradient. In parallel, the recruitment of pro-inflammatory cells is responsible of matrix metalloproteinases (MMPs) production that have the function to break the surrounding extracellular matrix and facilitate endothelial cell migration. Depending on their position in the angiogenic sprout, endothelial cells can differentiate into “tip” or “stalk” cells. “Tip” cells feel the VEGF gradient and move the growing sprout toward it. “Stalk” cells follow the tip cell and form the vascular lumen¹⁰⁰.

To prevent disordered vessels growth, angiogenic sprouting is regulated by the activation of Notch signaling at endothelial cell–cell link sites. VEGF induces DLL4 expression in “tip” cells. In contrast, Notch is expressed in the other surrounding “stalk” vascular cells, adjacent to the tip cells. This interaction induces the expression of genes that prevent excessive vascular growth¹⁰³.

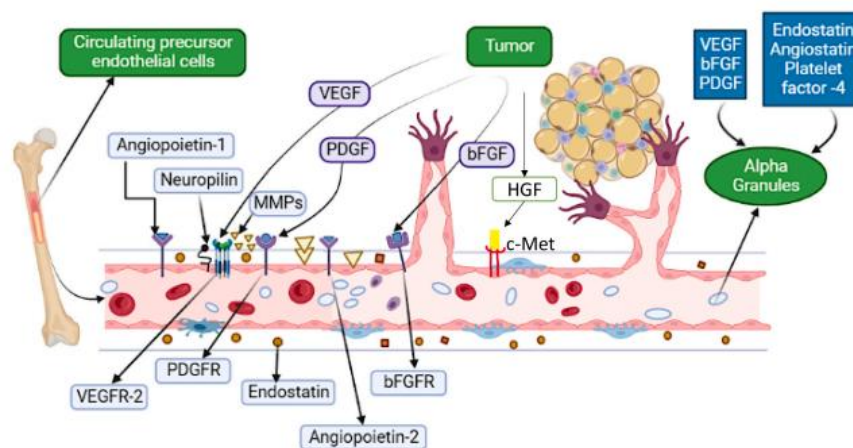


Figure 7. Signaling pathways and ligands involved in tumor angiogenesis. From Vimalraj et al.¹⁰⁴.

Angiogenesis is regulated by several pathways (**Figure 7**) that involve both pro- and anti-angiogenic factors¹⁰⁴ (**Table 2**).

A balanced expression of these factors allows neo vessels formation and prevents disorganized vessels growth. Deregulation of these pathways is observed in solid tumors-associated vessel¹⁰¹. In fact, neo-angiogenesis is a hallmark of cancer and represents a key factor for three-dimensional tumor growth, invasion, and metastasis¹⁰⁵. Deregulation of angiogenic pathways associated to disordered angiogenesis was also described in vascular tumors¹⁰⁶.

Table 2. Pro and anti- angiogenic factors, from Krock et al. ¹⁰⁷.

Pro-angiogenic	Anti-angiogenic
VEGF, Flt-1 (VEGF-R1), Kdr (VEGF-R2)	DLL1-4
Ang-1/2, Tie-2	VASH1
ADM	THBS1
FGF	CA-9
PGF	RGS5
PDGF-B	Angiostatin
SCF	Endostatin (precursor COL18A1)
Osteopontin	Canstatin (precursor COL4A2)
SERPINE1	Interferons (IFN- α , IFN- β , IFN- γ)
MMP, TIMP	
NOS	
COX-2	
Endoglin	
A1B-adrenergic receptor	
Endothelin-1	
Semaphorin 4D	
Integrins, leptin	
Endosialin	
Adenosine A2A receptor	
Oxygen-regulated protein-150	
SDF-1	
Interleukins (IL-1, IL-2, IL-4, IL-6, IL-8, IL-10)	
ADM, adrenomedullin; Ang-1/2, angiopoietin-1/2; COX-2, cyclo-oxygenase 2; DLL, delta-like ligand; FGF, fibroblast growth factor; Flt-1, fms-related tyrosine kinase 1; Kdr, kinase insert domain containing receptor; MMP, matrix metalloproteinases; NOS, nitric oxide synthases; PAI-1, plasminogen activator inhibitor-1; PGF, placenta growth factor; PDGF-B, platelet-derived growth factor beta; SCF, stem cell factor; SDF-1, stromal-derived growth factor; Tie-2, TEK tyrosine kinase endothelial; TIMP, tissue inhibitor of metalloproteinases; VEGF, vascular endothelial growth factor; VEGF-R, VEGF receptor.	

3.1. Angiogenic pathway alterations in vascular tumors

Several intracellular signaling are involved in endothelial cells tumors development ¹⁰⁶ (**Figure 8**). However, whilst angiosarcomas have been long studied, less information is available about the rarer EH and EHE.

In angiosarcoma, alterations of vascular endothelial growth factor receptor (VEGFR) and its signaling pathway have been reported, including high levels of VEGF-A, VEGFR1 (a.k.a. FLT1), VEGFR2 (a.k.a. KDR) or VEGFR3 (a.k.a. FLT4) ¹⁰⁸, angiopoietin-2 (Ang2), tyrosine kinase with immunoglobulin like and EGF like domains 1 (Tie1), and Tie2 ¹⁰⁹; activating VEGFR2 ¹¹⁰ and Phospholipase C Gamma 1 (PLCG1) mutations ¹¹¹; amplifications of VEGFR3 ¹¹². Moreover, angiosarcoma is characterized by loss of function mutations in the Protein Tyrosine Phosphatase Receptor Type B (PTPRB) ¹¹³ that result in increased Ang/Tie2 signaling and related pathways involved in survival, migration and proliferation ¹¹⁴.

Additional mutations include: K-H- and N-RAS, BRAF and MAPK1, Tsc1, together with amplification of B- C- RAF, MAPK1¹¹⁵ and C-MYC¹¹².

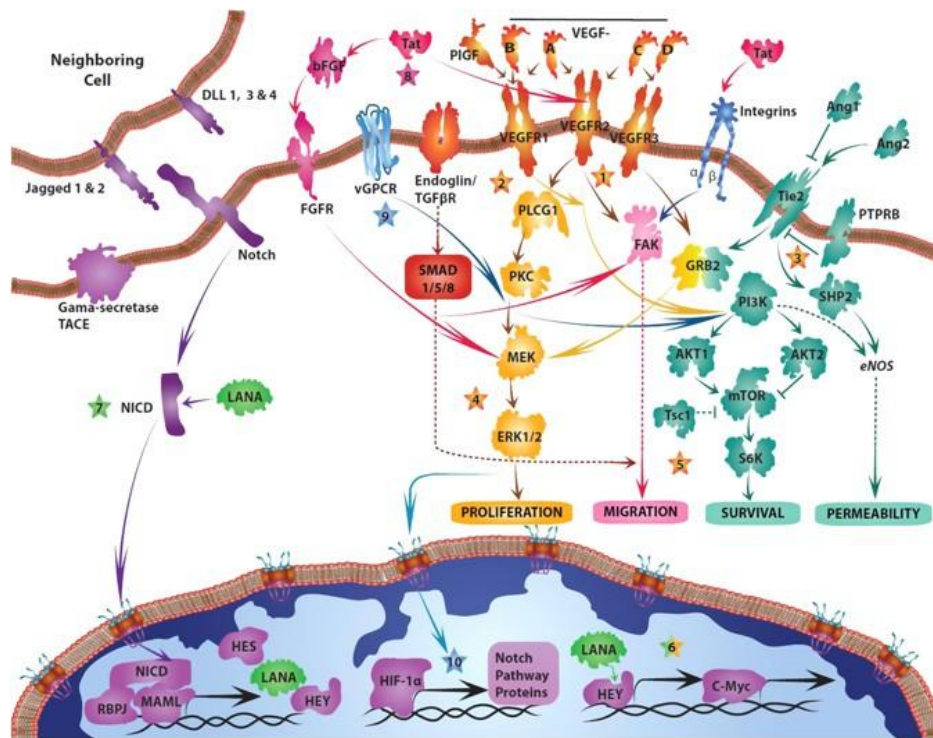


Figure 8. Common pathways deregulated in vascular tumors. From Wagner et al.¹⁰⁶.

Apart from the pathognomonic gene fusion, very little information is known about the pathways involved in EHE and EH. Regarding the typical vascular pathways, VEGF staining has been associated with more aggressive disease in EHE^{116,117}. The WWTR1::CAMTA1 gene fusion that typifies EHE has been shown to regulate the connective tissue growth factor (CTGF), that sustains VEGF production via the MAPK pathway¹¹⁸. Instead, truncated FOS-driven angiogenic sprouting is dependent on matrix metalloproteinases (MMPs) and Notch signaling⁶³.

The Hippo pathway, involved cell survival, proliferation and invasive migration and metastasis¹¹⁹ and activated in EHE via gene fusion, plays also a role in vascular development¹²⁰.

4. Passive and active mechanisms of tumor spreading

Tumor cells are known to be able to detach from the tumor mass and to enter circulation as circulating tumor cells (CTCs). CTCs have been shown to be able to disseminate to distant sites but can also re-seed in the site of origin¹²¹. Nevertheless, self-seeding, as well as cancer dissemination to distant sites, can generate tumors that are even more aggressive of the initial ones¹²¹.

During metastatic dissemination (**Figure 9**), tumor cells bypass a number of barriers: detach from the primary site, enter into circulation, survive in the lymphatic/circulatory system, exit the circulation, colonize secondary sites and expand¹²².

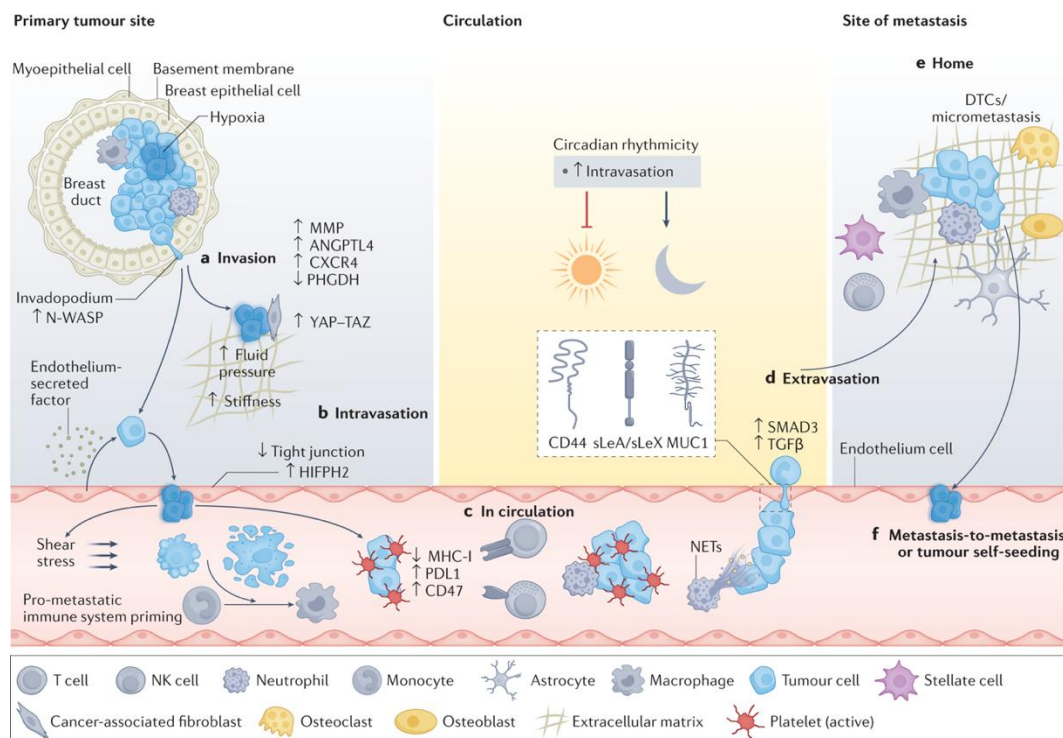


Figure 9. Steps of tumor spreading. From Ring et al.¹²².

Metastatic dissemination is usually considered an active process where all these steps are regulated by specific signaling pathways, but a number of evidence suggest that tumor spreading may occur also as a passive phenomenon¹²³. Pathways that are shown to contribute to active metastatic dissemination include hypoxia¹²⁴, Wnt signaling, epithelial-to-mesenchymal transition (EMT), integrins and other pathways related to reorganization of cytoskeleton proteins for polarization and migration¹²².

As mentioned above, an increasing body of evidence support the notion that tumor cells may disseminate and relocate distally from the primary site also through a passive phenomenon. Evidence in support of passive intravasation include the demonstration that CTCs are mostly unviable cells ¹²⁵, that primary tumors shed more tumor cells after traumatic stresses ¹²⁶, that tumors, especially large masses, can generate stress factors by themselves through uncontrolled growth that may facilitate an inert penetration of vessels ^{127,128}. Finally, the fact that a tumor develop as a vascular structure may be per se a facilitating factor of intravasation.

AIMS

The main aim of this thesis was to understand whether tumor multifocality in the context of EH subtends tumor multiplicity (multiple independent tumors) or dissemination of a primary tumor (metastatization). To shed light on this issue, fusion transcriptome profiling was performed using fusion breakpoints as clonality markers. Metastatic EHEs were also included in the study and used as a positive control.

Subsequently, we aimed to identify deregulated genes and pathways that are responsible of the different biology of EH and EHE, shedding light on the molecular bases of EHE malignant phenotype.

RESULTS

5. Clinical data of EH of bone patients

The most recent classification of the WHO classifies EHs of soft tissues as benign tumors and EHs of bone as intermediate-locally aggressive tumors. In fact, despite being composed of “benign looking cells”, EH of bone may show a local destructive growth pattern and has often multifocal presentation, generating doubts on its benign nature and suspecting a malignant behavior. Although the series of EH of bone reported so far suggest an indolent clinical behavior, the rarity of this disease has so far prevented a definitive assessment of the prognosis. Ambiguity in tumor classification, along with lack of consensus on treatment strategies, contribute to the consideration of EH as a controversial entity.

To gain insights into the clinical behavior and biology of EH of bone, we took advantage of an ongoing clinical trial (NCT03169595) to retrospectively analyze a series of 42 patients cured at the Rizzoli Institute from 1978 to 2021. This is one of the largest cohorts of EH of bone analyzed so far.

Of 42 patients (see **Table 3**), 17 showed multifocal presentation (16 synchronous, 1 metachronous). Tumor mean size was 4.5 cm, the range was between 1.4-11.0 cm. Treatment included: en-bloc resection (n=12), intralesional curettage (n=24) and biopsy, occasionally followed by radiotherapy (n=6). Follow-up information was available for 38 patients (range 12-120 months) and only 5/38 presented local recurrence. In none of the cases death of disease was observed.

Table 3. Details of the 42 patients with Epithelioid Hemangioma of bone

Patient ID	Age	Gender	Location	Presentation	Treatment	Outcome (FUmonths)
EH1	29	F	Bone (vertebra)	Solitary	Surgery (WM)	NED (276)
EH2	35	M	Bone (humerus)	Solitary	Surgery (WM) RXT	NED (84)
EH3*	83	M	Bone (tibia)	Multifocal	Surgery (IL)	DOO (94)
EH4*	45	M	Bone (tibia, calcaneus)	Multifocal	Surgery (IL)	NED (24)
EH5*	33	M	Bone (tibia, cuboid, cuneiform)	Multifocal	Surgery (IL), RXT	NED (92)
EH6*	40	M	Bone (calcaneus, fibula)	Multifocal	Surgery (IL)	NED (33)
EH7*	60	F	Bone (metatarsal)	Multifocal	Surgery (IL), RXT	NED (106)
EH8	42	M	Bone (metatarsal, cuneiform)	Multifocal	Surgery (WM)	NED (38)
EH9*	39	F	Bone (tibia, rotula)	Multifocal	Surgery (IL)	Lost
EH10	31	M	Bone (humerus)	Solitary	Surgery (WM)	NED (126)
EH11	48	F	Bone (femur)	Solitary	Surgery (WM)	NED (166)
EH12	45	F	Bone (vertebra, rib)	Multifocal	Surgery (WM)	NED (52)
EH13	22	M	Bone (tibia)	Solitary	Surgery (IL)	NED (25)
EH14	38	F	Bone (vertebra)	Solitary	Surgery (IL) RXT	NED (200)
EH15	58	M	Bone (ulna)	Solitary	Surgery (WM)	NED (314)
EH16	28	F	Bone (pelvis)	Solitary	Surgery (IL)	NED (256)

EH17	42	M	Bone (femur)	Multifocal	Surgery (WM)	NED (32)
EH18	51	M	Bone (femur, tibia)	Multifocal	Surgery (IL)	DOO (96)
EH19	55	F	Bone (vertebra)	Solitary	Biopsy, RXT	NED (27)
EH20	39	F	Bone (vertebra, rib)	Multifocal	Biopsy, SAE	NED (70)
EH21	12	M	Bone (humerus)	Solitary	Surgery (IL)	NED (44)
EH22	12	F	Bone (femur, tibia)	Multifocal	Surgery (WM,IL)	Lost
EH23	65	M	Bone (fibula, calcaneus)	Multifocal	Surgery (IL) RXT	NED (202)
EH24	22	F	Bone (sacrum)	Solitary	Surgery (IL)	NED (211)
EH25	28	M	Bone (vertebra)	Solitary	Biopsy	AWD (39)
EH26	57	F	Bone (cuneiform)	Solitary	Surgery (IL)	NED (53)
EH27	33	M	Bone (humerus)	Solitary	Surgery (WM)	NED (182)
EH28	25	M	Bone (femur, pelvis)	Multifocal	Biopsy, RXT	NED (79)
EH29	41	M	Bone (metacarpal)	Solitary	Surgery (IL)	NED1 (178)
EH30	44	M	Bone (humerus)	Solitary	Surgery (WM)	NED (185)
EH31	40	M	Bone (tibia)	Multifocal	Surgery (WM)	NED (202)
EH32	21	F	Bone (vertebra)	Solitary	Biopsy, SAE	NED (28)
EH33	20	F	Bone (humerus, radius, skull, sacrum)	Multifocal	Surgery (WM, IL)	NED2 (240)
EH34	34	M	Bone (clavicle)	Solitary	Surgery (WM)	NED (195)
EH35	34	F	Bone (talus, tibia)	Multifocal	Surgery (IL)	Lost
EH36	28	M	Bone (tibia)	Solitary	Surgery (IL)	NED (102)
EH37	28	F	Bone (humerus)	Solitary	Surgery (IL)	NED1 (239)
EH38	60	M	Bone (sternum)	Solitary	Surgery (IL), SAE	NED1 (72)
EH39	39	F	Bone (pelvis)	Solitary	Biopsy	AWD (30)
EH40	46	F	Bone (cervical vertebra)	Solitary	Surgery (IL)	NED (24)
EH41	58	F	Bone (distal phalanx, second finger, foot)	Solitary	Surgery (IL)	NED1 (29)
EH42	28	M	Bone (clavicle)	Solitary	Surgery (IL)	Lost

M, male; F, female; RXT, radiation therapy; SAE, Selective arterial embolization; WM, wide margin; IL, intralesional curettage; NED, no evidence of disease; NED1, no evidence of disease after one local recurrence; NED2, no evidence of disease after two local recurrence; AWD, alive with disease; DOO, dead of other cause; FU, follow up; *cases with biological material available.

One patient presented with metachronous lesions (EH33): He underwent resection and curettage of the various lesions involving skull, humerus, radius and sacrum. Despite these multiple lesions, the patient had a favorable prognosis at 19-years follow-up⁶². Thus, overall the prognosis of EH, irrespective of tumor multifocality, is excellent.

6. Fusion transcriptome profiling of multiple EHs

To understand if multiple EHs developed in the same patient were clonally related, cases for which biological material of matched lesion was available, were selected (**Table 4**). In 2 of 6 such cases (EH3, EH6), however, RNA quality in one of the matched lesions was poor, leaving 4 cases suitable for molecular characterization by targeted RNA-sequencing, whole transcriptome analysis and relative orthogonal validations.

Table 4. EH cases with multifocal presentation selected for molecular analysis.

Patient ID	Sample	Anatomic site	Diagnosis	Paired samples suitable for RNA analysis
EH3	EH3A	Distal tibia (B)	Atypical/cellular	No
	EH3B	Proximal tibia (B)		
EH4	EH4A	Tibia (B)	Classic	Yes
	EH4B	Calcaneus (B)		
EH5	EH5A	Distal tibia (B)	Classic	Yes
	EH5B	III cuneiform (B)		
EH6	EH6A	Calcaneus (B)	Classic	No
	EH6B	Distal fibula (B)		
EH7	EH7A	IV metatarsus (B)	Classic	Yes
	EH7B	II metatarsus (B)		
EH9	EH9A	Left tibia (B)	Atypical/cellular	Yes
	EH9B	Rotula (B)		
	EH9C	Proximal tibia (B)		
B=Bone				

Separate EH lesions were all synchronous and with bone localization. They involved contiguous bones (EH5, EH7, EH9) or non-contiguous bones (EH4).

Targeted RNA-sequencing was performed by using a customized Archer assay, a commercially available kit based on Anchored Multiplex PCR-NGS sequencing approach. Briefly, the Archer assay (schema in **Figure 10**)¹²⁹ relies on the use of gene-specific and universal PCR primers, that anneal on a pre-modified cDNA in which adapters were previously ligated. After the annealing, two cycles of PCR allow the production of NGS libraries, that are then sequenced and analyzed with a dedicated bioinformatic pipeline (Archer suite) that relies on a proprietary fusion transcript database (Quiver). Theoretically this approach may allow the identification of fusion events affecting one of the genes covered by the primers of the assay even without prior knowledge of the fusion partner.

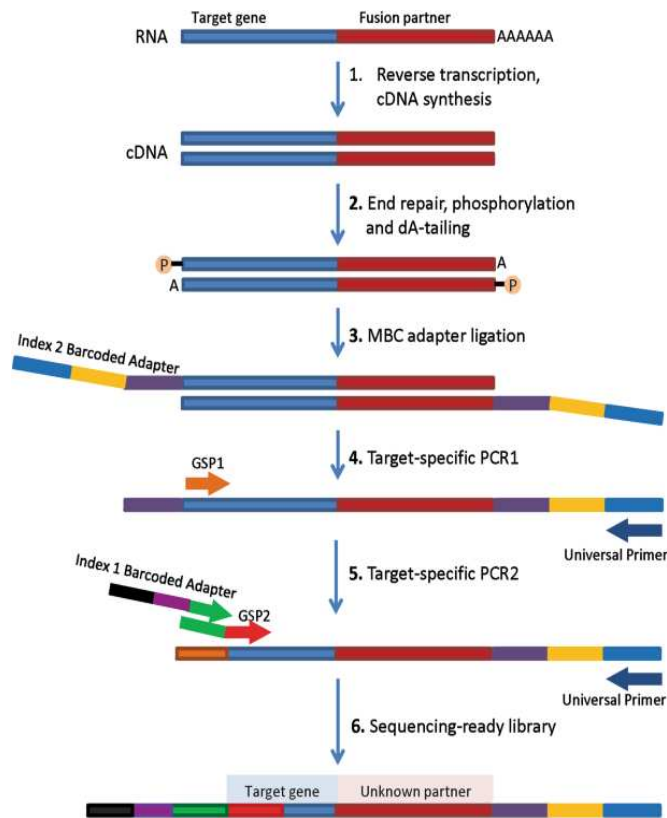


Figure 10 : Steps of an anchored multiplex PCR, from Zhu et al. ³⁶.

The commercial assay was customized in order to include also primers for the detection of FOS and FOSB fusions. After, sequencing raw data were analyzed using the Archer bioinformatic suite.

This Archer-based analysis yielded as “high confidence” the expression of a WWTR1::FOSB fusion transcript in case EH9 and a fusion involving FOS and a non-coding sequence on chromosome 11 in case EH4 (**Table 5**). In both cases the multiple lesions of the same patient expressed the same fusion with identical breakpoints. No “high confidence fusion” was detected by the Archer bioinformatics suite in cases EH5 and EH7.

The fact of having detected oncogenic FOS fusion in only 1 of 4 EH was in contradiction with literature data that indicated that over 70% of bone EH express FOS fusions. For this reason, we sought to “manually” re-analyze the raw data using a different RNA-sequencing fusion caller, namely Arriba. This “manual” approach allowed us to identify FOS fusion events also in cases EH5 and EH7 (**Table 5**). Intriguingly, these fusions were not reported even in the list of “discarded/low confidence fusion” of the Archer suite.

Table 5. Fusion transcriptome profiling in EH cases: Analysis of Archer data with the Archer bioinformatics suite and the Arriba fusion caller.

Targeted RNA- sequencing (Archer)					
Patient ID	Sample	Bioinformatic approach: Archer suite		Bioinformatic approach: Arriba	
		Gene1	Gene2	Gene1	Gene2
EH9	EH9A	WWTR1 chr3:149542335	FOSB chr19:45470629	WWTR1 chr3:149542335	FOSB chr19:45470629
	EH9B	WWTR1 chr3:149542335	FOSB chr19:45470629	WWTR1 chr3:149542335	FOSB chr19:45470629
	EH9C	WWTR1 chr3:149542335	FOSB chr19:45470629	WWTR1 chr3:149542335	FOSB chr19:45470629
EH4	EH4A	FOS chr14:75281167	ENSG00000255202 chr11:33694437	FOS chr14:75281167	ENSG00000255202 chr11:33694437
	EH4B	FOS chr14:75281167	ENSG00000255202 chr11:33694437	FOS chr14:75281167	ENSG00000255202 chr11:33694437
EH5	EH5A	No fusion detected		FOS chr14:75281016	chr21 (~ADAMTS1) chr21:26829622
	EH5B	No fusion detected		FOS chr14:75281016	chr21 (~ADAMTS1) chr21:26829622
EH7	EH7A	No fusion detected		FOS chr14:75281108	chr10 (~VIM) chr10:17238133
	EH7B	No fusion detected		FOS chr14:75281108	chr10 (~VIM) chr10:17238133

This finding has a diagnostic relevance. The Archer approach (kit and relative bioinformatic suite) is widely utilized in diagnostic laboratories for the diagnosis of fusion-driven tumors. However, it should be kept in mind that if the fusion is not annotated in the Archer proprietary fusion database (Quiver), the fusion may not be recognized as a high confidence fusion by the Archer suite. As better explained below, the FOS fusions that characterize EH are truncating fusions that do not yield a fusion protein and do not usually recognize a canonical fusion partner. Truncating fusions without recurrent fusion partner have been reported in other sarcomas, such as also in tenosynovial giant cell tumor (e.g. CSF1::ERV-LTR1B)¹³⁰ and in Dedifferentiated Liposarcoma (e.g. HMGA2 fusions)¹³¹. These fusions may be missed by the Archer suite, thus yielding false negative results. This is an aspect that diagnostic laboratories should be aware of when dealing with tumors that may produce truncating fusions.

The fusions identified by the “manual” annotation of raw Archer sequencing data with the Arriba fusion caller in cases EH4, 5, and 7 are illustrated in **Figure 11** and were all orthogonally validated by RT-PCR/Sanger sequencing.

In detail, in case EH4 FOS fusion partner on chromosome 11 was a long non-coding RNA in opposite orientation (FOS::ENSG00000255202 fusion). Case EH7 expressed in both lesions an identical FOS::chr10 fusion, involving FOS and an intergenic region on chromosome 10 located between VIM and ST8SIA6. A fusion of FOS with an intergenic region present on chromosome 21, located between ADAMTS1 and CYR1 genes, was detected in the multiple EH lesions of EH5 (FOS::chr21 fusion) with identical breakpoints.

All FOS fusions occurred between the exon 4 of FOS and a non-coding region (intergenic or intronic), resulting in a truncated version of FOS with a stop codon close to the breakpoint. According to previous data and the biological significance of these truncating fusions^{24,63}, a recurrent fusion partner was not identified among different EH cases.

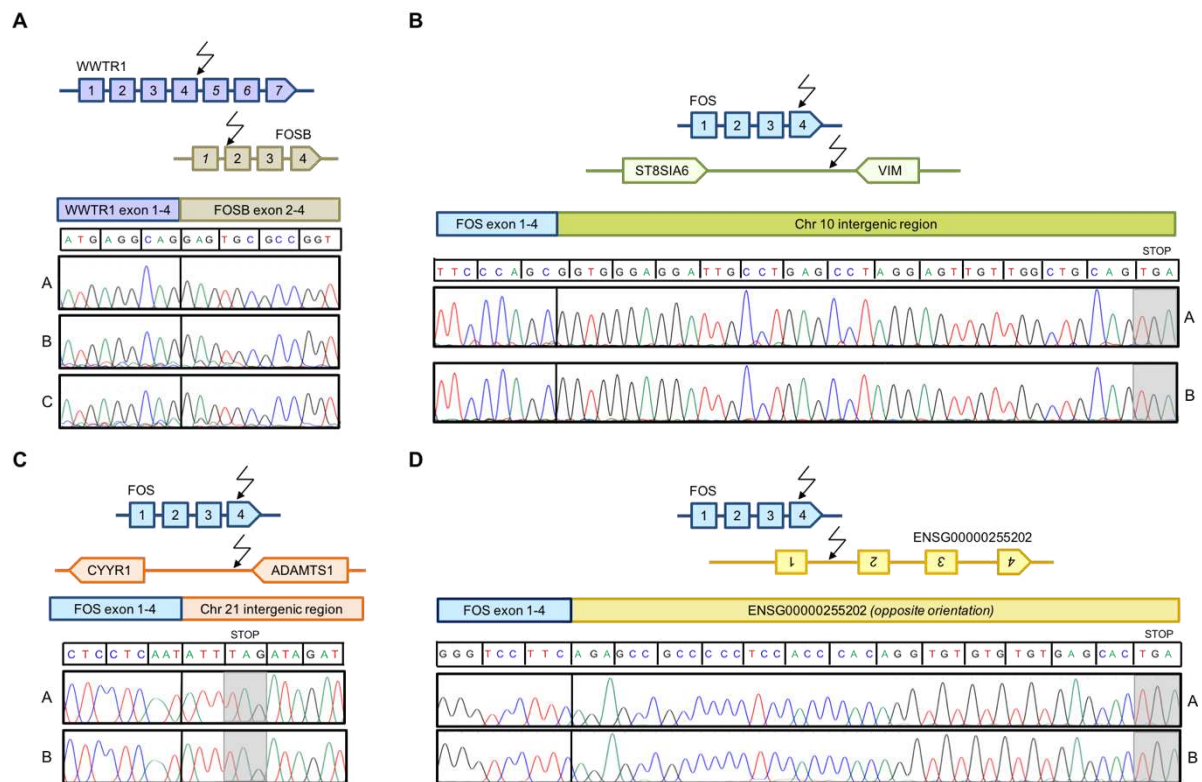


Figure 11. Schematic representation of the fusion breakpoints at RNA level. In the upper panel and chromatogram of the sequence in the lower panel. The arrows indicate the breakpoints at the RNA (cDNA) level. **(A)** Schematic representation of WWTR1::FOSB detected in the multifocal lesions of patient EH9 (A, left tibia; B, rotula; C, proximal tibia). **(B)** Schematic representation of the FOS::chr10 fusion detected in both lesions of EH7. The fusion involved FOS exon 4 and an intergenic region of chromosome 10, close to the VIM gene. An identical breakpoint in lesion A (IV metatarsus) and lesion B (II metatarsus) was identified. The greyish area indicates the de-novo STOP codon provided by the 3' partner. **(C)** Illustration of the FOS::chr21 fusion detected in case EH5 involving FOS exon 4 and an intergenic region of chromosome 21 close to the ADAMTS1 gene. Breakpoint sequence detected in both lesions of this patient was exactly the same in both lesions (A, distal tibia; B, III cuneiform). **(D)** EH4 lesions carried an identical FOS fusion (FOS exon 4 with lncRNA ENSG00000255202) in the lesions of the tibia and calcaneus (A and B, respectively).

The equivalence in the breakpoint sequence was further confirmed at the level of genomic DNA in the multiple lesions of cases EH9 and EH5 (**Figure 12**) adding further support to the common clonal origin.

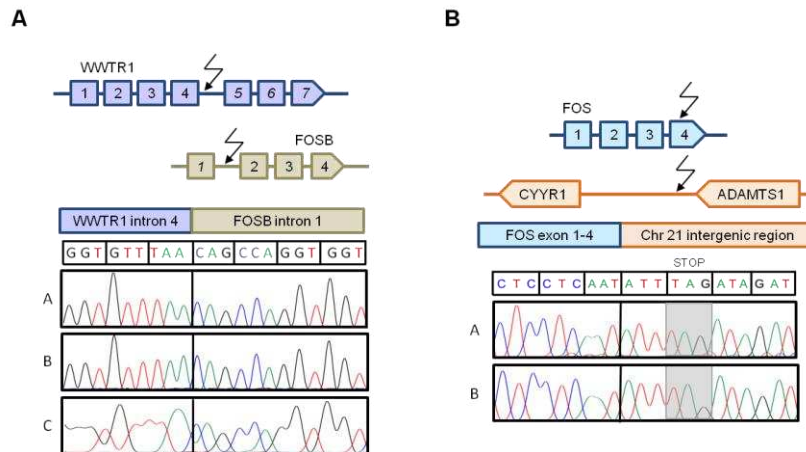


Figure 12. Fusion analysis of multifocal lesions at the genomic DNA level. **(A)** Schematic representation of the WWTR1::FOSB fusion detected in EH9. The chromatogram in the lower panel confirms that the three EH lesions in this patient (A, left tibia; B, rotula; C, proximal tibia) also share the same breakpoint at the DNA level. **(B)** Illustration of the FOS::chr21 fusion detected in case EH5. In both lesions of this patient (A, distal tibia; B, III cuneiform) The same breakpoint sequence was also detected at the genomic DNA level.

The clonal relationship between paired lesions of a same patients was also corroborated by the analysis of the transcriptome. Separate EHs of a same patient showed highly similar transcriptomes, as highlighted by Unsupervised hierarchical clustering and Principal Component Analysis (PCA) (**Figure 13**). Moreover, whole transcriptome fusion analysis, with Arriba and Fusion Catcher fusion callers, allowed us to identify additional fusion events. Importantly, these additional fusion events were shared by the tumor lesions of a same patient and showed identical breakpoints (**Table 6**). In cases EH5 and EH9 the additional fusions that were identified by both fusion callers (PSME3IP1::WWOX, FOSB::WWTR1 and TFG::ADGRG7) were also orthogonally validated through RT-PCR (not shown).

Unexpectedly, in EH9 (see **Table 6**), whole transcriptome profiling highlighted the presence of a FOSB::WWTR1. This fusion event involved the N-terminus of FOSB and the region corresponding to the transactivation domain of WWTR1, but did not the precisely correspond to the reciprocal of the WWTR1::FOSB transcript. The pathological significance of this additional event prompts further investigation.

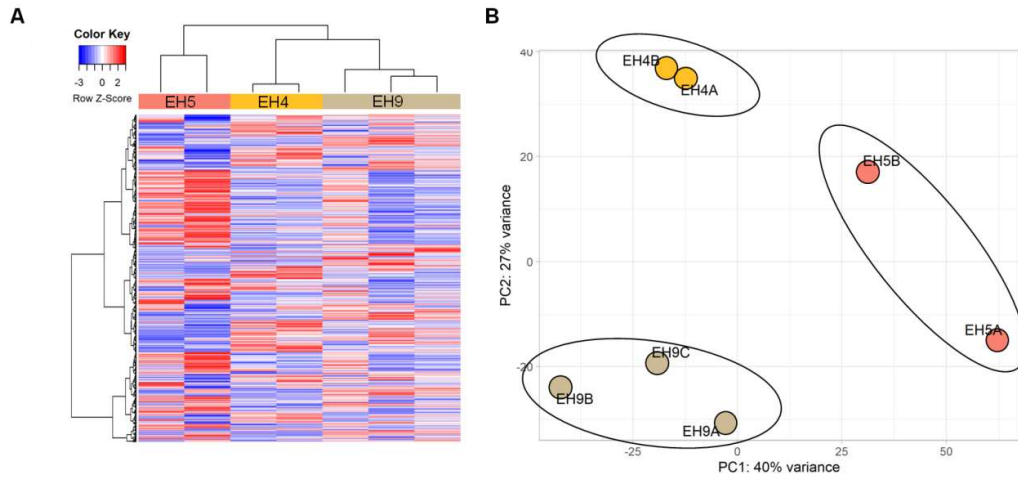


Figure 13. Unsupervised hierarchical clustering (A) and Principal Component Analysis (B), of the multifocal EHS of patients EH4, EH5 and EH9 show co-clustering of paired lesions of the same patient.

Table 6. Additional fusion events identified by whole RNA-sequencing in the separate tumor lesions of cases EH4, EH5 and EH9.

Pt ID	Sample	Gene1	Gene2	breakpoint_1	breakpoint_2	Arriba§	Fusion Catcher§
EH4	EH4A	SYN2	ACTG1	chr3:12071910 Intron	chr17:81510151 3'UTR	high	-
	EH4B	SYN2	ACTG1	chr3:12071910 Intron	chr17:81510151 3'UTR	low	-
EH5	EH5A	PSME3IP1	WWOX	chr16:57185821 5'UTR/splice-site	chr16:78164183 CDS/splice-site	high	high
	EH5B	PSME3IP1	WWOX	chr16:57185821 5'UTR/splice-site	chr16:78164183 CDS/splice-site	high	high
	EH5A	NDUFS8	chr11 (~GSTP1)	chr11:68033283 CDS/splice-site	chr11:67577746 intergenic	high	-
	EH5B	NDUFS8	chr11 (~GSTP1)	chr11:68033283 CDS/splice-site	chr11:67577746 intergenic	high	-
	EH5A	PMEPA1	PURB	chr20:57651860 UTR	chr7:44879426 UTR	-	high
	EH5B	PMEPA1	PURB	chr20:57651861 UTR	chr7:44879426 UTR	-	high
EH9	EH9A	WWTR1*	FOSB*	chr3:149528238 intron	chr19:45469785 intron	high	-
	EH9B	WWTR1*	FOSB*	chr3:149528238 intron	chr19:45469785 intron	high	-
	EH9C	WWTR1*	FOSB*	chr3:149528238 intron	chr19:45469785 intron	low	-
	EH9A	FOSB	WWTR1	chr19:45472706 CDS/splice-site	chr3:149527969 CDS/splice-site	high	high
	EH9B	FOSB	WWTR1	chr19:45472706 CDS/splice-site	chr3:149527969 CDS/splice-site	low	-
	EH9C	FOSB	WWTR1	chr19:45472706 CDS/splice-site	chr3:149527969 CDS/splice-site	low	-
	EH9A	TFG	ADGRG7	chr3:100720058 CDS/splice-site	chr3:100629598 CDS/splice-site	low	high

	EH9B	TFG	ADGRG7	chr3:100720058 CDS/splice-site	chr3:100629598 CDS/splice-site	low	high
	EH9C	TFG	ADGRG7	chr3:100720058 CDS/splice-site	chr3:100629598 CDS/splice-site	high	high
Pt=patient, *Pre-splicing transcript, §Confidence Level							

7. Fusion transcriptome profiling of multiple EHEs

Malignant EHEs were analyzed as a reference, to confirm the validity of the approach used in EH. Given the malignant nature of EHE, the presence of tumor multifocality or metachronous lesion development is by default considered symptomatic of metastatic dissemination. Indeed, the metastatic nature of liver metastasis from EHE has been previously molecular demonstrated ¹².

Table 7. EHE cases with multiple presentations.

Patient ID	Sample	Anatomic site	Diagnosis	M/S
EHE1	EHE1A	Thigh (ST)	Classic	M
	EHE1C	Lung		
EHE3	EHE3A	Iliac Wing (B)	Classic	S
	EHE3B	Lymph node		
EHE6	EHE6A	Thigh (ST)	Classic	M
	EHE6B	Thigh (ST)		
EHE7	EHE7A	L4 vertebra (B)	Classic	M
	EHE7B	Back (ST)		
EHE8	EHE8A	Thigh (ST)	Classic	S
	EHE8B	Thigh (ST)		
	EHE8C	Thigh (ST)		
ST=Soft tissue, B=Bone, M=Metachronous, S=Synchronous				

To corroborate the clonal relationship between multiple EHE lesions, 5 EHE cases (3 soft tissue and 2 bone EHE) were selected for having synchronous or metachronous EHEs (**Table 7**). A targeted RNA-sequencing was performed on one of the paired lesions and specifically on the one with better RNA quality. In the case of detection of fusion product, the same fusion was searched in the paired lesion by RT-PCR followed by Sanger sequencing.

The results of these analyses are summarized in **Table 8**. In all cases, the targeted RNA-sequencing approach (Archer) identified a pathognomonic WWTR1::CAMTA1 gene fusion.

Table 8. Fusion transcriptome profiling in EHE cases.

		Targeted RNA- sequencing (Archer approach)	RT-PCR validation of the fusion detected in one of the paired lesions
Pt ID	Sample	Fusion	Fusion
EHE1	EHE1A	WWTR1::CAMTA1 chr3:149572864-chr1:7663755	WWTR1::CAMTA1 chr3:149572864-chr1:7663755
	EHE1C	ND	WWTR1::CAMTA1 chr3:149572864-chr1:7663755
EHE3	EHE3A	WWTR1::CAMTA1 chr3:149572864-chr1:7661726	WWTR1::CAMTA1 chr3:149572864-chr1:7661726
	EHE3B	ND	WWTR1::CAMTA1 chr3:149572864-chr1:7661726
EHE6	EHE6A	WWTR1::CAMTA1 chr3:149572864-chr1:7661726	WWTR1::CAMTA1 chr3:149572864-chr1:7661726
	EHE6B	ND	WWTR1::CAMTA1 chr3:149572864-chr1:7661726
EHE7	EHE7A	ND	WWTR1::CAMTA1 chr3:149573000-chr1:7663928
	EHE7B	WWTR1::CAMTA1 chr3:149573000-chr1:7663928	WWTR1::CAMTA1 chr3:149573000-chr1:7663928
EHE8	EHE8A	WWTR1::CAMTA1 chr3:149572864-chr1:7661726	WWTR1::CAMTA1 chr3:149572864-chr1:7661726
	EHE8B	WWTR1::CAMTA1 chr3:149572864-chr1:7661726	WWTR1::CAMTA1 chr3:149572864-chr1:7661726
	EHE8C	WWTR1::CAMTA1 chr3:149572864-chr1:7661726	WWTR1::CAMTA1 chr3:149572864-chr1:7661726

Pt= Patient, ND=Not Done

RT-PCR/Sanger sequencing analyses confirmed the expression of the specific fusion in the paired lesion of the same patient. In cases EHE 3, 6, and 8 type A fusion (exon 3 WWTR1, exon 8 CAMTA1) was detected in both lesions; EHE1 and EHE7 carried a type B fusion (exon 3 WWTR1, exon 9 CAMTA1) and a type C fusion (exon 2 WWTR1, exon 9 CAMTA1), respectively.

Thus, all separate EHE tumors derived from a same patient expressed the same fusion transcript, confirming a common clonal origin (**Figure 14**). In one case (EHE7) the WWTR1::CAMTA1 fusion breakpoint was also validated at the genomic DNA level (**Figure 14D**). Also, whole transcriptome profiling confirmed the presence of WWTR1::CAMTA1 fusions detected by the targeted RNA-sequencing approach.

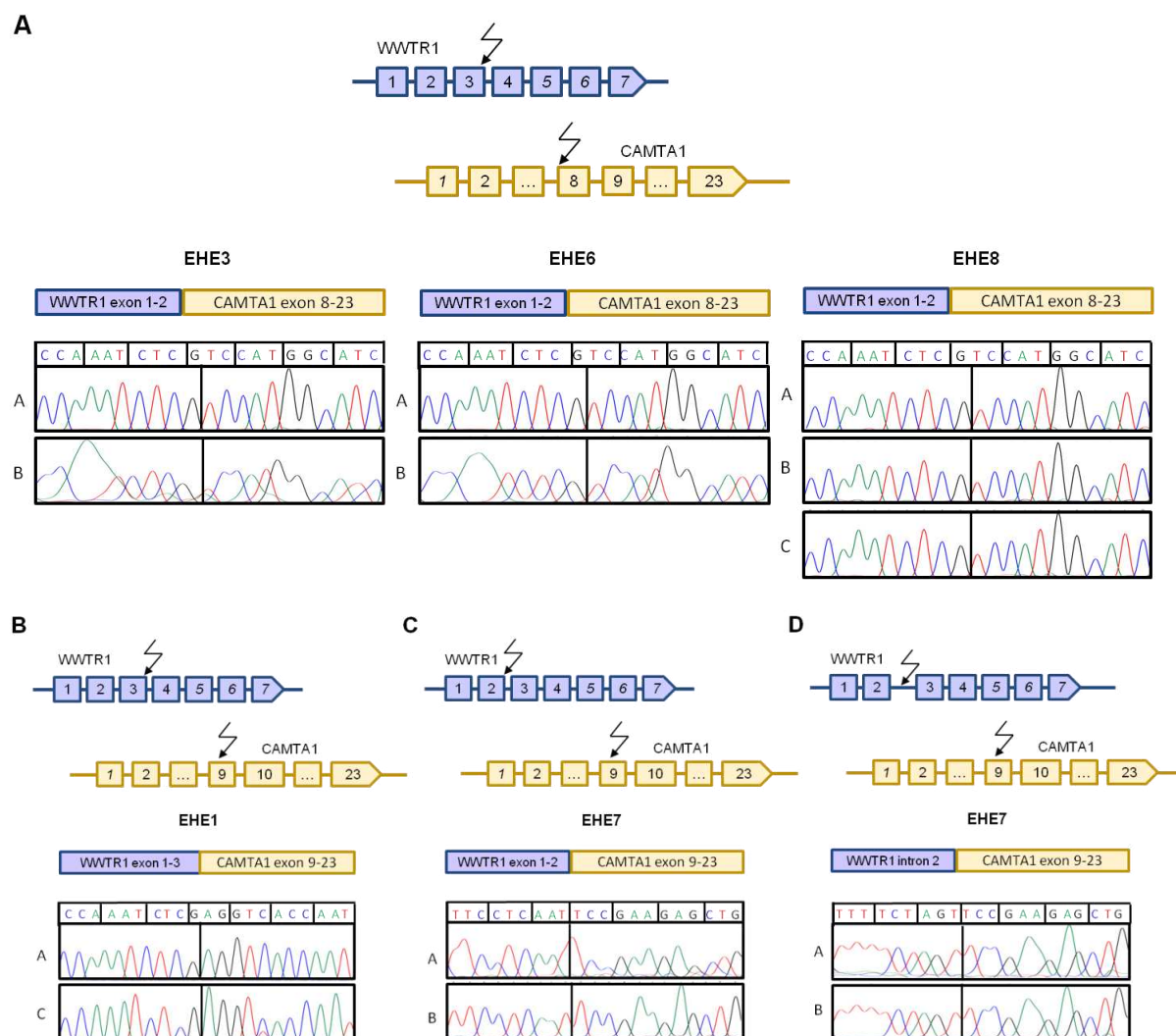


Figure 14. Fusion analysis of multifocal EHEs (A) Schematic representation of type A (exon 3 WWTR1, exon 8 CAMTA1) breakpoint, shared by EHE3, 6 and 8. In all the cases multiple EHE lesions of a same patient shared an identical breakpoint sequence. (B) Schematic representation of type B (exon 3 WWTR1, exon 9 CAMTA1) breakpoint found in EHE1, with identical breakpoint in lesion A (thigh) and C (lung). (C) Schematic representation of type C (exon 2 WWTR1, exon 9 CAMTA1) breakpoint found in EHE7, with identical breakpoint in lesion A (L4 vertebra) and B (back soft tissue). (D) Schematic representation and chromatogram of a WWTR1 intron 2 and CAMTA1 exon 9 fusion at the genomic DNA level.

8. Whole transcriptome profiling of EHE vs. EH

To identify molecular pathways that may support the aggressive behavior of EHE, the transcriptional profile of EHE was compared to that of EH (Table 9). This analysis was conducted on 6 single EHs and 4 single EHEs included in the clonality study. Three additional EHE (EHE4, 10 and 11), all scoring negative for CAMTA1 or TFE3 fusion analysis, were also included. All samples had tumor cellularity above 70%, thus were highly representative of the tumor transcriptome.

Table 9. EHE single lesions and EH single lesions employed in whole-transcriptome analysis.

EHE	Patient ID	Sample	Anatomic site	Diagnosis	Molecular data
	EHE1	EHE1A	Thigh (ST)	Classic	WWTR1::CAMTA1
	EHE3	EHE3A	Iliac Wing (B)	Classic	WWTR1::CAMTA1
	EHE4	EHE4A	Leg (ST)	Classic	No fusion detected
	EHE6	EHE6A	Thigh (ST)	Classic	WWTR1::CAMTA1
	EHE8	EHE8A	Thigh (ST)	Classic	WWTR1::CAMTA1
	EHE10	EHE10	Clavicle (B)	Classic	No fusion detected
	EHE11	EHE11	T12 vertebra (B)	Classic	No fusion detected
EH	Patient ID	Sample	Anatomic site	Diagnosis	Molecular data
	EH3	EH3A	Distal tibia (B)	Classic	No fusion detected
	EH4	EH4A	Tibia (B)	Classic	FOS::ENSG00000255202
	EH5	EH5A	Distal tibia	Classic	FOS::chr21
	EH6	EH6A	Calcaneus (B)	Classic	No fusion detected
	EH7	EH7B	II metatarsus (B)	Classic	FOS::chr10
	EH9	EH9A	Left tibia (B)	Atypical/cellular	WWTR1::FOSB

ST=Soft tissue, B=Bone

Unsupervised Hierarchical Clustering and PCA indicated a net separation between the two tumor types (**Figure 15**).

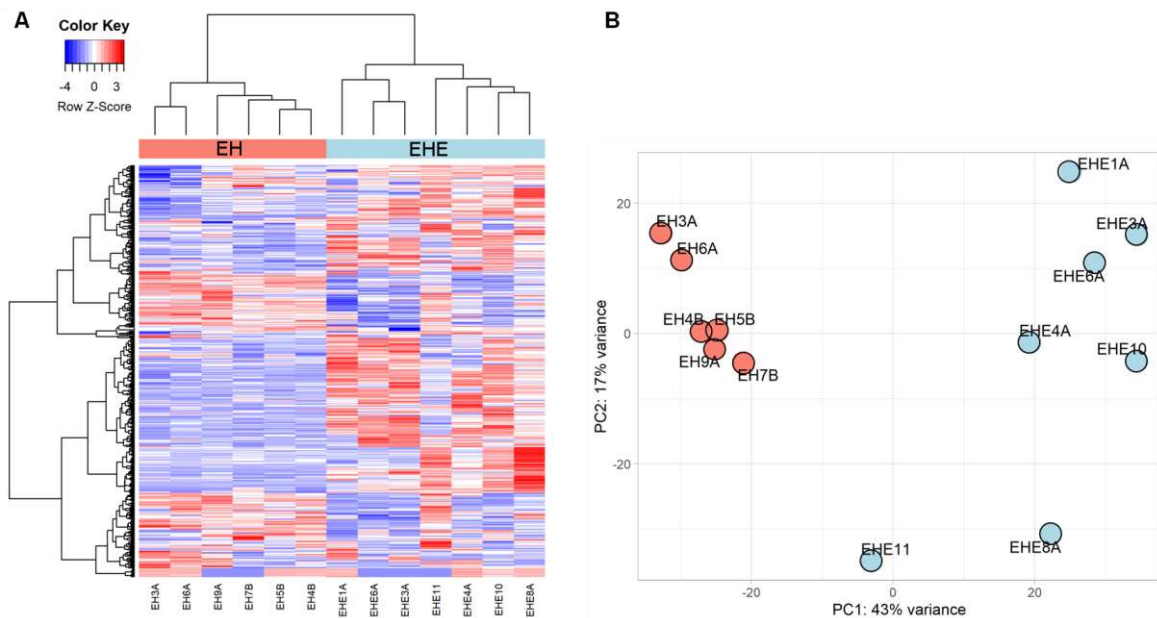


Figure 15. Unsupervised hierarchical clustering (**A**) and Principal Component Analysis (**B**), show co-clustering of EHs (salmon) and EHEs (light blue).

The separation between EH and EHE was maintained also when their transcriptome was analyzed in the context of a larger and diversified tumor series by t-SNE dimensionality reduction analysis that allow to better emphasize similarity between samples (**Figure 16**).

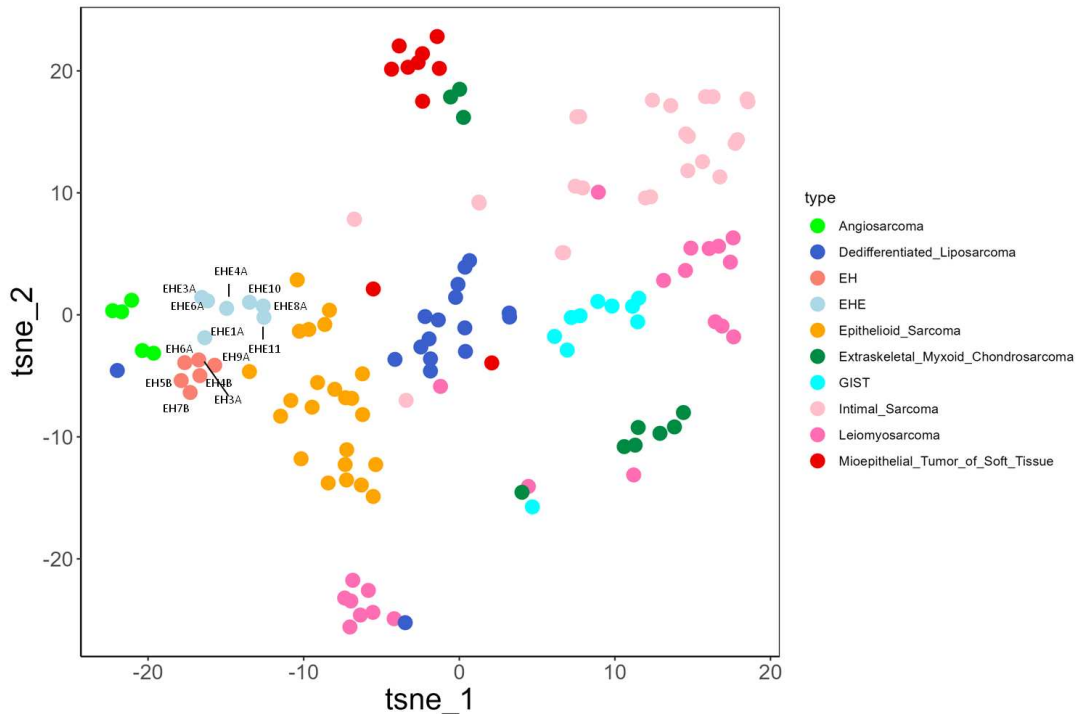


Figure 16. t-SNE was performed on different sarcoma types available in our laboratory. EH and EHE samples analyzed in my cohort are labeled with the sample ID (EH cluster is colored in salmon and EHE in light blue).

We then performed Differential Expression (DE) analysis and compared EHE vs. EH. Over 1000 genes were differentially expressed, 1149 up-regulated and 544 down-regulated (filtered by $\log_2\text{FoldChange} \geq |1|$ and p-value adjusted ≤ 0.05).

Functional annotation of DE genes was performed by a pre-ranked gene set enrichment analysis (GSEA) on MSigDB Gene Ontology Biological Processes (GOBP), Hallmarks and Oncogenic Signatures (**Figures 17-19**). Surprisingly, the top enriched signatures in EHE were muscle-related processes (**Figure 17**) and several muscle-related molecules such as ACTA1, MYOG and MYOD1, were indeed upregulated in a fraction of EHE. A consultation with the pathologist revealed that EHE do not express skeletal muscle markers but that muscular invasion is a very common feature of EHE. Our samples were selected for having a tumor cell fraction always greater than 70%. Thus, the fact that a limited presence of non-tumoral cells determines such an impact on the differential expression analysis of EHE vs. EH suggests that the transcriptome of EHE and EH tumor cells is quite similar.

In addition to the preponderant representation of muscle-related pathways, GSEA of differentially expressed genes indicated that EHEs featured also overactivation of mTORC, MEK and hypoxia (**Figure 17**). The implication of MEK and mTORC pathways in EHE has been previously reported and these molecules are currently exploited in clinics for therapeutic purposes^{82,83}.

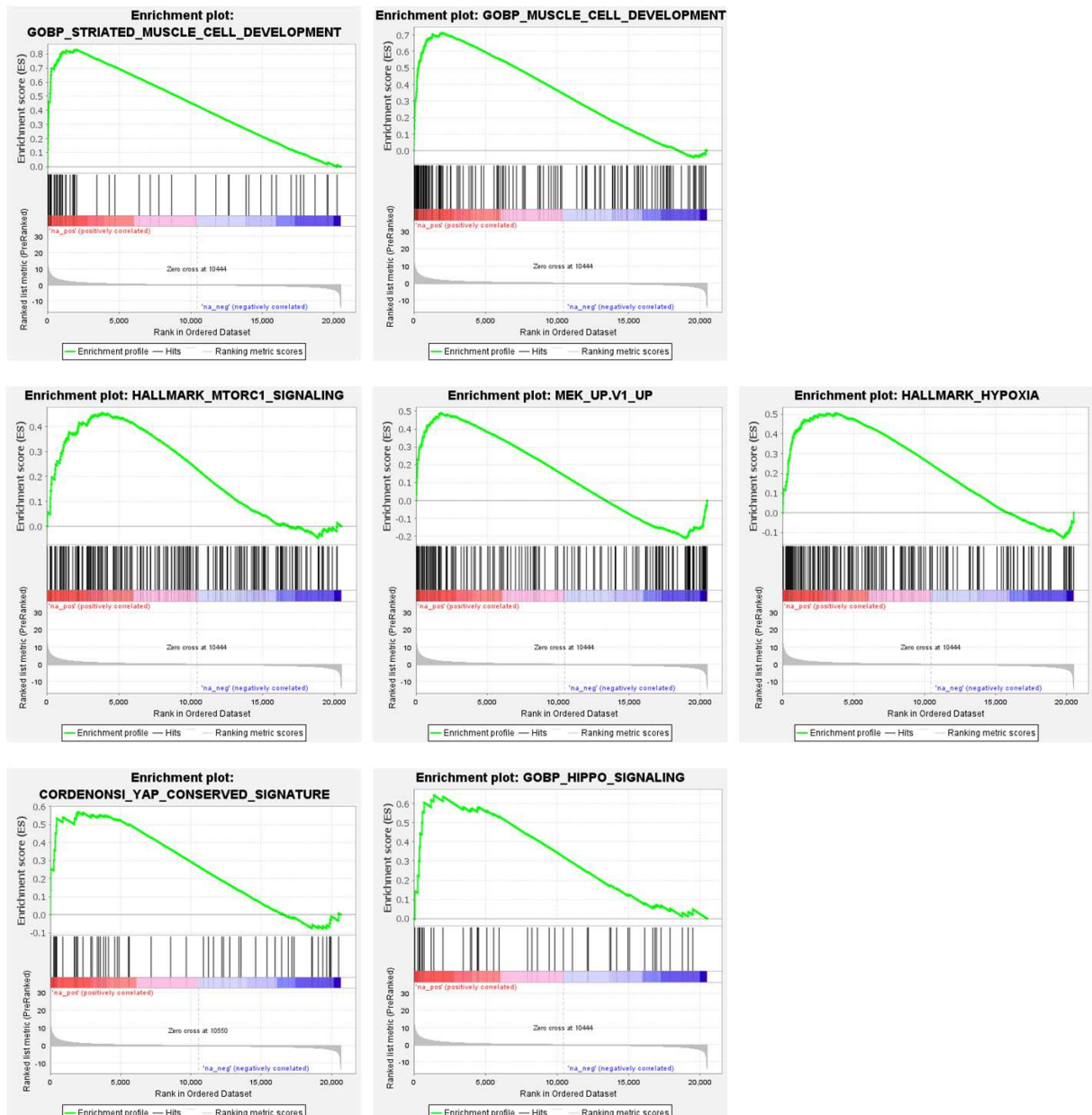


Figure 17. GSEA of the GOBP, hallmarks and oncogenic signatures enriched in EHE selected by $FDR \leq 0.25$ and $p\text{-value} \leq 0.05$.

EHE featured also enrichment of signatures related to YAP/TAZ (**Figure 17**).

The activation of YAP/TAZ is in keeping with the presence of the pathognomic fusions involving these genes in the majority of EHEs. A focused single sample GSEA (ssGSEA) analysis highlighted an overrepresentation of the Hippo signature (**Figure 18**) even in two samples scoring negative in fusion analysis (EHE4 and EHE10), thus supporting the relevance of the activation this pathway in the pathogenesis of EHE.

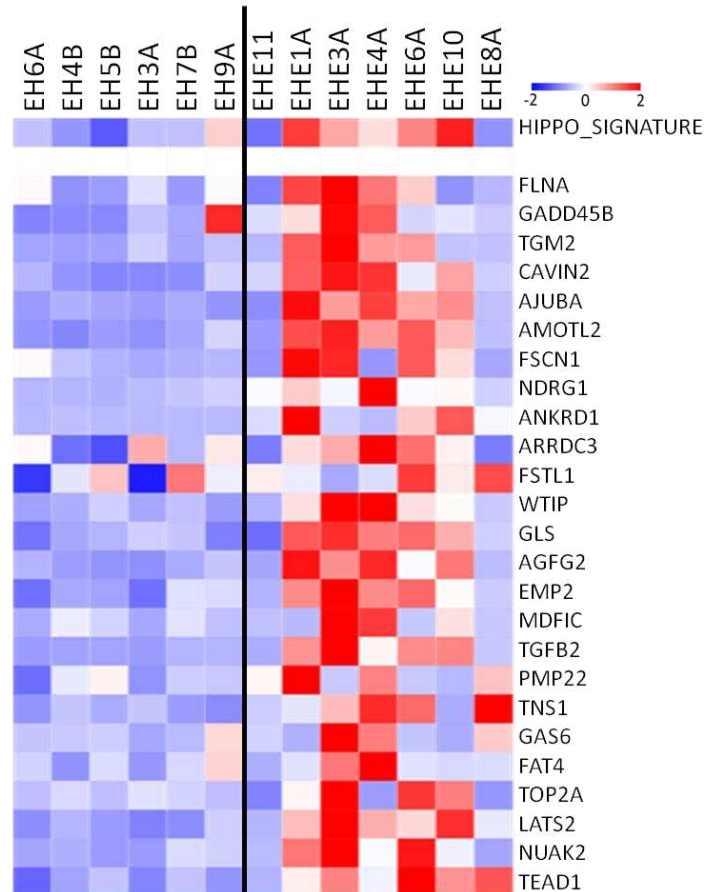


Figure 18. ssGSEA showing the expression of a Hippo signature and the top25 genes expressed in each sample.

Among the genes included in the signature overexpressed in EHE, it is worth mentioning transglutaminase 2 (TGM2)¹³², an enzyme that stabilizes the cross linking of the extracellular matrix, thus promoting matrix stiffness that induces the Hippo pathway. Moreover, TGM2 has been shown to bind and inhibit p53¹³³ and p53 and YAP are known to crosstalk¹³⁴. Thus, TGM2 might contribute to the EHE tumorigenic phenotype through converging pathways.

A scrutiny of the list of the genes differentially expressed genes between EHE and EH highlighted also upregulation of the secreted frizzled-related protein 2 (SFRP2), which is known to be overexpressed also in angiosarcomas¹³⁵. Also, multimerin-2 (MMNR2) was

downregulated in EHE, and loss of MMNR2, an extracellular matrix glycoprotein that regulates VEGFA/VEGFR2 signaling axis, induces reduced vessels perfusion and vascular leakage, which correlates with tumor hypoxia, a known trigger of metastatization ¹³⁶.

The output of GSEA analysis suggested also that EH features characteristics of a regulated vessel formation. In fact, EH showed enrichment in signaling pathways related to angiogenesis (e.g. VEGF-A) (**Figure 19**). Moreover, a greater immunogenicity, compared to EHE, was suggested by the overrepresentation of pathways related to antigen processing and presentation and allograft rejection (**Figure 19**).

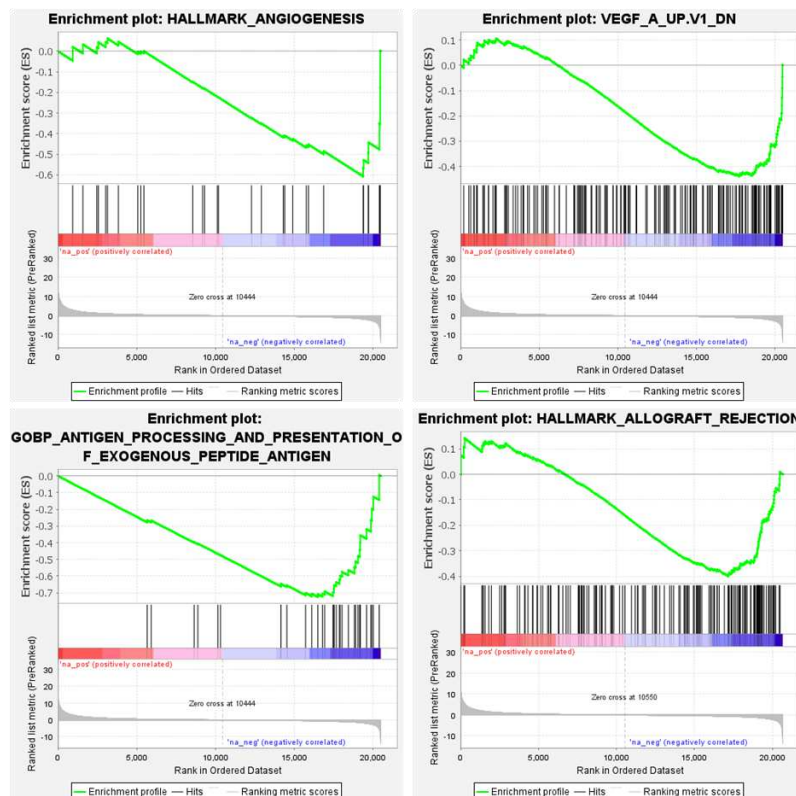


Figure 19. GSEA of the GOBP, hallmarks and oncogenic signatures enriched in EH selected by $FDR \leq 0.25$ and $p\text{-value} \leq 0.05$.

Indeed, EH overexpressed both pro- and anti-angiogenic factors (**Figure 20**).

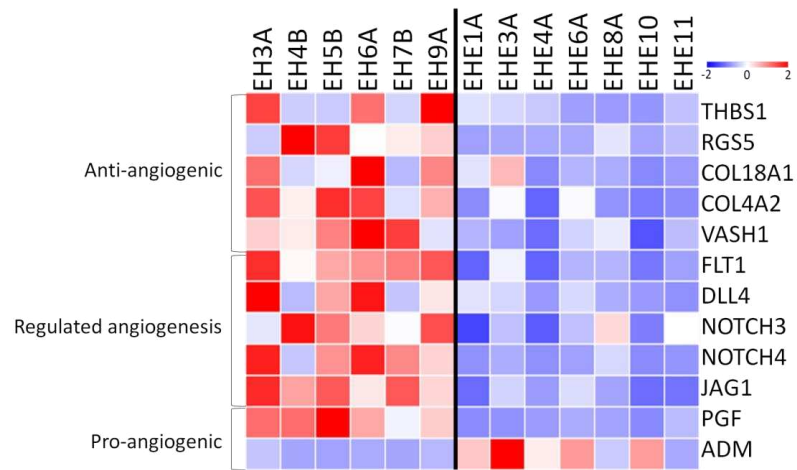


Figure 20. Heatmap showing the expression levels of anti- angiogenic factors (top), genes involved in regulated angiogenesis (middle) and pro-angiogenic factors (bottom).

DISCUSSION

EHE and EH are vascular tumors with the common feature of multifocal presentation, but of different histological and clinical characteristics. EHE is a malignant tumor, with 20% of mortality rate and a high propensity to distal metastasis¹². Clinically, EHE can be indolent for several years and suddenly become aggressive and the molecular mechanisms or biomarkers associated with the clinical course of the disease have not been identified yet⁸⁵. Conversely, the nature of multifocal presentation in EH is a matter of debate^{56,58}. In fact, the WHO classifies EH of soft tissue and EH of bone in different ways. The former are classified as benign tumors, the latter as intermediate, locally aggressive tumors¹. Indeed, in the absence of objective criteria, the classification of EH of bone remains controversial^{1,59}. Some authors consider EH of bone as benign as a EH of soft tissue due to the relatively benign looking appearance of EH cells; others argue that EH has traits of aggressiveness because frequently shows local destructive growth with demolition of cortex and extension to soft tissues. Moreover it often shows multifocal presentation^{1,18,19,21,58}.

To resolve this ambiguity, the clinical and biological characteristics of 42 patients with EH of bone were studied. The study, which is based on a retrospective cohort because of the rarity of EH, represents one of the largest case series analyzed so far. The study of the clinical history of the patients with EH of bone showed that prognosis was excellent. No patient died of the disease and most patients were cured with relatively non-aggressive treatments (curettage or resection). Only 5 patients experienced local recurrence (13%), all of them treated with curettage. Almost half of the patients presented at the diagnosis with multifocal disease (17/42 patients, 40%), and the multiple EH lesions could involve the same, contiguous but also non-contiguous bones. Yet, irrespectively of this multifocality, surgical treatment was curative. The nature of this multiple lesions was then analyzed molecularly. We used the fusion breakpoint as a clonality marker and demonstrated that separated lesions affecting the same patient expressed the same fusion transcripts with identical gene breakpoints. These results are in keeping with a previous work²⁴ in which it was concluded that EH foci affecting adjacent bones represent multifocal regional spread. Our work extends this observation also to EHs involving non-contiguous bones and supports the concept that multifocal presentations in this tumor represent the spread of a same neoplastic clone rather than simultaneous independent tumors. Thus, even if EH cells have a benign appearance and the clinical course is benign, the tumor shows a high propensity to metastasis. These concepts are only apparently contradictory. It is estimated that a tumor sheds millions of cells every day, but only a tiny fraction of these cells will eventually create secondary colonies¹²². Metastasis relies on tumor cells bypassing a series of obstacles: they must detach from the primary site,

survive in the lymphatic/circulatory system and colonize secondary sites ^{123,137}. Vascular tumors appear to be facilitated in some of these steps. Indeed, the multifocal presentation is a distinctive feature of vascular tumors of bone, including classical hemangioma, hemangioendothelioma and angiosarcoma. Although some cases present lymph node invasion and distal metastasis ^{26,56,62}, EH shows regional reseeding, suggesting that the capacity of EH cells to survive in the lymphatic/blood stream is limited, and that their congenial soil is the organ of origin. In multifocal EH, the separate tumor lesions maintain their intrinsic “benign” nature, as the presence of secondary seeding does not associate with poor outcome. Thus, EH dissemination does not appear to be associated with aggressive biological traits having rather features of a passive phenomenon. Indeed, it has been previously reported that tumors may shed passively into the blood or lymphatic vessels in the absence of active cell migration ¹²³.

In conclusion, the excellent prognosis of EH of bone supports the notion that it is a clinically benign tumor. Like other vascular tumors, EH of bone may present in a multifocal way. Although tumor multifocality in EH of bone is the manifestation of a disseminative process, as established by clonality analysis, this has no major impact on the clinical course of the disease, even for patients treated exclusively by surgery or biopsy. Therefore, EH of bone is a tumor with disseminative potential but of benign clinical nature.

The development of distal metastasis not associated with poor outcome is also a characteristic of the giant cell tumor ¹³⁸ which, despite its "metastatic" potential, is not ranked among sarcomas by the current WHO. This fact somehow reinforces the concept of the “benign metastases” or “benign dissemination”.

This study highlighted also a fact of paramount importance in the diagnostic setting. We demonstrate that the Archer approach (kit and relative bioinformatic suite), an approach widely utilized in diagnostic laboratories for the diagnosis of fusion-driven tumors, shows important limitation when dealing with tumors hallmarked by truncating fusions without recurrent fusion partners. As in the case of CSF1 fusions found in tenosynovial giant cell tumor ¹³⁰ or in the HMGA2 fusions detected in Dedifferentiated Liposarcoma ¹³¹, the use of the Archer bioinformatic suite associated to the kit may easily yield false negative results. Thus, using this kit for the diagnosis of tumors that may produce truncating fusions, a manually curated bioinformatic approach should be considered.

From a genetic standpoint, the fusions detected in our EH series (3 FOS and 1 FOSB fusion) are in line with literature data which indicate that about 70% of the cases bear FOS fusions and the remaining fraction carry FOSB fusions ^{24,26–28,30}. In detail, the WWTR1::FOSB fusion

detected in one case had been previously reported in EH (3 cases)^{26,28,30} but also in PHE (2 cases)^{38,39}. About the FOS fusions, the fusion involving a genomic sequence proximal to the VIM gene (FOS::VIM, labelled FOS::chr10 in our work in the light that the coding sequence of VIM was not directly involved in the fusion) had been previously described^{24,26,27}. Conversely, the other two FOS fusions identified in our study (FOS::ENSG00000255202 and FOS::chr21) are novel. Thus, our study extends the knowledge about FOS fusion partners in EH.

In this work we used EHE as a reference metastatic tumor for validating the use of the fusion breakpoint as a clonality marker and compared the transcriptome profiling of this malignant vascular tumor to that of EH with the intend to identify signaling pathway sustaining the aggressive clinical behavior of the former.

According to the literature the WWTR1::CAMTA1 fusion hallmarks about 90% of EHE while the remaining cases are either fusion-negative or carry YAP1::TFE3 fusions^{1,23,40,41,49}. Differential gene expression analysis, besides supporting a drift from a “controlled” angiogenic process in EHE vs. EH, highlighted in EHE the role of the Hippo, YAP/TAZ mediated pathway in EHE aggressiveness. In our series the canonical TAZ fusion, namely the WWTR1::CAMTA1 fusion, was detectable only in 5/8 cases (63%), despite a high RNA sequencing coverage. Noteworthy, the expression levels of WWTR1 mRNA was comparable in translocated and non-translocated cases and the Hippo signaling was found to be deregulated also in the subset of EHE devoid of YAP/TAZ fusions. Thus, besides chromosome translocations, it is possible that other mechanisms sustain YAP/TAZ signaling activation in these tumors. For instance, hypoxia is known to induce YAP/TAZ¹³⁹ and the hypoxia signaling was enriched in EHE. Thus, it is tempting to speculate that the lousy organization of the vessels in EHE may favor hypoxic conditions that sustain the pro-metastatic YAP/TAZ signaling. Intriguingly, we found that EHE overexpress TGM2. TGM2 is a YAP/TAZ transcriptional target that has been shown to directly bind and inhibit p53¹³³. Most EHEs retain the TP53 gene in a wild type status and secondary alterations, besides the fusion, are rare and not recurrent⁹⁵. Thus, overexpression of TGM2 might contribute to attenuate the p53 response in this tumor thus favoring malignant progression.

Differential gene expression analysis highlighted also a high expression of SFRP2, a molecule that stimulates angiogenesis via a Calcineurin/NFAT Signaling¹³⁵. Since it is highly expressed also in angiosarcoma, recently a novel humanized monoclonal antibody to this protein was proposed as an innovative therapeutic strategy¹⁴⁰. Provided that the *in vivo*

results are promising, it will be interesting to determine the eligibility to anti-SFRP2 treatments also for EHE.

CONCLUSIONS AND FUTURE PERSPECTIVES

Fusion transcriptome profiling revealed a common clonal origin of the multiple lesions in patients affected by EH. The discovery that a histological and clinically benign tumor metastasizes was unexpected. This result suggests that EH dissemination is probably due to a phenomenon of passive spreading. Investigations by using *in vivo* EH models are needed to corroborate this hypothesis.

Intriguingly, in one EH case (EH9) besides the WWTR1::FOSB fusion, a fusion already described in literature, transcriptome profiling highlighted the presence of an additional fusion event of FOSB with WWTR1, only apparently reciprocal of the driver fusion (WWTR1::FOSB). The analysis of the protein domain retained by the FOSB::WWTR1 fusion suggests the generation of an oncogenic fusion protein. We are planning to validate the pathogenicity of the FOSB::WWTR1 fusion and its contribution to the malignant phenotype of WWTR1::FOSB engineered HUVEC cells.

MATERIALS AND METHODS

9. Tumor samples analyzed

Formalin-Fixed Paraffin-Embedded (FFPE) blocks or Fresh Frozen samples from 13 EH and 14 EHE, were retrieved from the pathology files of the Rizzoli Orthopedic Institute in Bologna. Only specimens with a tumor cell fraction greater than 70% were analyzed.

10. RNA and DNA extraction

Nucleic acids were extracted using the AllPrep DNA/RNA mini kit columns (Qiagen, Germantown, MD, USA) for frozen samples and either the QIAamp DNA FFPE Tissue Kit (QIAGEN) or the FFPE RNA/DNA purification plus kit (Norgen Biotek Corporation, Ontario, Canada) for FFPE specimens, according to the manufacturer's instructions. Frozen EHE of bone were extracted according to Carter et al. protocol¹⁴¹. RNA and DNA were quantified with a fluorometer using the Qubit RNA HS Assay Kit or DNA BR Assay Kit (ThermoFisher Scientific). RNA and DNA qualities were evaluated by electrophoresis using the RNA and gDNA Assay Kit (Agilent Technologies) on the Agilent 2200 TapeStation instrument.

11. Targeted RNA-sequencing and fusion calling

Libraries were generated starting from 100-250 ng of total RNA. A customised Archer FusionPlex sarcoma RNA-sequencing panel v1.1 (ArcherDX, Boulder, CO, USA) was employed for library generation, covering 26 genes involved in sarcoma-associated fusions and supplemented with spike-ins primers for FOS (exon 4, forward primer) and FOSB (exons 1 and 2, reverse primers). Libraries were run on an Illumina MiSeq sequencing platform and were analyzed with the Archer Analysis suite software version 7.1.0. Raw data were also analyzed with the Arriba fusion caller^{142,143}.

12. Retro-transcription (RT)-PCR and Sanger sequencing

RT-Polymerase Chain Reaction (RT-PCR) and RT-PCR/Sanger sequencing were employed for orthogonal validations.

Total RNA (from 50ng to 500 ng) was reverse-transcribed into cDNA using the Superscript III reverse transcriptase protocol (Invitrogen) following the manufacturer's instructions.

PCR was carried out using the GoTaq Green Master Mix Kit (Promega), using the primers listed in **Table 10**.

Table 10. Primer list.

Case	Fusion	Forward (5'→3')	Reverse (5'→3')
EH5	FOS::chr21	GCTTCCCTTGATCTGACTGGG FOS exon 4	GGACCATTCAAAACATAGCCCT Intergenic chr21
	PSME3IP1::WVOX	GTGAGGTCTGCTCGCCTCC PSME3IP1 5'UTR	ATGCGTGACACTGCTTCACT WVOX exon 5
EH4	FOS::ENSG00000255202	TGATGACTTCCTGTTCCCAGC FOS exon 4	AGCCATCTCCAGAAGACTTGG ENSG00000255202
EH7	FOS::chr10	TGAAGACCGAGCCCTTTGA FOS exon 4	ATCTTCCGCTAGCAAGATGC Intergenic chr10
EH9	WWTR1::FOSB	AGGATTCTGAATGCGCCAAGA WWTR1 exon 4	AAGAGATGAGGGTGGGTTGC FOSB exon 2
	WWTR1::FOSB	GTCTCTGACAAAGTGTTTTGA GAGG WWTR1 intron 4	CCGACCAATCAGAGTCCTGG FOSB intron 2
	FOSB::WWTR1	CAAACCGGGCTGCAAGATCC FOSB exon 4	CCTGAACTGGGGCAAGAGTC WWTR1 exon 5
	FOSB::WWTR1	CTTCCGATCCCCTGAACTCG FOSB 3'UTR	ACCAGGCAACCATTAGTATCTT WWTR1 intron 4
	TFG::ADGRG7	TTCCTTTGCAATTCAGTGCAG TA TFG exon 3	CCATTTTCCCAGGTTCCACC ADGRG7 exon2
EHE1	WWTR1::CAMTA1	AAGACCCTAGGAAGGCGATG WWTR1 exon 3	CGTCCTGGGAAAGGCGAAC CAMTA1 exon 9
	WWTR1::CAMTA1	GTCAGTTCCACACCAGTGCCT WWTR1 exon 3	CATGGTGTACACGGCCTCATT CAMTA1 exon 9
EHE3,6,8	WWTR1::CAMTA1	AAGACCCTAGGAAGGCGATG WWTR1 exon 3	GCTGTTCCACCGAGAAGCCT CAMTA1 exon 8
	WWTR1::CAMTA1	GTCAGTTCCACACCAGTGCCT WWTR1 exon 3	ATTGCTGCAGGTCCACTTGAT CAMTA1 exon 8
EHE7	WWTR1::CAMTA1	GTCCTACGACGTGACCGAC WWTR1 exon 2	CTGGCCCTGCTTTGGGTTAT CAMTA1 exon 9
	WWTR1::CAMTA1	GGCTGGGAGATGACCTTACAG WWTR1 exon 2	GGGGTCAAAGTTCATGGTGGT CAMTA1 exon 9
	WWTR1::CAMTA1	TCTCAGTCCCGCCTCATACA WWTR1 intron 2	TTCTGGAATCTTCCGGCCAC CAMTA1 exon 9

PCR reactions were carried out by using an initial denaturing step (95°C for 2 min) followed by 40 cycles of amplification including denaturation (95°C for 30 sec), 30 sec annealing (from 56°C to 59°C depending on the primer pair) and extension (72°C for 30sec). Final extension was performed for 4 min at 72°C.

DNA Wizard® SV Gel-PCR Clean-Up System (Promega) was used for the DNA extraction of PCR products from agarose gel. Sanger sequencing was carried out with the BigDye™ Terminator v3.1 Cycle Sequencing Kit and the same primers used for PCR generation. Sequences were run on an Applied Biosystems® 3130xl Genetic Analyzer.

13. Whole transcriptome RNA-sequencing and data processing

An amount ranging from 50 to 250 nanograms of total RNA was used for the generation of RNA-sequencing libraries using the Illumina Stranded Total Ribo-Zero Plus

RNA library prep kit (Illumina, San Diego, CA, USA), according to the manufacturer's protocol. Briefly, RNA was first depleted from ribosomal RNA (rRNA) by using enzymatic rRNA depletion; then it was converted into double-stranded cDNA. cDNA fragments were then adenylated at the 3' end. After ligation of adapters, libraries were amplified by PCR with concomitant incorporation of indexes.

Libraries were quantified by a fluorometric assay (Qubit dsDNA High Sensitivity Assay Kit, ThermoFisher Scientific) and evaluated for size and purity by TapeStation electrophoresis (D1000 Assay Kit, Agilent Technologies). Finally, libraries were diluted, pooled to a 2 nM total concentration and loaded to an Illumina HiSeq 1000 or Nextseq 550 platforms using the HiSeq Rapid PE Cluster v2 Kit or the Nextseq 500/550 high output kit v2.5 (Illumina, San Diego, CA, USA) to reach a sequencing depth ≥ 40 million paired-end reads per sample. Once sequencing was completed, data (in the form of bcl files) were converted into FASTQ files using the bcl2fastq software (Illumina). FastQC (v0.11.9), MultiQC (v1.0), and Trimmomatic (v0.39) software were used for FASTQ sequence quality measurements and trimming.

The reads obtained were then aligned to the human reference genome assembly hg38 (GRCh38.p13) using STAR (v2.7.10a)¹⁴⁴. The RSEM tool (v1.3.1)¹⁴⁵ was used for reads quantification and GENCODE v.27¹⁴⁶ was employed for gene annotation.

Since some rRNA genes were not efficiently depleted by the probes for ribosomal depletion included in the kit, genes corresponding to this gene type ("Mt_rRNA", "Mt_tRNA", "rRNA", "rRNA_pseudogene") as well as genes showing sequence identity with ribosomal RNA ("ENSG00000283907.1", "ENSG00000280800.1", "ENSG00000281383.1", "ENSG00000280614.1", "ENSG00000281181.1", "ENSG00000284419.1") were computationally removed from the expression matrix.

Arriba (v2.3.0)¹⁴³ and FusionCatcher¹⁴⁷ fusion calling tools were used for fusion transcript identification.

Raw expression data (read counts from RSEM) were loaded in R (v4.2.2) and converted into normalized read counts using the Variance Stabilizing Transformation (VST) function in DESeq2 package (v1.26)¹⁴⁸ as input for Principal Component Analysis (PCA), unsupervised hierarchical clustering analysis (UHCA) and t-Distributed Stochastic Neighbor Embedding (t-SNE).

PCA is a an algorithm used to reduce the dimensionality of the data, while preserving the variation among the samples¹⁴⁹. PCA analysis was performed using the prcomp function built

in DESeq2, while UHCA was performed using the “Euclidean method” to calculate the distances and the “complete linkage method” to calculate the hierarchical cluster. t-SNE is a technique used to reduce the dimensionality of the data, well suited to emphasize the similarities in high-dimensional datasets¹⁵⁰. t-SNE analysis was performed using the Rtsne package. For all the graphical representation ggplot2, ggrepel, gplots, RColorBrewer packages were employed.

PCA and UHCA were performed on the top 5000 variant genes (EH multiple lesions comparison) or top 500 variant genes (EHE vs. EH primary lesions) with highest variance. t-SNE used to visualize EH and EHE in a larger tumor series, was performed on the top1000 variant genes (perplexity 3 to 40; perplexity 8 is shown in figure 16).

Differential expression analysis was performed using the DESeq2 R package. Genes expressed at a very low level were excluded from the analysis and filtered using the filterByexpress function of the EdgeR package (filterByexpress>10). Genes were considered differentially expressed (DE) if the absolute value of the log2 Fold Change (log2FC) was ≥ 1 and the adjusted p-value was ≤ 0.05 ($|\log_2(\text{FC})| \geq 1$ and $\text{padj} \leq 0.05$).

Read counts from RSEM were converted Transcripts per million (TPM). TPM calculation is based on sequencing depth and gene length and it is useful to compare gene expression within a sample and among samples^{145,151,152}. Protein coding TPM (pTPM) were employed as input for heatmaps generation. Heatmap plots were generated by using the Morpheus web app (<https://software.broadinstitute.org/morpheus>), in which input pTPM data were Z-score normalized.

14. Functional data annotation

Functional annotation of RNA-sequencing data was done using a pre-ranked Gene Set Enrichment Analysis (GSEA) and Overrepresentation Analysis (ORA).

Pre-ranked GSEA uses the list of DE genes and define whether a reference, pre-defined geneset, shows statistically significance and concordant differences between two conditions. To rank our list of DE genes (EHE vs. EH), according to the statistical significance and fold change, we used the formula $[-\log_{10}(\text{p-value}) * (\text{sign of } \log_2(\text{Fold-Change}))]$ as in Plaisier et al.¹⁵³.

Pre-ranked GSEA was performed using the GSEA desktop app (version 4.3.2) using the following parameters: number of permutations = 1000; enrichment statistic = weighted;

minimum size = 3; maximum size = 2000; collapse/remap to gene symbols = no collapse¹⁵⁴. We interrogated the following reference datasets: MSigDB Hallmark gene sets (Hallmarks=h.all.v2022.1.Hs.symbols.gmt) (<https://www.gsea-msigdb.org/gsea/msigdb/human/genesets.jsp?collection=H>) Gene Ontology Biological Processes gene sets (GOBP=c5.go.bp.v2022.1.Hs.symbols.gmt) (<https://www.gsea-msigdb.org/gsea/msigdb/human/genesets.jsp?collection=GO:BP>) and Oncogenic Signatures gene set (Oncogenic signature= c6.all.v2022.1.Hs.symbols.gmt) (<https://www.gsea-msigdb.org/gsea/msigdb/human/genesets.jsp?collection=C6>).

We also performed single-sample GSEA (ssGSEA) on a HIPPO_SIGNATURE obtained combining CORDENONSI_YAP_CONSERVED_SIGNATURE and GOBP_HIPPO_SIGNATURE using GSVA (v1.46) and GSEABase (v1.60) libraries in R. ssGSEA is an extension of GSEA that calculates separate enrichment scores for each pairing of a sample and gene set. Each ssGSEA enrichment score represents the degree to which the genes in a particular gene set are coordinately up- or down-regulated within a sample. Input data used in these analyses were pTPM and heatmaps were generated with the Morpheus web app.

Functional annotation of DE genes was also performed by ORA, a statistical method that determines whether genes from pre-defined sets are over-represented in a subset of your data. To this end we used the “ShinyGo” online tool (<http://bioinformatics.sdstate.edu/go/>) against the gene ontology biological processes, hallmark, oncogenic signatures. Genes up and down-regulated were annotated separately.

REFERENCES

1. WHO Classification of Tumours Editorial Board. *Soft Tissue and Bone Tumours*. 5th ed.; 2020. <https://publications.iarc.fr/Book-And-Report-Series/Who-Classification-Of-Tumours/Soft-Tissue-And-Bone-Tumours-2020>
2. Helman LJ, Meltzer P. Mechanisms of sarcoma development. *Nat Rev Cancer*. 2003;3(9):685-694. doi:10.1038/nrc1168
3. Brenca M, Maestro R. Massive parallel sequencing in sarcoma pathobiology: state of the art and perspectives. *Expert Rev Anticancer Ther*. 2015;15(12):1473-1488. doi:10.1586/14737140.2015.1108192
4. Bunting SF, Nussenzweig A. End-joining, translocations and cancer. *Nat Rev Cancer*. 2013;13(7):443-454. doi:10.1038/nrc3537
5. Taniue K, Akimitsu N. Fusion Genes and RNAs in Cancer Development. *Non-Coding RNA*. 2021;7(1):10. doi:10.3390/ncrna7010010
6. Oh E, Jeong HM, Kwon MJ, et al. Unforeseen clonal evolution of tumor cell population in recurrent and metastatic dermatofibrosarcoma protuberans. Bandapalli OR, ed. *PLOS ONE*. 2017;12(10):e0185826. doi:10.1371/journal.pone.0185826
7. Bridge JA, Cushman-Vokoun AM. Molecular Diagnostics of Soft Tissue Tumors. *Arch Pathol Lab Med*. 2011;135(5):588-601. doi:10.5858/2010-0594-RAIR.1
8. Mitelman F, Johansson B, Mertens F. The impact of translocations and gene fusions on cancer causation. *Nat Rev Cancer*. 2007;7(4):233-245. doi:10.1038/nrc2091
9. Gounder MM, Agaram NP, Trabucco SE, et al. Clinical genomic profiling in the management of patients with soft tissue and bone sarcoma. *Nat Commun*. 2022;13(1):3406. doi:10.1038/s41467-022-30496-0
10. Melotti CZ, Amary MFC, Sotto MN, Diss T, Sanches JA. Polymerase Chain Reaction-Based Clonality Analysis of Cutaneous B-Cell Lymphoproliferative Processes. *Clinics*. 2010;65(1):53-60. doi:10.1590/S1807-59322010000100009
11. Antonescu CR, Elahi A, Healey JH, et al. Monoclonality of multifocal myxoid liposarcoma: confirmation by analysis of TLS-CHOP or EWS-CHOP rearrangements. *Clin Cancer Res Off J Am Assoc Cancer Res*. 2000;6(7):2788-2793.
12. Errani C, Sung YS, Zhang L, Healey JH, Antonescu CR. Monoclonality of multifocal epithelioid hemangioendothelioma of the liver by analysis of WWTR1-CAMTA1 breakpoints. *Cancer Genet*. 2012;205(1-2):12-17. doi:10.1016/j.cancergen.2011.10.008
13. Antonescu C. Malignant vascular tumors—an update. *Mod Pathol*. 2014;27:S30-S38. doi:10.1038/modpathol.2013.176
14. Ko JS, Billings SD. Diagnostically Challenging Epithelioid Vascular Tumors. *Surg Pathol Clin*. 2015;8(3):331-351. doi:10.1016/j.path.2015.05.001
15. Folpe AL, Chand EM, Goldblum JR, Weiss SW. Expression of Fli-1, a Nuclear Transcription Factor, Distinguishes Vascular Neoplasms From Potential Mimics: *Am J Surg Pathol*. 2001;25(8):1061-1066. doi:10.1097/00000478-200108000-00011

16. O'Connell JX, Nielsen GP, Rosenberg AE. Epithelioid Vascular Tumors of Bone: A Review and Proposal of a Classification Scheme: *Adv Anat Pathol*. 2001;8(2):74-82. doi:10.1097/00125480-200103000-00003
17. Ong SLM, Szuhai K, Bovée JVMG. Gene fusions in vascular tumors and their underlying molecular mechanisms. *Expert Rev Mol Diagn*. 2021;21(9):897-909. doi:10.1080/14737159.2021.1950533
18. Evans HL, Raymond AK, Ayala AG. Vascular tumors of bone: a study of 17 cases other than ordinary hemangioma, with an evaluation of the relationship of hemangioendothelioma of bone to epithelioid hemangioma, epithelioid hemangioendothelioma, and high-grade angiosarcoma. *Hum Pathol*. 2003;34(7):680-689. doi:10.1016/S0046-8177(03)00249-1
19. Errani C, Zhang L, Panicek DM, Healey JH, Antonescu CR. Epithelioid Hemangioma of Bone and Soft Tissue: A Reappraisal of a Controversial Entity. *Clin Orthop*. 2012;470(5):1498-1506. doi:10.1007/s11999-011-2070-0
20. O'Connell JX, Kattapuram SV, Mankin HJ, Bhan AK, Rosenberg AE. Epithelioid hemangioma of bone. A tumor often mistaken for low-grade angiosarcoma or malignant hemangioendothelioma. *Am J Surg Pathol*. 1993;17(6):610-617.
21. Wenger DE, Wold LE. Benign vascular lesions of bone: radiologic and pathologic features. *Skeletal Radiol*. 2000;29(2):63-74. doi:10.1007/s002560050012
22. Nielsen GP, Srivastava A, Kattapuram S, et al. Epithelioid Hemangioma of Bone Revisited: A Study of 50 Cases. *Am J Surg Pathol*. 2009;33(2):270-277. doi:10.1097/PAS.0b013e31817f6d51
23. Mendlick MR, Nelson M, Pickering D, et al. Translocation t(1;3)(p36.3;q25) Is a Nonrandom Aberration in Epithelioid Hemangioendothelioma: *Am J Surg Pathol*. 2001;25(5):684-687. doi:10.1097/00000478-200105000-00019
24. van IJzendoorn DGP, de Jong D, Romagosa C, et al. Fusion events lead to truncation of *FOS* in epithelioid hemangioma of bone: *FOS* REARRANGEMENT IN EPITHELIOID HEMANGIOMA. *Genes Chromosomes Cancer*. 2015;54(9):565-574. doi:10.1002/gcc.22269
25. Antonescu CR, Le Loarer F, Mosquera JM, et al. Novel *YAPI-TFE3* fusion defines a distinct subset of epithelioid hemangioendothelioma: Novel *YAPI-TFE3* Fusion Defining Distinct EHE. *Genes Chromosomes Cancer*. 2013;52(8):775-784. doi:10.1002/gcc.22073
26. Tsuda Y, Suurmeijer AJH, Sung Y, Zhang L, Healey JH, Antonescu CR. Epithelioid hemangioma of bone harboring *FOS* and *FOSB* gene rearrangements: A clinicopathologic and molecular study. *Genes Chromosomes Cancer*. 2021;60(1):17-25. doi:10.1002/gcc.22898
27. Huang SC, Zhang L, Sung YS, et al. Frequent *FOS* Gene Rearrangements in Epithelioid Hemangioma: A Molecular Study of 58 Cases With Morphologic Reappraisal. *Am J Surg Pathol*. 2015;39(10):1313-1321. doi:10.1097/PAS.0000000000000469

28. Antonescu CR, Chen HW, Zhang L, et al. *ZFP36-FOSB* fusion defines a subset of epithelioid hemangioma with atypical features: *ZFP36-FOSB* FUSION. *Genes Chromosomes Cancer*. 2014;53(11):951-959. doi:10.1002/gcc.22206
29. Righi A, Sbaraglia M, Gambarotti M, et al. Primary Vascular Tumors of Bone: A Monoinstitutional Morphologic and Molecular Analysis of 427 Cases With Emphasis on Epithelioid Variants. *Am J Surg Pathol*. 2020;44(9):1192-1203. doi:10.1097/PAS.0000000000001487
30. Yuen LC, Baker ML, Sin JM, Linos K, Kerr DA. A Rare Case of Primary Epithelioid Hemangioma of Bone with *WWTR1::FOSB* Fusion: A Benign Lesion with the Potential to Mimic Malignancy. *Int J Surg Pathol*. 2023;31(5):667-674. doi:10.1177/10668969221117438
31. Ooi LY, Goh JY, Kuick CH, Chang KTE, Mok Y. Intravascular epithelioid haemangioma of deep soft tissue with novel SETD1B-FOSB gene rearrangement. *Pathology (Phila)*. 2021;53(2):270-273. doi:10.1016/j.pathol.2020.06.020
32. Agaram NP, Zhang L, Cotzia P, Antonescu CR. Expanding the Spectrum of Genetic Alterations in Pseudomyogenic Hemangioendothelioma With Recurrent Novel ACTB-FOSB Gene Fusions. *Am J Surg Pathol*. 2018;42(12):1653-1661. doi:10.1097/PAS.0000000000001147
33. Antonescu CR, Huang SC, Sung YS, et al. Novel GATA6-FOXO1 fusions in a subset of epithelioid hemangioma. *Mod Pathol*. 2021;34(5):934-941. doi:10.1038/s41379-020-00723-4
34. Walther C, Tayebwa J, Lilljebjörn H, et al. A novel *SERPINE1-FOSB* fusion gene results in transcriptional up-regulation of *FOSB* in pseudomyogenic haemangioendothelioma: *SERPINE1-FOSB* fusion in pseudomyogenic haemangioendothelioma. *J Pathol*. 2014;232(5):534-540. doi:10.1002/path.4322
35. Trombetta D, Magnusson L, Von Steyern FV, Hornick JL, Fletcher CDM, Mertens F. Translocation t(7;19)(q22;q13)—a recurrent chromosome aberration in pseudomyogenic hemangioendothelioma? *Cancer Genet*. 2011;204(4):211-215. doi:10.1016/j.cancergen.2011.01.002
36. Zhu G, Benayed R, Ho C, et al. Diagnosis of known sarcoma fusions and novel fusion partners by targeted RNA sequencing with identification of a recurrent ACTB-FOSB fusion in pseudomyogenic hemangioendothelioma. *Mod Pathol*. 2019;32(5):609-620. doi:10.1038/s41379-018-0175-7
37. Bridge JA, Sumegi J, Royce T, Baker M, Linos K. A novel *CLTC-FOSB* gene fusion in pseudomyogenic hemangioendothelioma of bone. *Genes Chromosomes Cancer*. 2021;60(1):38-42. doi:10.1002/gcc.22891
38. Panagopoulos I, Lobmaier I, Gorunova L, Heim S. Fusion of the Genes *WWTR1* and *FOSB* in Pseudomyogenic Hemangioendothelioma. *Cancer Genomics - Proteomics*. 2019;16(4):293-298. doi:10.21873/cgp.20134

39. Murshed KA, Torres-Mora J, ElSayed AM, Ammar A, Al-Bozom I. Pseudomyogenic hemangioendothelioma of bone with rare *WWTR1-FOSB* fusion gene: Case report and literature review. *Clin Case Rep*. 2021;9(3):1494-1499. doi:10.1002/ccr3.3808
40. Errani C, Zhang L, Sung YS, et al. A novel *WWTR1-CAMTA1* gene fusion is a consistent abnormality in epithelioid hemangioendothelioma of different anatomic sites. *Genes Chromosomes Cancer*. 2011;50(8):644-653. doi:10.1002/gcc.20886
41. Tanas MR, Sboner A, Oliveira AM, et al. Identification of a Disease-Defining Gene Fusion in Epithelioid Hemangioendothelioma. *Sci Transl Med*. 2011;3(98). doi:10.1126/scitranslmed.3002409
42. Tsukamoto Y, Futani H, Watanabe T, et al. Two cases of *WWTR1-CAMTA-1* fusion-positive epithelioid hemangioendotheliomas with extremely different outcomes. *Hum Pathol Case Rep*. 2018;14:25-32. doi:10.1016/j.ehpc.2018.07.003
43. Flucke U, Vogels RJ, De Saint Aubain Somerhausen N, et al. Epithelioid Hemangioendothelioma: clinicopathologic, immunohistochemical, and molecular genetic analysis of 39 cases. *Diagn Pathol*. 2014;9(1):131. doi:10.1186/1746-1596-9-131
44. Patel NR, Salim AA, Sayeed H, et al. Molecular characterization of epithelioid haemangioendotheliomas identifies novel *WWTR1 - CAMTA1* fusion variants. *Histopathology*. 2015;67(5):699-708. doi:10.1111/his.12697
45. Anderson T, Zhang L, Hameed M, Rusch V, Travis WD, Antonescu CR. Thoracic Epithelioid Malignant Vascular Tumors: A Clinicopathologic Study of 52 Cases With Emphasis on Pathologic Grading and Molecular Studies of *WWTR1-CAMTA1* Fusions. *Am J Surg Pathol*. 2015;39(1):132-139. doi:10.1097/PAS.0000000000000346
46. Shah AA, Ohori NP, Yip L, Coyne C, Antonescu CR, Seethala RR. Epithelioid Hemangioendothelioma: a Rare Primary Thyroid Tumor with Confirmation of *WWTR1* and *CAMTA1* Rearrangements. *Endocr Pathol*. 2016;27(2):147-152. doi:10.1007/s12022-016-9428-5
47. Lee SJ, Yang WI, Chung WS, Kim SK. Epithelioid hemangioendotheliomas with *TFE3* gene translocations are compossible with *CAMTA1* gene rearrangements. *Oncotarget*. 2016;7(7):7480-7488. doi:10.18632/oncotarget.7060
48. Suurmeijer AJH, Dickson BC, Swanson D, Sung YS, Zhang L, Antonescu CR. Variant *WWTR1* gene fusions in epithelioid hemangioendothelioma—A genetic subset associated with cardiac involvement. *Genes Chromosomes Cancer*. 2020;59(7):389-395. doi:10.1002/gcc.22839
49. Dermawan JK, Azzato EM, Billings SD, et al. *YAP1-TFE3*-fused hemangioendothelioma: a multi-institutional clinicopathologic study of 24 genetically-confirmed cases. *Mod Pathol*. 2021;34(12):2211-2221. doi:10.1038/s41379-021-00879-7
50. Anderson WJ, Fletcher CDM, Hornick JL. Loss of expression of *YAP1* C-terminus as an ancillary marker for epithelioid hemangioendothelioma variant with *YAP1-TFE3* fusion and other *YAP1*-related vascular neoplasms. *Mod Pathol*. 2021;34(11):2036-2042. doi:10.1038/s41379-021-00854-2

51. Lotfalla MM, Folpe AL, Fritchie KJ, et al. Hepatic *YAPI-TFE3* Rearranged Epithelioid Hemangioendothelioma. *Case Rep Gastrointest Med.* 2019;2019:1-5. doi:10.1155/2019/7530845
52. Puls F, Niblett A, Clarke J, Kindblom LG, McCulloch T. YAP1-TFE3 epithelioid hemangioendothelioma: a case without vasoformation and a new transcript variant. *Virchows Arch.* 2015;466(4):473-478. doi:10.1007/s00428-015-1730-y
53. Kuo FY, Huang HY, Chen CL, Eng HL, Huang CC. *TFE3*- rearranged hepatic epithelioid hemangioendothelioma-a case report with immunohistochemical and molecular study. *APMIS.* 2017;125(9):849-853. doi:10.1111/apm.12716
54. Huang SC, Zhang L, Sung YS, et al. Recurrent CIC Gene Abnormalities in Angiosarcomas: A Molecular Study of 120 Cases With Concurrent Investigation of *PLCG1*, *KDR*, *MYC*, and *FLT4* Gene Alterations. *Am J Surg Pathol.* 2016;40(5):645-655. doi:10.1097/PAS.0000000000000582
55. Shimozone N, Jinnin M, Masuzawa M, et al. NUP160–SLC43A3 Is a Novel Recurrent Fusion Oncogene in Angiosarcoma. *Cancer Res.* 2015;75(21):4458-4465. doi:10.1158/0008-5472.CAN-15-0418
56. Floris G, Deraedt K, Samson I, Brys P, Sciote R. Epithelioid Hemangioma of Bone: A Potentially Metastasizing Tumor? *Int J Surg Pathol.* 2006;14(1):9-15. doi:10.1177/106689690601400102
57. Errani C, Vanel D, Gambarotti M, Alberghini M, Picci P, Faldini C. Vascular bone tumors: a proposal of a classification based on clinicopathological, radiographic and genetic features. *Skeletal Radiol.* 2012;41(12):1495-1507. doi:10.1007/s00256-012-1510-6
58. Verbeke SLJ, Bovée JVMG. Primary vascular tumors of bone: a spectrum of entities? *Int J Clin Exp Pathol.* 2011;4(6):541-551.
59. van IJzendoorn DGP, Bovée JVMG. Vascular Tumors of Bone. *Surg Pathol Clin.* 2017;10(3):621-635. doi:10.1016/j.path.2017.04.003
60. Zhou Q, Lu L, Fu Y, Xiang K, Xu L. Epithelioid hemangioma of bone: a report of two special cases and a literature review. *Skeletal Radiol.* 2016;45(12):1723-1727. doi:10.1007/s00256-016-2482-8
61. Sirikulchayanonta V, Jinawath A, Jaovisidha S. Epithelioid Hemangioma Involving Three Contiguous Bones: a Case Report with a Review of the Literature. *Korean J Radiol.* 2010;11(6):692. doi:10.3348/kjr.2010.11.6.692
62. Xian J, Righi A, Vanel D, Baldini N, Errani C. Epithelioid hemangioma of bone: A unique case with multifocal metachronous bone lesions. *J Clin Orthop Trauma.* 2019;10(6):1068-1072. doi:10.1016/j.jcot.2019.03.009
63. van IJzendoorn DGP, Forghany Z, Liebelt F, et al. Functional analyses of a human vascular tumor FOS variant identify a novel degradation mechanism and a link to tumorigenesis. *J Biol Chem.* 2017;292(52):21282-21290. doi:10.1074/jbc.C117.815845

64. Van IJzendoorn DGP, Sleijfer S, Gelderblom H, et al. Telatinib Is an Effective Targeted Therapy for Pseudomyogenic Hemangioendothelioma. *Clin Cancer Res.* 2018;24(11):2678-2687. doi:10.1158/1078-0432.CCR-17-3512
65. Gomard T, Jariel-Encontre I, Basbous J, Bossis G, Mocquet-Torcy G, Piechaczyk M. Fos family protein degradation by the proteasome. *Biochem Soc Trans.* 2008;36(5):858-863. doi:10.1042/BST0360858
66. Milde-Langosch K. The Fos family of transcription factors and their role in tumourigenesis. *Eur J Cancer.* 2005;41(16):2449-2461. doi:10.1016/j.ejca.2005.08.008
67. Dustymiller A, Curran T, Verma I. c-fos protein can induce cellular transformation: A novel mechanism of activation of a cellular oncogene. *Cell.* 1984;36(1):51-60. doi:10.1016/0092-8674(84)90073-4
68. Lam SW, Cleven AHG, Kroon HM, Briaire-de Bruijn IH, Szuhai K, Bovée JVMG. Utility of FOS as diagnostic marker for osteoid osteoma and osteoblastoma. *Virchows Arch.* 2020;476(3):455-463. doi:10.1007/s00428-019-02684-9
69. Fittall MW, Mifsud W, Pillay N, et al. Recurrent rearrangements of FOS and FOSB define osteoblastoma. *Nat Commun.* 2018;9(1):2150. doi:10.1038/s41467-018-04530-z
70. Abarrategi A, Gambera S, Alfranca A, et al. c-Fos induces chondrogenic tumor formation in immortalized human mesenchymal progenitor cells. *Sci Rep.* 2018;8(1):15615. doi:10.1038/s41598-018-33689-0
71. Sugita S, Hirano H, Kikuchi N, et al. Diagnostic utility of FOSB immunohistochemistry in pseudomyogenic hemangioendothelioma and its histological mimics. *Diagn Pathol.* 2016;11(1):75. doi:10.1186/s13000-016-0530-2
72. Van IJzendoorn DGP, Salvatori DCF, Cao X, et al. Vascular Tumor Recapitulated in Endothelial Cells from hiPSCs Engineered to Express the SERPINE1-FOSB Translocation. *Cell Rep Med.* 2020;1(9):100153. doi:10.1016/j.xcrm.2020.100153
73. Stacchiotti S, Miah AB, Frezza AM, et al. Epithelioid hemangioendothelioma, an ultra-rare cancer: a consensus paper from the community of experts. *ESMO Open.* 2021;6(3):100170. doi:10.1016/j.esmoop.2021.100170
74. Kleer CG, Unni KK, McLeod RA. Epithelioid hemangioendothelioma of bone. *Am J Surg Pathol.* 1996;20(11):1301-1311. doi:10.1097/00000478-199611000-00001
75. Lau K, Massad M, Pollak C, et al. Clinical Patterns and Outcome in Epithelioid Hemangioendothelioma With or Without Pulmonary Involvement. *Chest.* 2011;140(5):1312-1318. doi:10.1378/chest.11-0039
76. Gill R, O'Donnell RJ, Horvai A. Utility of immunohistochemistry for endothelial markers in distinguishing epithelioid hemangioendothelioma from carcinoma metastatic to bone. *Arch Pathol Lab Med.* 2009;133(6):967-972. doi:10.5858/133.6.967
77. Kulkarni KR, Jambhekar NA. Epithelioid hemangioendothelioma of bone--a clinicopathologic and immunohistochemical study of 7 cases. *Indian J Pathol Microbiol.* 2003;46(4):600-604.

78. Mentzel T, Beham A, Calonje E, Katenkamp D, Fletcher CDM. Epithelioid Hemangioendothelioma of Skin and Soft Tissues: Clinicopathologic and Immunohistochemical Study of 30 Cases: *Am J Surg Pathol*. 1997;21(4):363-374. doi:10.1097/00000478-199704000-00001
79. Doyle LA, Fletcher CDM, Hornick JL. Nuclear Expression of CAMTA1 Distinguishes Epithelioid Hemangioendothelioma From Histologic Mimics. *Am J Surg Pathol*. 2016;40(1):94-102. doi:10.1097/PAS.0000000000000511
80. Shibuya R, Matsuyama A, Shiba E, Harada H, Yabuki K, Hisaoka M. CAMTA1 is a useful immunohistochemical marker for diagnosing epithelioid haemangioendothelioma. *Histopathology*. 2015;67(6):827-835. doi:10.1111/his.12713
81. Gaur S, Torabi A, O'Neill TJ. Activity of angiogenesis inhibitors in metastatic epithelioid hemangioendothelioma: a case report. *Cancer Biol Med*. 2012;9(2):133-136. doi:10.3969/j.issn.2095-3941.2012.02.010
82. Schuetze S, Ballman KV, Ganjoo KN, et al. P10015/SARC033: A phase 2 trial of trametinib in patients with advanced epithelioid hemangioendothelioma (EHE). *J Clin Oncol*. 2021;39(15_suppl):11503-11503. doi:10.1200/JCO.2021.39.15_suppl.11503
83. Stacchiotti S, Simeone N, Lo Vullo S, et al. Activity of sirolimus in patients with progressive epithelioid hemangioendothelioma: A case-series analysis within the Italian Rare Cancer Network. *Cancer*. 2021;127(4):569-576. doi:10.1002/cncr.33247
84. Kobayashi E, Naito Y, Asano N, et al. Interim results of a real-world observational study of eribulin in soft tissue sarcoma including rare subtypes. *Jpn J Clin Oncol*. 2019;49(10):938-946. doi:10.1093/jjco/hyz096
85. Rosenberg A, Agulnik M. Epithelioid Hemangioendothelioma: Update on Diagnosis and Treatment. *Curr Treat Options Oncol*. 2018;19(4):19. doi:10.1007/s11864-018-0536-y
86. Garcia K, Gingras AC, Harvey KF, Tanas MR. TAZ/YAP fusion proteins: mechanistic insights and therapeutic opportunities. *Trends Cancer*. 2022;8(12):1033-1045. doi:10.1016/j.trecan.2022.08.002
87. Katoh M, Katoh M. Identification and characterization of FLJ10737 and CAMTA1 genes on the commonly deleted region of neuroblastoma at human chromosome 1p36.31-p36.23. *Int J Oncol*. 2003;23(4):1219-1224.
88. Vuong-Brender TT, Flynn S, Vallis Y, De Bono M. Neuronal calmodulin levels are controlled by CAMTA transcription factors. *eLife*. 2021;10:e68238. doi:10.7554/eLife.68238
89. Lamar J, Motilal Nehru V, Weinberg G. Epithelioid Hemangioendothelioma as a Model of YAP/TAZ-Driven Cancer: Insights from a Rare Fusion Sarcoma. *Cancers*. 2018;10(7):229. doi:10.3390/cancers10070229
90. Tanas MR, Ma S, Jadaan FO, et al. Mechanism of action of a WWTR1(TAZ)-CAMTA1 fusion oncoprotein. *Oncogene*. 2016;35(7):929-938. doi:10.1038/onc.2015.148

91. Szulzewsky F, Holland EC, Vasioukhin V. YAP1 and its fusion proteins in cancer initiation, progression and therapeutic resistance. *Dev Biol.* 2021;475:205-221. doi:10.1016/j.ydbio.2020.12.018
92. Merritt N, Garcia K, Rajendran D, et al. TAZ-CAMTA1 and YAP-TFE3 alter the TAZ/YAP transcriptome by recruiting the ATAC histone acetyltransferase complex. *eLife.* 2021;10:e62857. doi:10.7554/eLife.62857
93. Zanconato F, Cordenonsi M, Piccolo S. YAP/TAZ at the Roots of Cancer. *Cancer Cell.* 2016;29(6):783-803. doi:10.1016/j.ccell.2016.05.005
94. Deel MD, Li JJ, Crose LES, Lincardic CM. A Review: Molecular Aberrations within Hippo Signaling in Bone and Soft-Tissue Sarcomas. *Front Oncol.* 2015;5. doi:10.3389/fonc.2015.00190
95. Seligson ND, Awasthi A, Millis SZ, et al. Common Secondary Genomic Variants Associated With Advanced Epithelioid Hemangioendothelioma. *JAMA Netw Open.* 2019;2(10):e1912416. doi:10.1001/jamanetworkopen.2019.12416
96. Seavey CN, Hallett A, Li S, et al. Loss of CDKN2A Cooperates with WWTR1(TAZ)-CAMTA1 Gene Fusion to Promote Tumor Progression in Epithelioid Hemangioendothelioma. *Clin Cancer Res Off J Am Assoc Cancer Res.* 2023;29(13):2480-2493. doi:10.1158/1078-0432.CCR-22-2497
97. Neil E, Paredes R, Pooley O, Rubin B, Kouskoff V. The oncogenic fusion protein TAZ::CAMTA1 promotes genomic instability and senescence through hypertranscription. *Commun Biol.* 2023;6(1):1174. doi:10.1038/s42003-023-05540-4
98. Schmidt M, Mattern S, Singer S, et al. NOTCH3 missense mutations as predictor of long-term response to gemcitabine in a patient with epithelioid hemangioendothelioma. *J Cancer Res Clin Oncol.* 2023;149(9):6753-6757. doi:10.1007/s00432-023-04598-1
99. Guo W, Zhou D, Huang H, et al. Successful chemotherapy with continuous immunotherapy for primary pulmonary endovascular epithelioid hemangioendothelioma: A case report. *Medicine (Baltimore).* 2023;102(7):e32914. doi:10.1097/MD.00000000000032914
100. Lee HW, Shin JH, Simons M. Flow goes forward and cells step backward: endothelial migration. *Exp Mol Med.* 2022;54(6):711-719. doi:10.1038/s12276-022-00785-1
101. Liu ZL, Chen HH, Zheng LL, Sun LP, Shi L. Angiogenic signaling pathways and anti-angiogenic therapy for cancer. *Signal Transduct Target Ther.* 2023;8(1):198. doi:10.1038/s41392-023-01460-1
102. Sherwood LM, Parris EE, Folkman J. Tumor Angiogenesis: Therapeutic Implications. *N Engl J Med.* 1971;285(21):1182-1186. doi:10.1056/NEJM197111182852108
103. Kerbel RS. Tumor Angiogenesis. *N Engl J Med.* 2008;358(19):2039-2049. doi:10.1056/NEJMra0706596
104. Vimalraj S. A concise review of VEGF, PDGF, FGF, Notch, angiopoietin, and HGF signalling in tumor angiogenesis with a focus on alternative approaches and future

105. Hanahan D, Folkman J. Patterns and Emerging Mechanisms of the Angiogenic Switch during Tumorigenesis. *Cell.* 1996;86(3):353-364. doi:10.1016/S0092-8674(00)80108-7
106. Wagner MJ, Ravi V, Menter DG, Sood AK. Endothelial cell malignancies: new insights from the laboratory and clinic. *Npj Precis Oncol.* 2017;1(1):11. doi:10.1038/s41698-017-0013-2
107. Krock BL, Skuli N, Simon MC. Hypoxia-Induced Angiogenesis: Good and Evil. *Genes Cancer.* 2011;2(12):1117-1133. doi:10.1177/1947601911423654
108. Itakura E, Yamamoto H, Oda Y, Tsuneyoshi M. Detection and characterization of vascular endothelial growth factors and their receptors in a series of angiosarcomas. *J Surg Oncol.* 2008;97(1):74-81. doi:10.1002/jso.20766
109. Buehler D, Rush P, Hasenstein JR, et al. Expression of angiopoietin-TIE system components in angiosarcoma. *Mod Pathol.* 2013;26(8):1032-1040. doi:10.1038/modpathol.2013.43
110. Antonescu CR, Yoshida A, Guo T, et al. *KDR* Activating Mutations in Human Angiosarcomas Are Sensitive to Specific Kinase Inhibitors. *Cancer Res.* 2009;69(18):7175-7179. doi:10.1158/0008-5472.CAN-09-2068
111. Kunze K, Spieker T, Gamerding U, et al. A Recurrent Activating *PLCG1* Mutation in Cardiac Angiosarcomas Increases Apoptosis Resistance and Invasiveness of Endothelial Cells. *Cancer Res.* 2014;74(21):6173-6183. doi:10.1158/0008-5472.CAN-14-1162
112. Guo T, Zhang L, Chang NE, Singer S, Maki RG, Antonescu CR. Consistent *MYC* and *FLT4* gene amplification in radiation-induced angiosarcoma but not in other radiation-associated atypical vascular lesions. *Genes Chromosomes Cancer.* 2011;50(1):25-33. doi:10.1002/gcc.20827
113. Behjati S, Tarpey PS, Sheldon H, et al. Recurrent *PTPRB* and *PLCG1* mutations in angiosarcoma. *Nat Genet.* 2014;46(4):376-379. doi:10.1038/ng.2921
114. Huang H, Bhat A, Woodnutt G, Lappe R. Targeting the *ANGPT-TIE2* pathway in malignancy. *Nat Rev Cancer.* 2010;10(8):575-585. doi:10.1038/nrc2894
115. Murali R, Chandramohan R, Möller I, et al. Targeted massively parallel sequencing of angiosarcomas reveals frequent activation of the mitogen activated protein kinase pathway. *Oncotarget.* 2015;6(34):36041-36052. doi:10.18632/oncotarget.5936
116. Theurillat JPP, Vavricka SR, Went P, et al. Morphologic Changes and Altered Gene Expression in an Epithelioid Hemangioendothelioma during a Ten-Year Course of Disease. *Pathol - Res Pract.* 2003;199(3):165-170. doi:10.1078/0344-0338-00370
117. Emamaullee JA, Edgar R, Toso C, et al. Vascular endothelial growth factor expression in hepatic epithelioid hemangioendothelioma: Implications for treatment and surgical management. *Liver Transpl.* 2010;16(2):191-197. doi:10.1002/lt.21964

118. Ma S, Kanai R, Pobbati AV, et al. The TAZ-CAMTA1 Fusion Protein Promotes Tumorigenesis via Connective Tissue Growth Factor and Ras–MAPK Signaling in Epithelioid Hemangioendothelioma. *Clin Cancer Res.* 2022;28(14):3116-3126. doi:10.1158/1078-0432.CCR-22-0421
119. Wang Y, Xu X, Maglic D, et al. Comprehensive Molecular Characterization of the Hippo Signaling Pathway in Cancer. *Cell Rep.* 2018;25(5):1304-1317.e5. doi:10.1016/j.celrep.2018.10.001
120. Boopathy GTK, Hong W. Role of Hippo Pathway-YAP/TAZ Signaling in Angiogenesis. *Front Cell Dev Biol.* 2019;7:49. doi:10.3389/fcell.2019.00049
121. Kim MY, Oskarsson T, Acharyya S, et al. Tumor Self-Seeding by Circulating Cancer Cells. *Cell.* 2009;139(7):1315-1326. doi:10.1016/j.cell.2009.11.025
122. Ring A, Nguyen-Sträuli BD, Wicki A, Aceto N. Biology, vulnerabilities and clinical applications of circulating tumour cells. *Nat Rev Cancer.* 2023;23(2):95-111. doi:10.1038/s41568-022-00536-4
123. Bockhorn M, Jain RK, Munn LL. Active versus passive mechanisms in metastasis: do cancer cells crawl into vessels, or are they pushed? *Lancet Oncol.* 2007;8(5):444-448. doi:10.1016/S1470-2045(07)70140-7
124. Donato C, Kunz L, Castro-Giner F, et al. Hypoxia Triggers the Intravasation of Clustered Circulating Tumor Cells. *Cell Rep.* 2020;32(10):108105. doi:10.1016/j.celrep.2020.108105
125. Bockhorn M, Roberge S, Sousa C, Jain RK, Munn LL. Differential Gene Expression in Metastasizing Cells Shed from Kidney Tumors. *Cancer Res.* 2004;64(7):2469-2473. doi:10.1158/0008-5472.CAN-03-0256
126. Liotta LA, Saidel MG, Kleinerman J. The significance of hematogenous tumor cell clumps in the metastatic process. *Cancer Res.* 1976;36(3):889-894.
127. Jain RK. Molecular regulation of vessel maturation. *Nat Med.* 2003;9(6):685-693. doi:10.1038/nm0603-685
128. Padera TP, Stoll BR, Tooredman JB, Capen D, Tomaso ED, Jain RK. Cancer cells compress intratumour vessels. *Nature.* 2004;427(6976):695-695. doi:10.1038/427695a
129. Zheng Z, Liebers M, Zhelyazkova B, et al. Anchored multiplex PCR for targeted next-generation sequencing. *Nat Med.* 2014;20(12):1479-1484. doi:10.1038/nm.3729
130. Lipplaa A, Meijer D, van de Sande MAJ, et al. A novel colony-stimulating factor 1 (CSF1) translocation involving human endogenous retroviral element in a tenosynovial giant cell tumor. *Genes Chromosomes Cancer.* 2023;62(4):223-230. doi:10.1002/gcc.23116
131. Mansoori B, Mohammadi A, Ditzel HJ, et al. HMGA2 as a Critical Regulator in Cancer Development. *Genes.* 2021;12(2):269. doi:10.3390/genes12020269

132. Steppan J, Bergman Y, Viegas K, et al. Tissue Transglutaminase Modulates Vascular Stiffness and Function Through Crosslinking-Dependent and Crosslinking-Independent Functions. *J Am Heart Assoc.* 2017;6(2):e004161. doi:10.1161/JAHA.116.004161
133. Malkomes P, Lunger I, Oppermann E, et al. Transglutaminase 2 promotes tumorigenicity of colon cancer cells by inactivation of the tumor suppressor p53. *Oncogene.* 2021;40(25):4352-4367. doi:10.1038/s41388-021-01847-w
134. Furth N, Aylon Y, Oren M. p53 shades of Hippo. *Cell Death Differ.* 2018;25(1):81-92. doi:10.1038/cdd.2017.163
135. Courtwright A, Siamakpour-Reihani S, Arbiser JL, et al. Secreted Frizzled-Related Protein 2 Stimulates Angiogenesis via a Calcineurin/NFAT Signaling Pathway. *Cancer Res.* 2009;69(11):4621-4628. doi:10.1158/0008-5472.CAN-08-3402
136. Pellicani R, Poletto E, Andreuzzi E, et al. Multimerin-2 maintains vascular stability and permeability. *Matrix Biol.* 2020;87:11-25. doi:10.1016/j.matbio.2019.08.002
137. Norton L, Massagué J. Is cancer a disease of self-seeding? *Nat Med.* 2006;12(8):875-878. doi:10.1038/nm0806-875
138. Klenke FM, Wenger DE, Inwards CY, Rose PS, Sim FH. Recurrent Giant Cell Tumor of Long Bones: Analysis of Surgical Management. *Clin Orthop.* 2011;469(4):1181-1187. doi:10.1007/s11999-010-1560-9
139. Ma B, Chen Y, Chen L, et al. Hypoxia regulates Hippo signalling through the SIAH2 ubiquitin E3 ligase. *Nat Cell Biol.* 2015;17(1):95-103. doi:10.1038/ncb3073
140. Garcia D, Nasarre P, Bonilla IV, et al. Development of a Novel Humanized Monoclonal Antibody to Secreted Frizzled-Related Protein-2 That Inhibits Triple-Negative Breast Cancer and Angiosarcoma Growth In Vivo. *Ann Surg Oncol.* 2019;26(13):4782-4790. doi:10.1245/s10434-019-07800-2
141. Carter LE, Kilroy G, Gimble JM, Floyd ZE. An improved method for isolation of RNA from bone. *BMC Biotechnol.* 2012;12(1):5. doi:10.1186/1472-6750-12-5
142. Racanelli D, Brenca M, Baldazzi D, et al. Next-Generation Sequencing Approaches for the Identification of Pathognomonic Fusion Transcripts in Sarcomas: The Experience of the Italian ACC Sarcoma Working Group. *Front Oncol.* 2020;10:489. doi:10.3389/fonc.2020.00489
143. Uhrig S, Ellermann J, Walther T, et al. Accurate and efficient detection of gene fusions from RNA sequencing data. *Genome Res.* 2021;31(3):448-460. doi:10.1101/gr.257246.119
144. Dobin A, Davis CA, Schlesinger F, et al. STAR: ultrafast universal RNA-seq aligner. *Bioinformatics.* 2013;29(1):15-21. doi:10.1093/bioinformatics/bts635
145. Li B, Dewey CN. RSEM: accurate transcript quantification from RNA-Seq data with or without a reference genome. *BMC Bioinformatics.* 2011;12(1):323. doi:10.1186/1471-2105-12-323

146. Frankish A, Diekhans M, Jungreis I, et al. GENCODE 2021. *Nucleic Acids Res.* 2021;49(D1):D916-D923. doi:10.1093/nar/gkaa1087
147. Nicorici D, Satalan M, Edgren H, et al. *FusionCatcher - a Tool for Finding Somatic Fusion Genes in Paired-End RNA-Sequencing Data.* Bioinformatics; 2014. doi:10.1101/011650
148. Love MI, Huber W, Anders S. Moderated estimation of fold change and dispersion for RNA-seq data with DESeq2. *Genome Biol.* 2014;15(12):550. doi:10.1186/s13059-014-0550-8
149. Hotelling H. RELATIONS BETWEEN TWO SETS OF VARIATES. *Biometrika.* 1936;28(3-4):321-377. doi:10.1093/biomet/28.3-4.321
150. van der Maaten L, Hinton G. Visualizing data using t-SNE. *J Mach Learn Res.* 2008;9:2579-2605.
151. Conesa A, Madrigal P, Tarazona S, et al. A survey of best practices for RNA-seq data analysis. *Genome Biol.* 2016;17(1):13. doi:10.1186/s13059-016-0881-8
152. Zhao Y, Li MC, Konaté MM, et al. TPM, FPKM, or Normalized Counts? A Comparative Study of Quantification Measures for the Analysis of RNA-seq Data from the NCI Patient-Derived Models Repository. *J Transl Med.* 2021;19(1):269. doi:10.1186/s12967-021-02936-w
153. Plaisier SB, Taschereau R, Wong JA, Graeber TG. Rank–rank hypergeometric overlap: identification of statistically significant overlap between gene-expression signatures. *Nucleic Acids Res.* 2010;38(17):e169-e169. doi:10.1093/nar/gkq636
154. Subramanian A, Tamayo P, Mootha VK, et al. Gene set enrichment analysis: A knowledge-based approach for interpreting genome-wide expression profiles. *Proc Natl Acad Sci.* 2005;102(43):15545-15550. doi:10.1073/pnas.0506580102

ACKNOWLEDGEMENTS

First of all, I would like to thank my supervisor, Dr. Roberta Maestro, for her support during these three years. She showed me what laboratory work means and helped me to prepare for presentations, conferences and written papers. I will take with me all her scientific suggestions and the passion she gave me for research work.

I would also like to thank my external collaborators in Padua and Bologna who made this work possible and my collaborators in the lab.

And now...let's go to the best part of these three years. Moving from Naples to Aviano was not easy at first, but the special people I have met here have made this place one of my heart places and the PhD one of the best experiences in my life.

Many thanks to the staff of the Department of Oncogenetics and Functional Oncogenomics for all the scientific suggestions.

A special thank you goes to all my lab coffee girls who were there for me to share scientific ideas as well as life experiences. Lab days with you were not that hard!

Many thanks to my PhD friend Giulia T., who was always there for me in the most difficult moments of this journey. Your scientific advices and your moral support were fundamental. It was much more fun to share this experience with you and I will miss you every day. Thank you to Giulia Z., the other PhD student who shared these years with me and was always there to talk about bioinformatics and give me valuable advice.

Thank you, Elena Bells, for being such a great friend. I was lucky to find you, who always believed in me and encouraged me in the most difficult moments of this PhD. You were my lab partner who waited for me late at night in the lab, but also a true friend who listened to my life troubles. Your honest suggestions were valuable and your company always worthwhile. Sharing all the experiences in FVG with such a fun and positive person was of paramount importance to me!

Thank you so much, Veronica! Your support and the laughter we shared during our trips to escape the lab world were among the best moments of those three years. Despite the distance, I could always count on you, on your advice and understanding. Our friendship is one of the best things that has happened to me in these three years!

I thank all AperiCRO friends, and in particular my Befane, for the days and nights together, which were important to relieve the stress of lab work.



Last but not least, I would like to thank all my family and my best friend for their great support despite the distance.

Thank you, mom, for always listening to me and giving me comfort in difficult situations. Thank you, Dad, for always being there for me, believing in me and distracting me whenever I needed it. Thank you, Ary, for being there for me and supporting me even when I cried and felt lost. Thank you, Mary, for always being there for a video phone call to listen and encourage me. Thank you to my grandmother Adri for her loving support and kind words, and to my other grandmother. Thank you also to my second family in FVG.

I am grateful for this challenging experience because PhD has taught me to never give up and to find alternative solutions to any problem.

PUBLISHED ARTICLES

Fusion transcriptome profiling defines the monoclonal origin of multifocal epithelioid haemangioma of bone

Costantino Errani,¹ Ilaria De Benedictis,² Alberto Righi,³  Beatrice Valenti,² Elisa Del Savio,² Davide Baldazzi,² Stefania Benini,³ Marta Sbaraglia,^{4,5} Brayan Vega Jimenez,³ Daniel Vanel,³ Davide Maria Donati,¹ Angelo Paolo Dei Tos^{4,5} & Roberta Maestro² 

¹Clinica Ortopedica e Traumatologica III a Prevalente Indirizzo Oncologico, IRCCS Istituto Ortopedico Rizzoli, Bologna, ²Unit of Oncogenetics and Functional Oncogenomics, Centro di Riferimento Oncologico di Aviano (CRO Aviano) IRCCS, Aviano, ³Department of Pathology, IRCCS Istituto Ortopedico Rizzoli, Bologna, ⁴Department of Pathology, Azienda Ospedaliera Universitaria di Padova and ⁵Department of Medicine, University of Padua School of Medicine, Padua, Italy

Date of submission 26 May 2023

Accepted for publication 13 July 2023

Errani C, De Benedictis I, Righi A, Valenti B, Del Savio E, Baldazzi D, Benini S, Sbaraglia M, Vega Jimenez B, Vanel D, Donati D M, Dei Tos A P & Maestro R

(2023) *Histopathology*. <https://doi.org/10.1111/his.15016>

Fusion transcriptome profiling defines the monoclonal origin of multifocal epithelioid haemangioma of bone

Aims: Epithelioid haemangioma (EH) of bone remains a highly controversial entity. Indeed, the WHO classifies EHs of soft tissues as benign tumours, whereas bone EHs are considered intermediate–locally aggressive tumours due to common multifocal presentation and local destructive growth. To gain insights into the clinical behaviour and biology of EH of bone we retrospectively analysed 42 patients treated in a single institution from 1978 to 2021.

Methods and results: Multifocal presentation was detected in 17 of 42 patients (40%) primarily as synchronous lesions. Patients were treated with curettage (57%), resection (29%) or biopsy, followed by radiotherapy or embolisation (14%). Follow-up (minimum 24 months) was available for 38 patients, with only five local recurrences (13%) and no death of disease.

To clarify whether the synchronous bone lesions in multifocal EH represent multicentric disease or clonal dissemination, four cases were profiled by RNA-sequencing. Separate lesions from the same patient, which showed a similar transcriptional profile, expressed the same fusion transcript (involving FOS or FOSB) with identical gene breakpoints.

Conclusions: These results indicate that, in EH of bone, multifocal lesions are clonally related and therefore represent the spread of a same neoplastic clone rather than simultaneous independent tumours. This finding is in apparent contradiction with the benign clinical course of the disease, and suggests that tumour dissemination in bone EH probably reflects a phenomenon of passive spreading, with tumour cells colonising distal sites while maintaining their benign biological nature.

Keywords: clonal analysis, epithelioid haemangioma of bone, FOS, FOSB, fusion transcript, RNA-sequencing

Introduction

Vascular bone tumours represent controversial entities because of their rarity, unusual morphology, variable

classifications and unpredictable biological behaviour.^{1,2} Epithelioid haemangioma (EH) is a tumour of unclear aetiology and pathogenesis that may arise in diverse anatomical sites, including bone.^{1–4} The differential

Address for correspondence: R Maestro, Unit of Oncogenetics and Functional Oncogenomics, Centro di Riferimento Oncologico di Aviano (CRO Aviano) IRCCS, Via Gallini 2, 33081 Aviano, PN, Italy. e-mail: rmaestro@cro.it

Costantino Errani and Ilaria De Benedictis are co-first authors.

Angelo Paolo Dei Tos and Roberta Maestro are co-last authors.

© 2023 The Authors. *Histopathology* published by John Wiley & Sons Ltd.

This is an open access article under the terms of the [Creative Commons Attribution-NonCommercial-NoDerivs](https://creativecommons.org/licenses/by-nc-nd/4.0/) License, which permits use and distribution in any medium, provided the original work is properly cited, the use is non-commercial and no modifications or adaptations are made.

diagnosis of EH includes epithelioid haemangioendothelioma and epithelioid angiosarcoma, characterised by significantly different clinical courses.^{1,5} Imaging is of limited help, as this tumour lacks characteristic imaging features.⁶ The recent identification of FOS and FOSB gene rearrangements as a genetic hallmark of EH, and CAMTA1 and TFE3 gene rearrangements as recurrent alterations in epithelioid haemangioendothelioma, provides an objective and powerful diagnostic tool for distinguishing EH from other vascular tumours.^{7–12} EH of soft tissues is classified by the most recent World Health Organisation (WHO) Classification of Soft Tissue and Bone Tumours as a benign tumour, while EH of bone is classified as intermediate and locally aggressive tumour.¹ Despite the benign histological appearance, EH of bone may show a locally destructive growth pattern, lymph node involvement and multifocal presentation.^{1,6,13} These data would suggest an aggressive clinical behaviour and reinforce the concept that EH of bone is a controversial entity.^{14,15} Moreover, whether multifocal lesions of a EH of bone, similar to multifocal epithelioid haemangioendothelioma, are the result of tumour spreading of a primary lesion, as proposed,¹⁶ or rather represent independent tumours, due to a type of 'field effect', is still debated.^{1,13,17,18} This uncertainty, which is particularly relevant when separate lesions affect different bones, impacts upon clinical decision-making and, indeed, there is no consensus regarding the treatment that ranges from intralesional curettage to *en-bloc* resection.^{3,6,17}

In the attempt to shed light into the clinical and biological characteristics of EH of bone, we retrospectively analysed 42 patients treated in a single institution from 1978 to 2021.

Materials and methods

TUMOUR SERIES

The medical records of 42 patients with EH of bone treated in a single institution between 1978 and 2021 were retrospectively reviewed. Eight of these patients were described previously.¹⁷ Medical records were available for 38 patients with a mean follow-up of 100 months (range = 24–314 months). Demographics, clinical data and follow-up information were retrieved from medical records (Table 1). The study was approved by the ethics committee of our institution and registered at [ClinicalTrials.gov](https://clinicaltrials.gov) (identifier NCT03169595). Parents/guardians gave written informed consent for the retrospective analysis of clinical data according to the Institutional Review Board and before inclusion into ongoing protocols.

Diagnosis of EH of bone was based on morphological, immunohistochemical and molecular analysis. Histology was reviewed by musculoskeletal tumour pathology experts. Imaging was available for 23 patients at the onset of their disease [radiographs, 20 patients; computed tomography (CT), 16 patients; magnetic resonance (MR) imaging, 14 patients] and was reviewed by a musculoskeletal tumour radiologist. Surgical treatment ranged from biopsy alone to *en-bloc* resection.

IMMUNOHISTOCHEMISTRY (IHC)

Immunohistochemistry was performed as described previously.¹⁹ The following antibodies were used: ERG (monoclonal antibody V9; Ventana, Tucson, AZ, USA), CD31 (monoclonal antibody O13; Ventana), CK AE1/AE3 (mouse monoclonal antibody, 6F-H2; Cell Marque, Rocklin, CA, USA), INI1 (mouse monoclonal antibody, clone BAF47; Cell Marque), CAMTA1 (rabbit polyclonal antibody, dilution 1:200; Novusbio, Centennial, CO, USA), TFE3 (rabbit monoclonal antibody, clone RQ-37; Cell Marque) and FOSB (rabbit monoclonal antibody, clone 5G4, 1:100 dilution; Cell Signalling Technology, Danvers, MA, USA). Antibody detection was performed using UltraView Universal DAB detection kit (Ventana). FOSB positivity was defined as moderate-to-strong nuclear staining in at least 50% of cells, as in Huang *et al.*⁷ Samples were also stained with a FOS rabbit polyclonal antibody (ABE457; Millipore, Burlington, MA, USA), unfortunately providing unreliable results probably due to the decalcification procedure.

FISH ANALYSIS AND ZFP36::FOSB REVERSE TRANSCRIPTION-QUANTITATIVE POLYMERASE CHAIN REACTION (RT-QPCR) ANALYSIS

Fluorescence *in-situ* hybridisation (FISH) and ZFP36::FOSB RT-qPCR were performed as previously described¹⁷ and detailed in the [Supporting information](#). The following FISH probes were used: SPEC TFE3 (Xp11.23), SPEC WWTR1 (3q25.1) LSI dual colour break-apart DNA probes (Zytovision, Bremerhaven, Germany); FOS (14q24.3) dual colour break-apart probe (Empire Genomics, Williamsville, NY, USA).

TARGETED RNA-SEQUENCING AND WHOLE TRANSCRIPTOME ANALYSIS

Nucleic acids were extracted using the AllPrep DNA/RNA mini kit columns (Qiagen, Germantown, MD, USA) for frozen samples and the FFPE RNA/DNA

Table 1. Details of the 42 patients with epithelioid haemangioma of bone

Patient ID	Age (years)	Gender	Location	Presentation	Treatment	Outcome (FUmonths)
EH1	29	F	Bone (vertebra)	Solitary	Surgery (WM)	NED (276)
EH2	35	M	Bone (humerus)	Solitary	Surgery (WM) RXT	NED (84)
EH3	38	F	Bone (vertebra)	Solitary	Surgery (IL) RXT	NED (200)
EH4	12	M	Bone (humerus)	Solitary	Surgery (IL)	NED (44)
EH5	22	F	Bone (sacrum)	Solitary	Surgery (IL)	NED (211)
EH6	57	F	Bone (cuneiform)	Solitary	Surgery (IL)	NED (53)
EH7	34	M	Bone (clavicle)	Solitary	Surgery (WM)	NED (195)
EH8	42	M	Bone (metatarsal, cuneiform)	Multifocal	Surgery (WM)	NED (38)
EH9	60	M	Bone (sternum)	Solitary	Surgery (IL), SAE	NED1 (72)
EH10	31	M	Bone (humerus)	Solitary	Surgery (WM)	NED (126)
EH11	48	F	Bone (femur)	Solitary	Surgery (WM)	NED (166)
EH12	45	F	Bone (vertebra, rib)	Multifocal	Surgery (WM)	NED (52)
EH13	22	M	Bone (tibia)	Solitary	Surgery (IL)	NED (25)
EH14	60	F	Bone (metatarsal)	Multifocal	Surgery (IL), RXT	NED (106)
EH15	58	M	Bone (ulna)	Solitary	Surgery (WM)	NED (314)
EH16	28	F	Bone (pelvis)	Solitary	Surgery (IL)	NED (256)
EH17	42	M	Bone (femur)	Multifocal	Surgery (WM)	NED (32)
EH18	51	M	Bone (femur, tibia)	Multifocal	Surgery (IL)	DOO (96)
EH19	55	F	Bone (vertebra)	Solitary	Biopsy, RXT	NED (27)
EH20	39	F	Bone (vertebra, rib)	Multifocal	Biopsy, SAE	NED (70)
EH21	45	M	Bone (tibia, calcaneus)	Multifocal	Surgery (IL)	NED (24)
EH22	12	F	Bone (femur, tibia)	Multifocal	Surgery (WM, IL)	Lost
EH23	65	M	Bone (fibula, calcaneus)	Multifocal	Surgery (IL) RXT	NED (202)
EH24	33	M	Bone (tibia, cuboid, cuneiform)	Multifocal	Surgery (IL), RXT	NED (92)
EH25	28	M	Bone (vertebra)	Solitary	Biopsy	AWD (39)
EH26	83	M	Bone (tibia)	Multifocal	Surgery (IL)	DOO (94)
EH27	33	M	Bone (humerus)	Solitary	Surgery (WM)	NED (182)
EH28	25	M	Bone (femur, pelvis)	Multifocal	Biopsy, RXT	NED (79)
EH29	41	M	Bone (metacarpal)	Solitary	Surgery (IL)	NED1 (178)
EH30	44	M	Bone (humerus)	Solitary	Surgery (WM)	NED (185)
EH31	40	M	Bone (tibia)	Multifocal	Surgery (WM)	NED (202)
EH32	21	F	Bone (vertebra)	Solitary	Biopsy, SAE	NED (28)
EH33	20	F	Bone (humerus, radius, skull, sacrum)	Multifocal	Surgery (WM, IL)	NED2 (240)
EH34	40	M	Bone (calcaneus, fibula)	Multifocal	Surgery (IL)	NED (33)

Table 1. (Continued)

Patient ID	Age (years)	Gender	Location	Presentation	Treatment	Outcome (FUmonths)
EH35	34	F	Bone (talus, tibia)	Multifocal	Surgery (IL)	Lost
EH36	28	M	Bone (tibia)	Solitary	Surgery (IL)	NED (102)
EH37	28	F	Bone (humerus)	Solitary	Surgery (IL)	NED1 (239)
EH38	39	F	Bone (tibia, rotula)	Multifocal	Surgery (IL)	Lost
EH39	39	F	Bone (pelvis)	Solitary	Biopsy	AWD (30)
EH40	46	F	Bone (cervical vertebra)	Solitary	Surgery (IL)	NED (24)
EH41	58	F	Bone (distal phalanx, second finger, foot)	Solitary	Surgery (IL)	NED1 (29)
EH42	28	M	Bone (clavicle)	Solitary	Surgery (IL)	Lost

AWD, Alive with disease; DOO, Dead of other cause; F, Female; FU, Follow-up; IL, Intralesional curettage; M, Male; NED, No evidence of disease; NED1, No evidence of disease after one local recurrence; NED2, No evidence of disease after two local recurrence; RXT, Radiation therapy; SAE, Selective arterial embolisation; WM, Wide margin.

purification plus kit (Norgen Biotek Corporation, Ontario, Canada) for formalin-fixed paraffin-embedded (FFPE) specimens.

A customised Archer FusionPlex sarcoma RNA-sequencing panel version 1.1 (ArcherDX, Boulder, CO, USA), supplemented with spike-ins primers for FOS (exon 4, forward primer) and FOSB (exons 1 and 2, reverse primers) was employed for library generation. Libraries were run on an Illumina MiSeq sequencing platform and were first analysed with the Archer Analysis suite software version 6.0.4 (January 2022). Subsequently (June 2023), raw data were re-analysed with the most recent version 7.1.0 release. Raw data were also analysed with the Arriba fusion caller, as previously described.²⁰ RT-PCR and RT-PCR/Sanger sequencing were employed for orthogonal validations. Primer sequences are provided in the [Supporting information](#).

For whole transcriptome analysis, libraries were generated with the Illumina Stranded Total Ribo-Zero Plus RNA library prep kit (Illumina, San Diego, CA, USA) and run on an Illumina HiSeq 1000 platform. Sequencing depth was ≥ 50 million paired-end reads per sample. RNA-sequencing data were analysed as in Gasparotto *et al.*²¹ with minor modifications. Arriba (version 2.3.0)²² and FusionCatcher tools were used for fusion transcript identification (see [Supporting information](#) for details).

Results

TUMOUR SERIES: DEMOGRAPHIC AND CLINICAL FEATURES

The analysis of medical records of 42 patients with EH of bone (Table 1) showed no age predilection,

with patients' ages ranging between 12 and 83 years (mean age = 39 years). Twenty-three patients were male and 19 were female. Most EHs occurred in the extremities (seven humerus; one ulna; one radius; one hand; nine tibia; two fibula; five femur; eight foot) followed by the trunk (two rib; 10 vertebra; three pelvis; one clavicle; one sternum). Seventeen of 42 patients (40%) presented with multifocal bone involvement (13 lower limb; one pelvis and femur; one upper limb, sacrum and skull; two vertebra and rib; Figure 1). Except for one patient (EH33), multifocality was synchronous. In most cases the same or contiguous bones were involved, except in patients EH21, where non-contiguous bones were affected (tibia and calcaneus) and EH33 (see below).

Imaging data were available for 23 patients. All lesions were well-defined and lytic, associated with sclerosis in only two patients. The cortex was thin, with a calcified periosteal limitation in three patients (13%) and completely missing in six patients (26%). Soft tissues were involved in four patients (17%). Two patients presented with surface lesions (9%). The mean size of the bone lesions was 4.5 cm (range = 1.4–11.0 cm). On MR imaging all lesions showed a high signal on T2W images, but the signal was variable on T1W images (low in five patients, intermediate six patients and high in three patients). One vertebral lesion had MR imaging features similar to a typical haemangioma.

Twenty-four patients (57%) were treated with intralesional curettage, 12 patients (29%) underwent *en-bloc* resection with wide margins and six patients (14%) were treated with biopsy only, followed by radiation therapy or selective arterial embolisation.



Figure 1. Multifocal EH of the left lower limb of patient EH21. A, Laterolateral radiograph, B, sagittal CT and C, MRI show osteolytic lesions involving the distal tibia and calcaneus. D, Laterolateral radiograph showing the result after curettage and filling the bone defects with cement.

Follow-up information was available for 38 patients: five of 38 patients (13%) had a local recurrence at 12, 26, 28, 48 and 120 months, respectively. Four of these patients were treated with curettage and only one with resection. At the last follow-up, no patient was dead of disease. The only patient with metachronous presentation (EH33) underwent resection of lesions involving skull and proximal humerus and a curettage of proximal radius, distal humerus and sacrum. The patient had a favourable prognosis at 19-years' follow-up.²³

HISTOLOGICAL AND IMMUNOHISTOCHEMICAL FINDINGS

IHC showed a strong expression of vascular markers (CD31 and ERG), retained INI1/SMARCB1 expression and negativity for pan-keratin AE1/AE3, CAMTA1 and TFE3 in all patients. The diagnosis of EH of bone with exclusion of EH mimics was supported by molecular analyses (FISH or RT-PCR) whenever the quality

and quantity of biological material allowed. According to morphological, IHC and molecular features, 34 EHs were classified as classic variant and eight as atypical/cellular variant. On haematoxylin and eosin, classic EHs showed no significant cytological atypia (Figure 2). Focal tumoral necrosis was detected in three patients. The mitotic rate was low, with fewer than two mitoses per 10 high-power fields in all patients. The eight atypical/cellular EH presented solid neoplastic areas constituted of endothelial cells, and in six of these patients a strong nuclear immunoreactivity for FOSB was detected (Figure 2, Table 2). Unfortunately, in our series the FOS staining was unreliable, probably due to the decalcification procedure.

MOLECULAR ANALYSES AND CLONALITY ASSESSMENT

Molecular analyses were conducted in 15 patients for which biological material was available (Table 2).

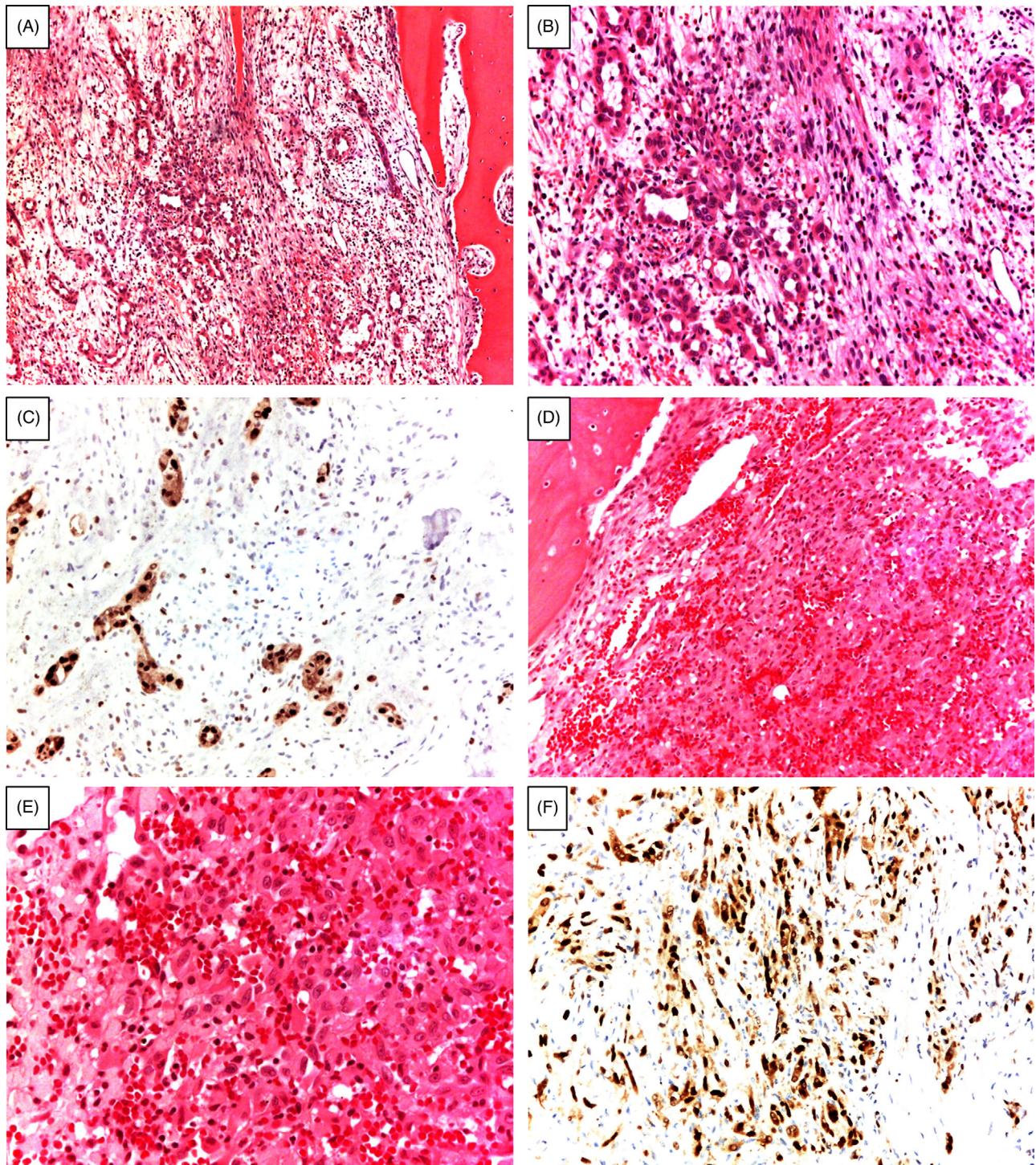


Figure 2. An example (EH22) of classic variant of epithelioid haemangioma composed of well-formed vascular channels lined by plump epithelioid endothelial cells, featuring moderate to abundant eosinophilic cytoplasm associated with eosinophils-rich inflammatory infiltrate: A, stain, haematoxylin and eosin, magnification; B, stain, haematoxylin and eosin, magnification; C, a nuclear immunohistochemical expression for FOSB antibody was observed in endothelial cells (magnification). An example (EH38) of atypical/cellular variant of epithelioid haemangioma of bone that shows solid neoplastic areas constituted of endothelial cells with abundant eosinophilic cytoplasm associated with extravasated red blood cells: D, stain, haematoxylin and eosin, magnification; E, stain, haematoxylin and eosin, magnification; F, nuclear FOSB immunoreactivity (magnification).

RT-qPCR indicated that 2/4 FOSB IHC-positive tumours (both atypical/cellular EH) expressed ZFP36::FOSB fusion; no ZFP36::FOSB fusion was detected in six FOSB IHC-negative EHs. An additional FOSB fusion (WWTR1::FOSB) was identified by both targeted and whole RNA-sequencing in a FOSB IHC-positive atypical/cellular EH. FISH highlighted FOS rearrangements in three of the four patients analysed, all classic EHs. RNA-sequencing revealed two further FOS rearrangements in classic EHs.

To determine the clonality relationship between separate EHs in the same patient, multifocal synchronous lesions of four patients were analysed for the expression of fusion transcripts. In these patients the separate lesions involved the same bone, contiguous bones (EH14, EH24, EH38) or non-contiguous bones (EH21). A targeted RNA-sequencing approach with a customised Archer fusion panel revealed the expression of a WWTR1::FOSB fusion with identical breakpoints in all three lesions of patient EH38 (Figure 3A, Table 3). Conversely, no high confidence fusions were detected by the Archer-suite software version 6.0.4 in cases EH14, EH21 and EH24. However, potential fusions involving FOS were included in the list of discarded/low-confidence calls. Raw sequencing data were then reanalysed with a more recent Archer-suite release (version 7.1.0) and with the Arriba fusion caller.²² The potential fusions reported as discarded/low-confidence calls by the Archer-suite version 6.0.4 were erroneous, while the Archer-suite version 7.1.0 detected, with high confidence, a fusion of FOS with a sequence located on chromosome 11 in both lesions of case EH21. The Arriba tool not only confirmed the expression of this chimeric transcript, involving FOS and a long non-coding RNA in opposite orientation (FOS::ENSG00000255202 fusion; Figure 3B–D, Table 3), but efficiently captured the fusion events in all cases and indicated that synchronous EHs of the same patient shared FOS fusions with identical breakpoints. A FOS::VIM fusion had been previously reported in a metatarsal lesion of patient EH14.¹⁶ Arriba analysis highlighted that both EH lesions of this patient carried indeed an identical FOS::chr10 fusion, involving FOS and an intergenic region on chromosome 10 located between VIM and ST8SIA6. An identical fusion of FOS with an intergenic region of chromosome 21, located between ADAMTS1 and CYYR1 genes, was also detected in the multiple EHs of patient EH24 (FOS::chr21 fusion).

These rearrangements, which were orthogonally validated by PCR-Sanger sequencing (Figure 3A–D), involved exon 4 of FOS and yielded a truncated FOS

protein, due to the generation of a *de-novo* stop codon a few amino acids downstream from the breakpoint. No recurrent fusion partner was identified, in line with the fact that the biological significance of these truncating fusions is the hyperactivation of FOS via the removal of the C-terminal regulatory region.^{16,24} The correspondence in the breakpoint sequence was also confirmed at the level of genomic DNA in the multiple lesions of cases EH14 and EH24 (not shown), and the presence of identical fusion events in separate EHs of the same patient strongly indicated a clonal origin.

We also analysed the global transcriptional profile of the multiple tumours of patients EH21, EH24 and EH38. Separate EHs of a same patient showed similar transcriptomes (Figure 3E,F). More importantly, RNA-sequencing not only confirmed the presence of the FOS or FOSB fusions but identified further identical fusion events shared by the tumour lesions of the same patient (Table 3). We focused upon the ones picked up by both Arriba and FusionCatcher tools and orthogonally validated by RT-PCR the expression of PSME3IP1::WWOX and TFG::ADGRG7 chimeras in cases EH24 and EH38, respectively (not shown). Both are intrachromosomal events and the TFG::ADGRG7 fusion was reported previously.²⁵

Discussion

The WHO ambivalently classifies EH of soft tissue and EH of bone. The former are classified as benign tumours, the latter as intermediate, locally aggressive tumours.¹ Indeed, in the absence of objective criteria, the classification of EH of bone remains controversial.^{1,2} Some authors consider EH a benign tumour, as none of the patients reported in the literature experienced an adverse outcome, while others argue that EH is an aggressive tumour because of its multifocal presentation and frequent local destructive growth with destruction of cortex and extension to soft tissues.^{1,14,15,26,27}

In an attempt to resolve this ambiguity, we studied the clinical and biological characteristics of 42 patients with EH treated at a single institution. Although the retrospective design could be considered a limitation, the rarity of EH mandates that such a study be retrospective to have sufficient patients for analysis²⁸ and the relatively large case series is an advantage of the present study.

The retrospective analysis of 38 patients with EH of bone showed that prognosis was excellent, with no death of disease. Most patients were treated with

Table 2. Immunohistochemical and molecular data of the 42 patients with EH of bone

Patient ID	Histological variant	TFE3 and WWTR1 FISH analysis	FOSB IHC	ZFP36::FOSB RT-PCR analysis	FOS FISH analysis	FOS and FOSB fusions identified by NGS in paired lesions
EH1	Classic	–	+	ND	ND	
EH2	Classic	ND	–	–	ND	
EH3	Classic	ND	+	ND	ND	
EH4	Classic	ND	–	–	ND	
EH5	Classic	ND	–	ND	ND	
EH6	Classic	ND	+	ND	ND	
EH7	Classic	ND	+	ND	ND	
EH8	Classic	ND	+	ND	ND	
EH9	Classic	ND	–	ND	ND	
EH10	Atypical/cellular	–	+	ND	ND	
EH11	Classic	–	–	–	ND	
EH12	Atypical/cellular	ND	+	ND	ND	
EH13	Classic	ND	–	–	ND	
EH14	Classic	–	–	ND	+	FOS::chr10
EH15	Classic	ND	+	ND	ND	
EH16	Classic	ND	–	ND	ND	
EH17	Classic	–	–	ND	+	
EH18	Classic	ND	+	–	ND	
EH19	Classic	ND	–	ND	ND	
EH20	Atypical/cellular	–	–	ND	ND	
EH21	Classic	ND	–	ND	ND	FOS::ENSG00000255202
EH22	Classic	ND	+	ND	ND	
EH23	Classic	–	–	ND	ND	
EH24	Classic	ND	–	–	ND	FOS::chr21
EH25	Classic	–	–	ND	ND	
EH26	Atypical/cellular	ND	+	+	ND	
EH27	Classic	–	–	ND	ND	
EH28	Classic	ND	+	ND	ND	
EH29	Classic	–	–	–	+	
EH30	Classic	ND	+	ND	ND	
EH31	Classic	ND	–	ND	ND	

Table 2. (Continued)

Patient ID	Histological variant	TFE3 and WWTR1 FISH analysis	FOSB IHC	ZFP36::FOSB RT-PCR analysis	FOS FISH analysis	FOS and FOSB fusions identified by NGS in paired lesions
EH32	Classic	ND	–	ND	ND	
EH33	Atypical/cellular	–	+	+	ND	
EH34	Classic	ND	+	ND	ND	
EH35	Classic	ND	+	–	ND	
EH36	Atypical/cellular	–	+	ND	–	
EH37	Atypical/cellular	ND	–	ND	ND	
EH38	Atypical/cellular	ND	+	ND	ND	WWTR1::FOSB
EH39	Classic	–	+	ND	ND	
EH40	Classic	–	+	ND	ND	
EH41	Classic	–	+	ND	ND	
EH42	Classic	ND	+	ND	ND	

ND, Not done or not feasible; +, Positive; –, Negative.

curettage or resection. Local recurrence occurred in five patients (13%) treated with curettage. Multifocal presentation was detected in 17 of 42 patients (40%), in all but one as synchronous EH lesions. The same contiguous, but in some cases also non-contiguous, bones were involved.

Molecular characterisation of multifocal tumours indicated a clonal origin. Synchronous lesions affecting the same patient expressed the same fusion transcripts with identical gene breakpoints. These results are in keeping with the work by van Ijzendoorn and co-workers¹⁶ who, by analysing two cases of multifocal EH, concluded that tumour foci affecting adjacent bones represent multifocal regional spread. Our work extends this observation also to EH lesions involving non-contiguous bones and supports the concept that multifocal presentations in this tumour represent the spread of a same neoplastic clone rather than simultaneous independent tumours.

Taken together, our data indicate that EH of bone is a tumour with a benign clinical course despite a disseminative potential. These two concepts are only seemingly contradictory. It has been estimated that millions of cells are shed by a tumour every day, although only a minute fraction of these will eventually seed into secondary colonies.²⁹ Metastatisation imposes that a tumour cell bypasses a number of roadblocks: to detach from the primary site, to survive

in the lymphatic/circulatory system and to colonise secondary sites with induction of neoangiogenesis for tumour support.^{30,31} Intriguingly, vascular tumours seem to be facilitated in some of these steps. Indeed, the multifocal presentation is somehow a distinctive feature of vascular tumours of bone, including classical haemangioma, haemangioendothelioma and angiosarcoma. Despite some cases of lymph node invasion and distal metastasis,^{9,13,23} EH primarily demonstrates regional reseeding, suggesting that the capacity of EH cells to survive in the lymphatic/blood stream is somehow limited, and that their congenial soil is the organ of origin. In multifocal EH, the separate tumour lesions maintain their intrinsic 'benign' nature, as the presence of secondary seedings does not correlate with poor outcome. Thus, EH dissemination does not appear to be associated with aggressive biological traits; rather, having features of a passive phenomenon. Indeed, it has been previously reported that tumours may shed passively into the blood or lymphatic vessels in the absence of active cell migration.³¹

In conclusion, the excellent prognosis of EH of bone supports the contention that it is indeed a clinically benign tumour. Like other vascular tumours, EH of bone may be multifocal. Although tumour multifocality in EH of bone is the manifestation of a disseminative process, as established by clonality

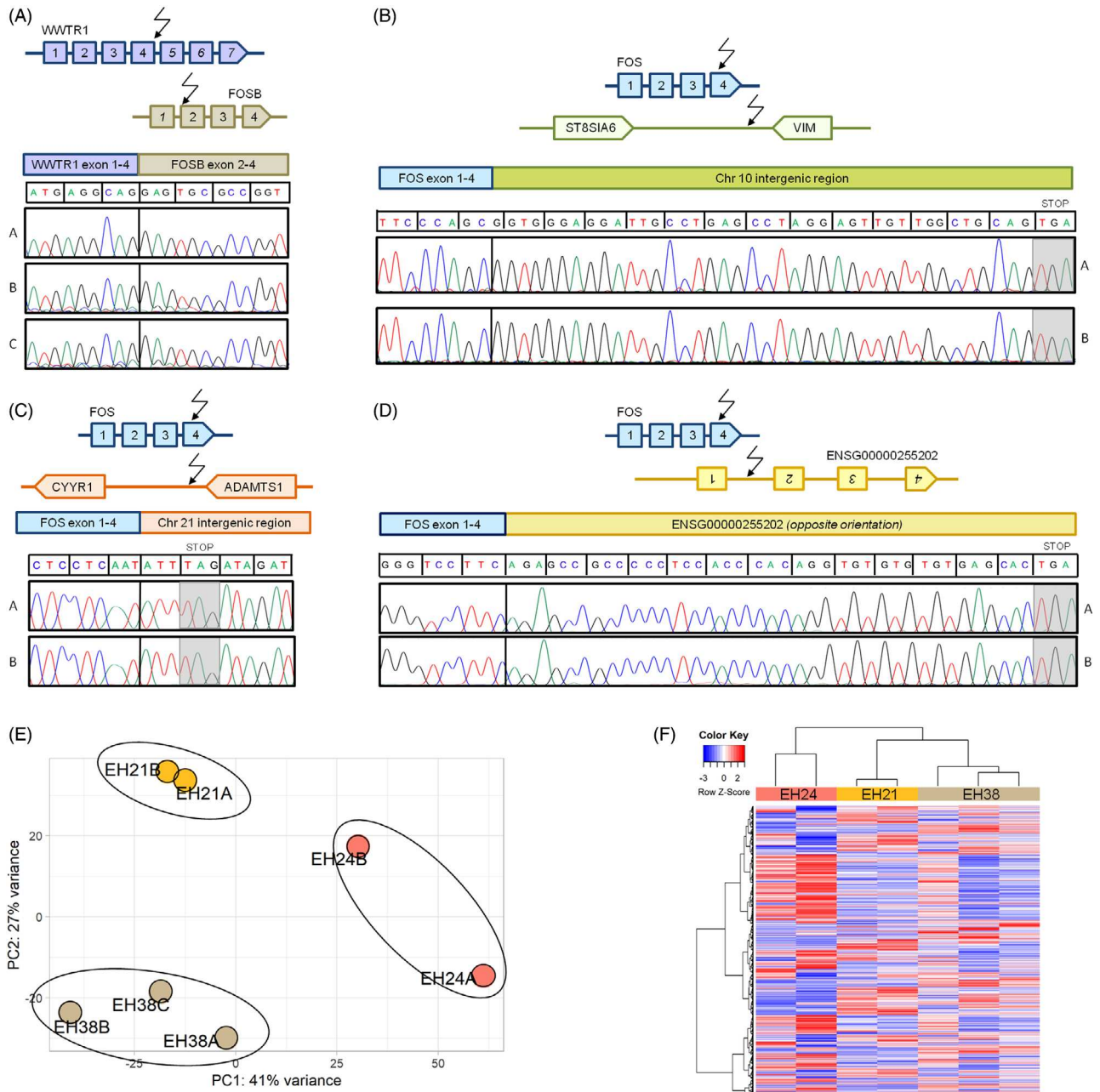


Figure 3. Fusion analysis of multifocal lesions indicates clonal relationship. **A**, Schematic representation of the WWTR1::FOSB fusion detected in the multifocal EHS of patient EH38. The arrows indicate the location of the breakpoints in the cDNA. The chromatogram in the lower panel confirms that the three EH lesions of this patient (A, left tibia; B, rotula; C, proximal tibia) share the same breakpoint. **B**, Schematic representation of the FOS::chr10 fusion detected in both EHS of case EH14. The fusion involved FOS exon 4 and an intergenic region of chromosome 10, close to the VIM gene. The chromatograms in the lower panel show that lesion A (IV metatarsus) and lesion B (II metatarsus) carry an identical breakpoint. The greyish area indicates the *de-novo* STOP codon provided by the 3' partner. **C**, Illustration of the FOS::chr21 fusion detected in case EH24 involving FOS exon 4 and an intergenic region of chromosome 21 close to the ADAMTS1 gene. The same breakpoint sequence was detected in both lesions of this patient (A, distal tibia; B, III cuneiform). **D**, Case EH21 carried an identical FOS fusion (FOS exon 4 and lncRNA ENSG00000255202) in the lesions of the tibia and calcaneus (A and B, respectively). PCA (**E**) and unsupervised hierarchical clustering (**F**) of the multifocal EHS of patients EH21, EH24 and EH38 show co-clustering of paired lesions of the same patient.

Table 3. Recurrent fusions identified by RNA-sequencing in the separate tumour lesions of cases EH21, EH24 and EH38

Patient ID	Gene 1	Gene 2	Breakpoint_1	Site1	Breakpoint_2	Site2	Arriba (confidence)	FusionCatcher (confidence)
EH21A	FOS	ENSG00000255202	chr14:75281167	CDS	chr11:33694437	Intron	High	–
EH21B	FOS	ENSG00000255202	chr14:75281175	CDS	chr11:33694437	Intron	Low	–
EH21A	SYN2	ACTG1	chr3:12071910	Intron	chr17:81510151	3' UTR	High	–
EH21B	SYN2	ACTG1	chr3:12071910	Intron	chr17:81510151	3' UTR	Low	–
EH24A	FOS	chr21 (~ADAMTS1)	chr14:75281016	CDS	chr21:26829622	Intergenic	High	–
EH24B	FOS	chr21 (~ADAMTS1)	chr14:75281016	CDS	chr21:26829622	Intergenic	High	–
EH24A	PSME3IP1	WVOX	chr16:57185821	5'UTR/splice	chr16:78164183	CDS/splice	High	High
EH24B	PSME3IP1	WVOX	chr16:57185821	5'UTR/splice	chr16:78164183	CDS/splice	High	High
EH24A	NDUF58	chr11 (~GSTP1)	chr11:68033283	CDS/splice	chr11:67577746	Intergenic	High	–
EH24B	NDUF58	chr11 (~GSTP1)	chr11:68033283	CDS/splice	chr11:67577746	Intergenic	High	–
EH24A	PMEPA1	PURB	chr20:57651860	UTR	chr7:44879426	UTR	–	High
EH24B	PMEPA1	PURB	chr20:57651861	UTR	chr7:44879426	UTR	–	High
EH38A	WWTR1	FOSB	chr3:149542335	CDS/splice	chr19:45470629	CDS/splice	High	High
EH38C	WWTR1	FOSB	chr3:149542335	CDS/splice	chr19:45470629	CDS/splice	High	High
EH38A	WWTR1 ¹	FOSB ¹	chr3:149528238	Intron	chr19:45469785	Intron	High	–
EH38B	WWTR1 ¹	FOSB ¹	chr3:149528238	Intron	chr19:45469785	Intron	High	–
EH38C	WWTR1 ¹	FOSB ¹	chr3:149528238	Intron	chr19:45469785	Intron	Low	–
EH38A	TFG	ADGRG7	chr3:100720058	CDS/splice	chr3:100629598	CDS/splice	Low	High
EH38B	TFG	ADGRG7	chr3:100720058	CDS/splice	chr3:100629598	CDS/splice	Low	High
EH38C	TFG	ADGRG7	chr3:100720058	CDS/splice	chr3:100629598	CDS/splice	High	High

Splice, Splice-site.

¹Presplicing transcript.

analysis, this has no major impact on the clinical course of the disease, even for patients treated exclusively by surgery or biopsy. Therefore, EH of bone is a tumour with disseminative potential but of benign nature.

Acknowledgements

This work was supported by the Italian Ministry of Health, Alleanza Contro il Cancro 'WG sarcoma', Associazione Italiana Ricerca sul Cancro to R.M.

Conflicts of interest

The authors declare that they have no conflicts of interest directly related to the topic of this article.

Clinical trial registration number

This study was registered at [ClinicalTrials.gov](https://clinicaltrials.gov) (identifier NCT03169595).

Data availability statement

The data that support the findings of this study are available from the corresponding author upon reasonable request. The data are not publicly available due to ethical restrictions.

Ethics approval

The study was approved by the ethics committee of IRCCS Istituto Ortopedico Rizzoli (Nr0030451del 10/09/2015).

References

- WHO Classification of Tumours Editorial Board. *Soft tissue and bone tumours*. Vol. 3. 5th ed. Lyon: IARC press; 2020.
- van IJzendoorn DGP, Bovée JVMG. Vascular tumors of bone. *Surg. Pathol. Clin.* 2017; **10**: 621–635.
- Nielsen GP, Srivastava A, Kattapuram S et al. Epithelioid hemangioma of bone revisited: a study of 50 cases. *Am. J. Surg. Pathol.* 2009; **33**: 270–277.
- Dei Tos AP. *Soft tissue sarcomas: a pattern-based approach to diagnosis*. 1st ed. Cambridge: Cambridge University Press, 2018.
- Zhang Y, Rosenberg AE. Epithelioid hemangioma. In Santini-Araujo E, Kalil RK, Bertoni F et al. eds. *Tumors and tumor-like lesions of bone*. Cham: Springer International Publishing, 2020; 497–503.
- Errani C, Vanel D, Gambarotti M, Alberghini M, Picci P, Faldini C. Vascular bone tumors: a proposal of a classification based on clinicopathological, radiographic and genetic features. *Skeletal Radiol.* 2012; **41**: 1495–1507.
- Huang S-C, Zhang L, Sung Y-S et al. Frequent FOS gene rearrangements in epithelioid hemangioma: a molecular study of 58 cases with morphologic reappraisal. *Am. J. Surg. Pathol.* 2015; **39**: 1313–1321.
- Antonescu CR, Chen H-W, Zhang L et al. ZFP36-FOSB fusion defines a subset of epithelioid hemangioma with atypical features: ZFP36-FOSB FUSION. *Genes Chromosomes Cancer* 2014; **53**: 951–959.
- Tsuda Y, Suurmeijer AJH, Sung Y et al. Epithelioid hemangioma of bone harboring FOS and FOSB gene rearrangements: a clinicopathologic and molecular study. *Genes Chromosomes Cancer* 2021; **60**: 17–25.
- Errani C, Zhang L, Sung YS et al. A novel WWTR1-CAMTA1 gene fusion is a consistent abnormality in epithelioid hemangioendothelioma of different anatomic sites. *Genes Chromosomes Cancer* 2011; **50**: 644–653.
- Antonescu CR, Le Loarer F, Mosquera J-M et al. Novel YAP1-TFE3 fusion defines a distinct subset of epithelioid hemangioendothelioma. *Genes Chromosomes Cancer* 2013; **52**: 775–784.
- Papke DJ, Hornick JL. What is new in endothelial neoplasia? *Virchows Arch.* 2020; **476**: 17–28.
- Floris G, Deraedt K, Samson I, Brys P, Scirot R. Epithelioid hemangioma of bone: a potentially metastasizing tumor? *Int. J. Surg. Pathol.* 2006; **14**: 9–15.
- Errani C, Zhang L, Panicek DM, Healey JH, Antonescu CR. Epithelioid hemangioma of bone and soft tissue: a reappraisal of a controversial entity. *Clin. Orthop.* 2012; **470**: 1498–1506.
- Verbeke SLJ, Bovée JVMG. Primary vascular tumors of bone: a spectrum of entities? *Int. J. Clin. Exp. Pathol.* 2011; **4**: 541–551.
- van IJzendoorn DGP, de Jong D, Romagosa C et al. Fusion events lead to truncation of FOS in epithelioid hemangioma of bone. *Genes Chromosomes Cancer* 2015; **54**: 565–574.
- Righi A, Sbaraglia M, Gambarotti M et al. Primary vascular tumors of bone: a monoinstitutional morphologic and molecular analysis of 427 cases with emphasis on epithelioid variants. *Am. J. Surg. Pathol.* 2020; **44**: 1192–1203.
- Errani C, Sung YS, Zhang L, Healey JH, Antonescu CR. Monoclonality of multifocal epithelioid hemangioendothelioma of the liver by analysis of WWTR1-CAMTA1 breakpoints. *Cancer Genet.* 2012; **205**: 12–17.
- Gambarotti M, Benini S, Gamberi G et al. CIC-DUX4 fusion-positive round-cell sarcomas of soft tissue and bone: a single-institution morphological and molecular analysis of seven cases. *Histopathology* 2016; **69**: 624–634.
- Racanello D, Brenca M, Baldazzi D et al. Next-generation sequencing approaches for the identification of pathognomonic fusion transcripts in sarcomas: the experience of the Italian ACC Sarcoma Working Group. *Front. Oncol.* 2020; **10**: 489.
- Gasparotto D, Sbaraglia M, Rossi S et al. Tumor genotype, location, and malignant potential shape the immunogenicity of primary untreated gastrointestinal stromal tumors. *JCI Insight* 2020; **5**: e142560.
- Uhrig S, Ellermann J, Walther T et al. Accurate and efficient detection of gene fusions from RNA sequencing data. *Genome Res.* 2021; **31**: 448–460.
- Xian J, Righi A, Vanel D, Baldini N, Errani C. Epithelioid hemangioma of bone: a unique case with multifocal metachronous bone lesions. *J. Clin. Orthop. Trauma* 2019; **10**: 1068–1072.
- van IJzendoorn DGP, Forghany Z, Liebelt F et al. Functional analyses of a human vascular tumor FOS variant identify a novel degradation mechanism and a link to tumorigenesis. *J. Biol. Chem.* 2017; **292**: 21282–21290.
- Chase A, Ernst T, Fiebig A et al. TFG, a target of chromosome translocations in lymphoma and soft tissue tumors, fuses to GPR128 in healthy individuals. *Haematologica* 2010; **95**: 20–26.
- Evans HL, Raymond AK, Ayala AG. Vascular tumors of bone: a study of 17 cases other than ordinary hemangioma, with an evaluation of the relationship of hemangioendothelioma of bone to epithelioid hemangioma, epithelioid hemangioendothelioma, and high-grade angiosarcoma. *Hum. Pathol.* 2003; **34**: 680–689.
- Wenger DE, Wold LE. Benign vascular lesions of bone: radiologic and pathologic features. *Skeletal Radiol.* 2000; **29**: 63–74.

28. Stacchiotti S, Maria Frezza A, Demetri GD *et al.* Retrospective observational studies in ultra-rare sarcomas: a consensus paper from the Connective Tissue Oncology Society (CTOS) community of experts on the minimum requirements for the evaluation of activity of systemic treatments. *Cancer Treat. Rev.* 2022; **110**: 102455.
29. Ring A, Nguyen-Sträuli BD, Wicki A, Aceto N. Biology, vulnerabilities and clinical applications of circulating tumour cells. *Nat. Rev. Cancer* 2023; **23**: 95–111.
30. Norton L, Massagué J. Is cancer a disease of self-seeding? *Nat. Med.* 2006; **12**: 875–878.
31. Bockhorn M, Jain RK, Munn LL. Active versus passive mechanisms in metastasis: do cancer cells crawl into vessels, or are they pushed? *Lancet Oncol.* 2007; **8**: 444–448.
32. Dobin A, Davis CA, Schlesinger F *et al.* STAR: ultrafast universal RNA-seq aligner. *Bioinformatics* 2013; **29**: 15–21.
33. Li B, Dewey CN. RSEM: accurate transcript quantification from RNA-Seq data with or without a reference genome. *BMC Bioinformatics* 2011; **12**: 323.
34. Frankish A, Diekhans M, Jungreis I *et al.* GENCODE 2021. *Nucleic Acids Res.* 2021; **49**: D916–D923.
35. Love MI, Huber W, Anders S. Moderated estimation of fold change and dispersion for RNA-seq data with DESeq2. *Genome Biol.* 2014; **15**: 550.

Supporting Information

Additional Supporting Information may be found in the online version of this article:

Supporting Information S1. Materials and methods details.